THE DETERMINATION OF THE DYNAMIC RESPONSE OF A SMALL SWEPT WING JET FIGHTER TO ATMOSPHERIC TURBULENCE USING THE POWER SPECTRUM METHOD OF ANALYSIS

PAUL SHERIDAN NORTON

THE DETERMINATION OF THE DYNAMIC RESPONSE OF A SMALL SWEPT WING JET FIGHTER TO ATMOSPHERIC TURBULENCE USING THE POWER SPECTRUM METHOD OF ANALYSIS

by

Paul Sheridan Norton
Lieutenant, United States Navy
B.S. U.S. Naval Academy, 1960

Submitted in partial fulfillment of the
requirements for the degree of

MASTER OF SCIENCE IN AERONAUTICAL ENGINEERING

from the

NAVAL POSTGRADUATE SCHOOL
December 1967

ABSTRACT

The power spectral techniques of generalized harmonic analysis were applied to determine the phase and amplitude of the transfer function between the vertical component of turbulence and the resultant pitch rate of a small swept wing jet fighter. The power spectrum analysis was based on actual flight test data. In addition the amplitude and phase of the aircraft's transfer function are determined theoretically by two different methods and compared with the results of the power spectrum analysis. It was established that the power spectrum method, as applied to random turbulence, can be used to determine an aircraft's response to this random input on a continuous basis and that power spectrum techniques have considerable potential value in the study of aircraft gust loading.

Thesis by Paul S. Norton, entitled "The Determination of the Dynamic Response of a Small Swept Wing Jet Fighter to Atmospheric Turbulence Using the Power Spectrum Method of Analysis"

ERRATA SHEET

Page	Line	Change	To
13	2	Aeronautical Engineering Department	Aeronautics Department
18	3rd para line 1	an	a
26	6 from bottom	Fig. 5	Table I.
32	15	longitudinal control inputs,	longitudinal control inputs;
37	2nd from bottom	$\sqrt{R_x(\infty)},$	$\sqrt{R_x(\infty)}$;
43	last line of text	imagi-nary	imagin-ary
45	4th para	"angular magnitude;"	"angular magnitude,"
48	5	F-100C;	F-100C,
63	6	0.6 cycles per second,	0.6 cycles per second;
63	20	agreement with theory;	agreement with theory,
63	bottom	param-eters	para-meters
66	2/3	signif-icant	signi-ficant

TABLE OF CONTENTS

LIST OF TABLES

LIST OF ILLUSTRATIONS

TABLE OF SYMBOLS

a_Z	vertical acceleration
$\bar{c}$	mean aerodynamic chord
C_D	total drag coefficient
C_{D_α}	change in drag coefficient with variation in angle of attack
C_{L_α}	change in lift coefficient with variation in angle of attack
C_L	total lift coefficient
C_{m_α}	change in pitching moment coefficient with variation in angle of attack
$C_{m_{\delta H}}$	change in pitching moment coefficient with variation in elevator deflection
C_{m_q}	change in pitching moment coefficient with variation in pitch angular velocity
C_{xy}	co-spectral density function (real part of the cross spectral density function)
e	natural logarithmic base
f	frequency, cps
$G_{(x)}$	power spectral density function of function x
G_{xy}	cross spectral density function of functions x and y
g	acceleration due to gravity
$H_{y/x}$	transfer function from input x(t) to output y(t)
I_{yy}	moment of inertia about the Y axis
j	$\sqrt{-1}$
L_α	change in lift with variation in angle of attack
l_x	longitudinal distance from accelerometer to flow vane

TABLE OF SYMBOLS (Continued)

$M_{\alpha} = -\left[L_{\alpha_{eff}}\right] M_q - \left[\omega_{sp}^2\right]$, change in pitching moment with variation in angle of attack

$M_{\delta B} = \frac{\rho V^2 S c}{2 I_{yy}} C_{m_{\delta B}}$, change in pitching moment with variation in speed brake deflection

$M_{\delta E} = \frac{\rho V^2 S c}{2 I_{yy}} C_{m_{\delta E}}$, change in pitching moment with variation in elevator deflection

$M_{\delta F} = \frac{\rho V^2 S c}{2 I_{yy}} C_{m_{\delta F}}$, change in pitching moment with variation in flap deflection

$M_q = \frac{\rho S V c^2}{4 I_{yy}} C_{m_q}$, change in pitching moment with variation in pitch angular velocity

$M_u = -\frac{\rho S c V}{2 I_{yy}} \left(\alpha_o C_{m_\alpha}\right)$, change in pitching moment with variation in forward velocity

$M_W = \frac{\rho S c V}{2 I_{yy}} C_{m_\alpha}$, change in pitching moment with variation in velocity along the Z axis

$M_{\dot{W}} = \frac{\rho S c^2}{4 I_{yy}} C_{m_{\dot{\alpha}}}$, change in pitching moment with variation in acceleration along the Z axis

Q_{xy} quadrature spectral density function (imaginary part of the cross spectral density function)

q pitch angular velocity; dynamic pressure

$\dot{q}$ pitch angular acceleration

$R_{(x)}$ autocorrelation function of random input x

R_{xy} cross correlation function of functions x and y

s wing area; La-Placian operator

T general time limit

t time

$T_{\delta RPM}$ change in engine thrust with variation of RPM

T_u change in engine thrust with variation in forward velocity

u linear velocity along the X axis

V aircraft velocity

$X_{\delta B} = \frac{-\rho V^2 S}{2m} C_{D_{\delta E}}$, change in force along the X axis with a variation in speed brake deflection

$X_{\delta E} \equiv \frac{-\rho V^2 S}{2m} C_{D_{\delta E}}$, change in force along the X axis with a variation in elevator deflection

$X_{\delta F} = \frac{-\rho V^2 S}{2m} C_{D_{\delta F}}$, change in force along the X axis with a variation in flap deflection

x_k k^{th} value of function x

$X_q \approx 0$, change in force along the X axis with a variation in pitch angular velocity

$X_u = \frac{-\rho S V}{m} C_D$, change in force along the X axis with a variation in forward velocity

$X_w = \frac{\rho S V}{2m}(C_{L_\alpha} - C_{D_\alpha})$, change in force along the X axis with a variation in velocity along the Z axis

$X_{\dot{w}} \approx 0$, change in force along the X axis with a variation in acceleration along the Z axis

w_g vertical component of atmospheric turbulence

$Z_{\delta B} = \frac{-\rho V^2 S}{2m} C_{L_{\delta B}}$, change in force along the Z axis due to a variation in speed brake deflection

$Z_{\delta E} = \frac{-\rho V^2 S}{2m} C_{L_{\delta E}}$, change in force along the Z axis with a variation in elevator deflection

$Z_{\delta F} = \frac{-\rho V^2 S}{2m} C_{L_{\delta F}}$, change in force along the Z axis with a variation in flap deflection

$Z_q = \frac{\rho S V C}{4m} C_{L_q}$, change in force along the Z axis with a variation in pitch angular velocity

$Z_u = \frac{-\rho S V}{m} C_L$, change in force along the Z axis with a variation in forward velocity

$Z_w = \frac{-\rho S V}{2m}(C_{L_\alpha} + C_D)$, change in force along the Z axis with a variation in velocity along the Z axis

$Z_{\dot{w}} = \frac{-\rho S V}{2m} C_{L_{\dot{\alpha}}}$, change in force along the Z axis with a variation in acceleration along the Z axis

α_V vertical vane angle

ε angle between X axis and thrust line

Ω reduced wavelength (radians/ft)

λ wavelength

θ pitch angle

θ_{xy} phase of the cross spectral density function based on the functions x and y

TABLE OF SYMBOLS (Continued)

μ	mass ratio
$\mu_{(\,)}$	mean value
ρ	air density
ω	angular or circular frequency
ζ	damping ratio
τ	time lag
ψ_x^2	mean square value

Subscripts:

Ph	phugoid
Sp	short period
n	n^{th} turbulence patch
x,y	general input or response quantities

A dot over a symbol denotes differentiation with respect to time.

A bar over a quantity denotes an average value.

u,v,w, are velocities along the X,Y, and Z axes respectively.

$\delta_B, \delta_E, \delta_F$ are variations in speed brake, elevator, and flap deflections respectively.

δ_{RPM} denotes a variation in engine RPM.

$(\,)_o$ denotes an initial value.

ACKNOWLEDGEMENTS

The author wishes to thank Cdr. D. M. Layton, instructor in the Aeronautical Engineering Department and Director of the Aviation Safety School, for his guidance and support as thesis advisor. The author would also like to express his appreciation to the personnel of the Flight Test Division of the NASA Ames Research Center who provided the flight test data and related information used in this thesis. In particular the author is indebted to Mr. Walter McNeil of the Flight Test Division and Mr. William Crawford of the Computer Facility at Ames for their professional advice and assistance. Original attempts were made to obtain the desired flight test data at the Naval Air Test Center, and although this information was not used for this thesis, the author wishes to thank the pilots of the Flight Test Division at Patuxent River for their efforts and cooperation.

INTRODUCTION

Atmospheric turbulence and the resulting aircraft disturbances from stabilized flight due to this turbulence are random and thus aperiodic and non-dissipative. These disturbances can only be defined on a non-precise basis with certain probability distributions and average values since they are random in nature. This leads to the application of probability and statistical concepts, which, in combination with classical Fourier techniques, form a general approach for the analysis of problems of this type. This technique is termed the power spectrum method.

Power spectral methods were derived from economic time studies at the beginning of this century. The initial applications were also directed toward turbulence studies and the Brownian motion of particles. During World War II power spectral methods were used to analyze problems in servomechanisms and communications; however, the application of power spectral analysis to the field of aeronautics, and in particular to the study of the dynamic response of aircraft to turbulence, is relatively new and still in the early stages of development.

Other recent studies in the field of aeronautics involving power spectral techniques have been applied to:

a. Wind tunnel turbulence
b. Gust loads on aircraft
c. Acoustic Noise
d. Buffeting loads
e. Electronic noise in guidance and gunnery systems

In particular, considering the gust loading and dynamic response of aircraft, statistical inference is a realistic approach since the problem is essentially one of a random process phenomena. Perhaps a more meaningful presentation of the effectiveness of the power spectrum method can be made if the earlier discrete gust design methods are mentioned in comparison.

The earliest discrete gust approach involved the assumptions of a rigid airplane, a ramp type gust, and a specified maximum vertical velocity. Subsequent discrete gust design methods were adjusted for different wing chords and pitch characteristics between different aircraft by expressing data in terms of the mass ratio, μ . The discrete gust concept was based primarily on the premise that the relative loads for single isolated gusts are a measure of the relative loads in a sequence of gusts.

However, in recent years a more general approach to turbulence analysis has been needed in order to account for the greater variety and degree of aircraft flexibility, mass distribution, configuration and dynamic response characteristics, as well as the varied operating speeds and altitudes. Therefore, the power spectral techniques of generalized harmonic analysis were developed for application to turbulence and dynamic response studies.

As conditions changed and the variety of aircraft and operating altitudes/airspeeds increased, the concept of the discrete gust design method was broadened to include flexible bodies as well as rigid bodies. Although the flexible aircraft was mathematically flown through discrete gusts of varying wavelengths, the discrete gust concept did not adequately account for the continuous nature of atmospheric turbulence, particularly as applied to lightly damped dynamic systems. Latest design philosophy embodies both the discrete gust concept and the power spectral approach, with the design initially analyzed and checked using the discrete gust method and then examined in greater detail using the power spectrum analysis. Further development of the power spectral method may result in its use in the future entirely for atmospheric turbulence studies.

The main advantages of the power spectral approach to turbulence analysis are outlined in Ref. 1:

1. It provides a more realistic representation of the continuous nature of atmospheric turbulence.
2. It allows airplane configurations and response characteristics to be taken into account in a rational manner.
3. It allows more rational consideration of design and operational variations such as configuration changes, mission changes and airplane degrees of freedom.

Most of the present day applications of power spectral methods are concerned with the analysis of the magnitude and distribution of the random data; for example, the intensity of atmospheric turbulence and its variation with frequency. However this thesis considers a more unique application of power spectral techniques by establishing the transfer function between pitch rate and turbulence for the F-100C airplane based upon the analysis of a random input, w_g, the vertical component of atmospheric turbulence. This application goes one step beyond the analysis of random data by considering its effect upon the dynamic response of an airframe. The particular transfer function, $\frac{\dot{\theta}}{w_g}$, is considered to provide a basic indication of the F-100 airplane's dynamic response characteristics in a turbulent environment. To measure the accuracy of the results obtained through the power spectral analysis, a comparison between $\frac{\dot{\theta}}{w_g}$, as determined from this method, is made with the values of $\frac{\dot{\theta}}{w_g}$, as determined by solving the longitudinal equations of dynamic motion for the F-100C airplane.

DISCUSSION OF THE CHARACTERISTICS AND ANALYSIS OF RANDOM DATA

Any recorded data which describe a physical process can be broadly classified into either one of two categories: deterministic or non-deterministic. Deterministic data are information which describe a process which can be represented and predicted with reasonable accuracy by exact mathematical relationships. Some common examples of this type of process are the electrical potential across a condenser as it discharges through a resistor or the motion of a satellite in a known orbit around the earth. Examples of non-deterministic data are the variation of an aircraft's vertical velocity in turbulence and the variation in the magnitude of the lift developed on an airfoil encountering buffeting in rough air. Due to the inherent randomness of the turbulence this non-deterministic data cannot be described, nor can its behavior be predicted by explicit mathematical relationships. In practical terms, the decision as to whether or not physical data are classified as being deterministic or non-deterministic (random) is based upon the ability to reproduce the data repeatedly through controlled experiments. If the experiment or phenomena which produced the data can be repeated with the same results, within the tolerances of experimental error, then the data obtained are classified as deterministic. Conversely, if identical results cannot be obtained upon repeating an experiment, then the data are considered to be non-deterministic or random in nature.

In considering random data, therefore, it is expected that an particular observation producing this data will effectively represent only one of many possible outcomes which might have occured as a result of this experiment. For example, assume that the lift developed on an airfoil during buffeting in flight is recorded as a function of time. A specific lift time history will be obtained as shown in Fig. 1. However, if a second airfoil of identical shape is flown through a similar type of disturbance simultaneously, it is likely that a different lift time history would result. Therefore, the lift time history for any one airfoil encountering a particular finite disturbance is only one example of an infinitely large number of time histories which might have occurred. If the random buffeting is observed over a finite time

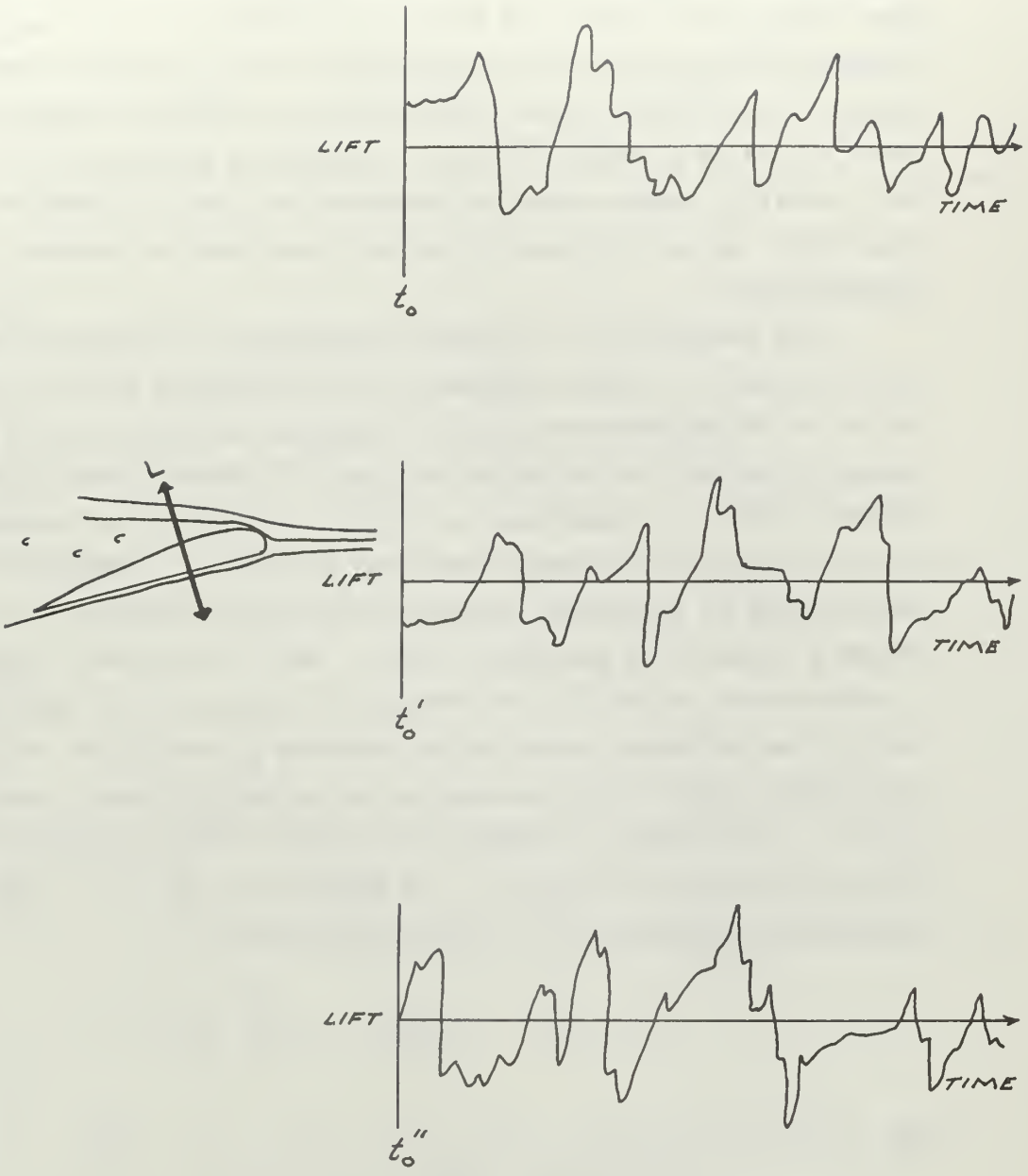

Figure 1. Sample records showing the lift developed on an airfoil in turbulence.

interval and is graphically or mathematically represented by a single time history, then this time history is referred to as a sample record by Bendat and Piersol (2). The collection of all possible sample records of lift versus time which the random buffeting might have produced is called a random process or stochastic process in Ref. 2. As a result, a sample record of observed data for a random physical occurrence can be considered to be only one physical outcome of a random process.

The properties of a physical experiment or occurrence which are described by a random process can be determined from the average values of the experimental data as computed over the range of sample records obtained. A collection of sample functions which comprise a random process is illustrated in Fig. 2. By taking the instantaneous values of each of the sample functions at time t_1, summing the values and dividing by the number of sample functions, the mean value of the random process for a particular time t_1 may be computed. In addition, a joint moment or correlation between the values of the random process at two different times can be computed by taking the average of the product of the instantaneous values at two different times t_1 and $t_1 + \tau$. The product obtained in the manner described above is termed the auto-correlation function. The mean value, $\mu_x(t_1)$, and the auto-correlation function $R_x(t_1, t_1+\tau)$ are defined as:

$$\mu_x(t_1) = \lim_{N\to\infty} \frac{1}{N} \sum_{k=1}^{N} x_k(t_1) \qquad (1)$$

and $$R_x(t_1, t_1+\tau) = \lim_{N\to\infty} \frac{1}{N} \sum_{k=1}^{N} x_k(t_1) \cdot x_k(t_1+\tau) \qquad (2)$$

According to Ref. 2, the random process is stationary if $\mu_x(t_1)$ and $R_x(t_1, t_1+\tau)$ do not vary as time t_1 is varied. In a more general sense, when the properties of a random process, as computed over short intervals, do not vary significantly from one interval to the next, then the process is considered to be stationary.

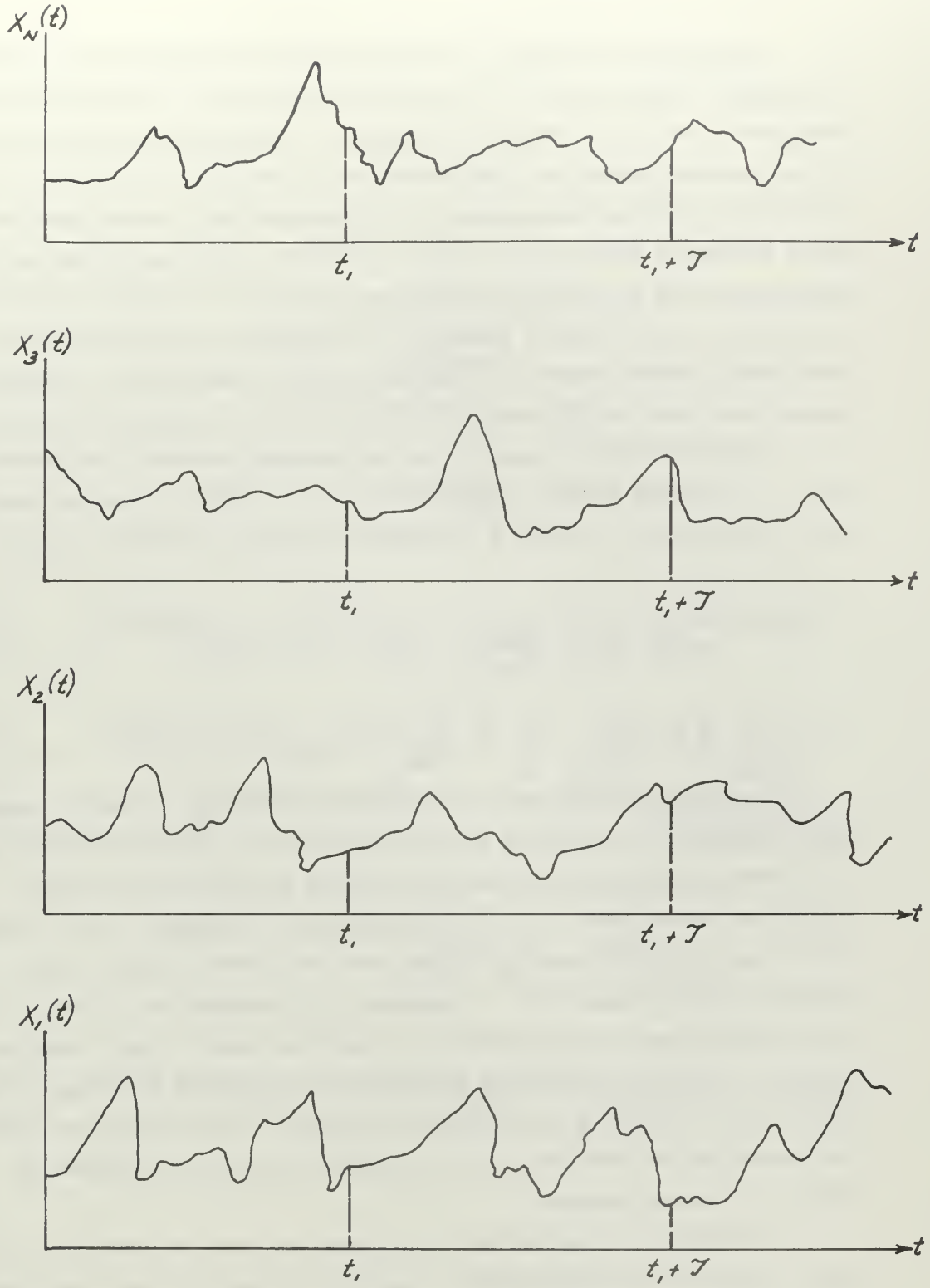

Figure 2. Ensemble of sample functions forming a random process. (Reproduced from Ref. 2).

Applying the concept of stationarity to atmospheric turbulence, it has been shown in Ref. 1 that the conditions of stationarity and homogeneity apply to large scale patterns of air motion within regions of one hundred miles and time durations of one hour. In cases of severe turbulence, such as encountered in a thunderstorm, these time and distance estimates would not be valid. However, the time duration for homogeneous and stationary conditions may still be almost five minutes in length. It is usually possible to determine the properties of a stationary random process by computing time averages over specified sample functions in the ensembles (collection of sample functions).

Consider the k^{th} sample for the random process illustrated in Fig. 2. The mean value, $\mu_x(k)$, and the autocorrelation function, $R_x(\tau, k)$, for the k^{th} sample function, according to Ref. 2, are:

$$\mu_x(k) = \lim_{T\to\infty} \frac{1}{T} \int_0^T x_k(t)\,dt \tag{3}$$

$$R_x(\tau, k) = \lim_{T\to\infty} \frac{1}{T} \int_0^T x_k(t) \cdot x_k(t+\tau)\,dt \tag{4}$$

Random processes may be classified as shown in Fig. 3, reproduced from Ref. 2, as being either stationary or non-stationary, and stationary random processes may be further subdivided as either ergodic or non-ergodic. The random process is ergodic if it is stationary and $\mu_x(k)$ and $R_x(\tau, k)$ do not vary when computed over different sample functions. Therefore, all properties of ergodic random processes can be determined by computing over a single sample function. In actual physical phenomena, as outlined in Ref. 2, most random data, including atmospheric turbulence, are ergodic so that the properties of the data can be computed from time averages of individual sample records.

Two types of statistical functions are used to describe the basic properties of random data: (a) the autocorrelation function and (b) the power spectral density function. The autocorrelation function and the power spectral density function provide an analysis

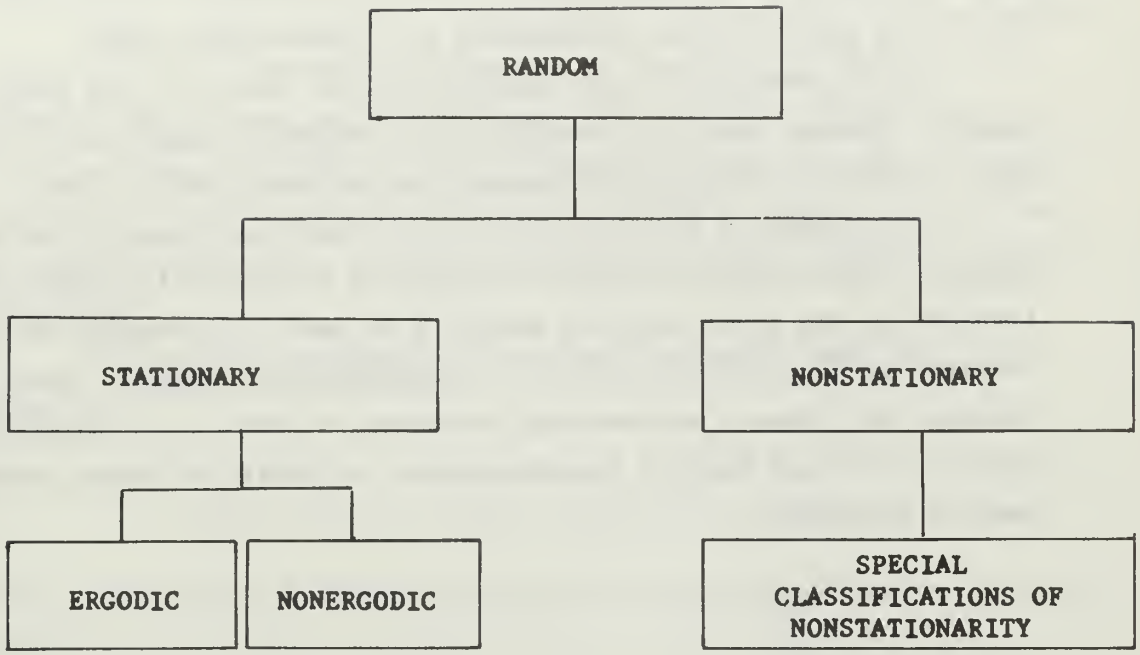

Figure 3. Classifications of random data (Reproduced from Ref. 2.)

of the amplitude of the random data with respect to time and frequency respectively. These functions are Fourier transform pairs, and therefore provide an analysis of the data in two different formats.

The autocorrelation function for random data provides an indication of the general dependence of the amplitude of the data at a particular time on the value of the data at a different time. An autocorrelation measurement can be used for detecting deterministic data which may be hidden or obscured in a random background.

As an extension of the autocorrelation function, the power spectral density function describes the frequency composition of the data in terms of the spectral density of its mean square value.

In Chapter IV an explicit and more detailed presentation is included which outlines both the analytical and digital computer steps involved in the power spectrum analysis as used to determine the pitch response of the F-100C airplane to atmospheric turbulence. This analysis will form a mathematical extension of the autocorrelation function, through Fourier transformation, to yield the power spectral density function.

The basic measurement used to determine atmospheric turbulence in flight is the angle of attack of the aircraft as measured by flow vanes. The flow angles measured are corrected for the effects of airplane motion, Chilton (3). In this particular analysis as applied to the power spectrum method, a continuous time history of the vertical component of the true gust velocity is to be initially determined. Although the lateral and longitudinal components of turbulence could have been measured as well, the vertical component has the most significant effect upon the aircraft's pitch dynamics, and in the interest of simplification only this vertical portion of the turbulence will be considered.

The vertical component of the gust velocity, from Ref. 1, is given by:

$$W_g = V\alpha_v - V\theta + \int a_z\,dt + \ell_x\dot{\theta} \tag{5}$$

The equation above is based upon the following assumptions as outlined in Ref. 1:

1. All disturbances are small enough to allow the use of the angle in radians in place of the sine of the angle.
2. Boom flexures are negligible.
3. The effects of variation in upwash on vane indications are negligible or allowed for by calibration.

In conducting the flight analysis, the average values of the measured parameters (denoted by a bar) are included to establish the flight measurements as increments from the mean values for the measured flight interval. Therefore, the time history of the vertical component of the gust velocity, from Ref. 1, is:

$$W_g = V(\alpha_v - \bar{\alpha}_v) - V(\theta - \bar{\theta}) + \int_0^t (a_z - \bar{a}_z)\,dt + \ell_x(\dot{\theta} - \bar{\dot{\theta}}) \tag{6}$$

A reading interval of 0.1 seconds was established as being an optimum value for this analysis after considering the aircraft speed at which the data were obtained (300 knots TAS) and the frequencies evaluated.

All turbulence data used for this analysis were obtained by the author during the month of June 1967 while participating in an industrial tour at the Flight Test Branch of NASA's Ames Research Center at Moffett Field, California. The flight test data used for this thesis are only a portion of the total data obtained by NASA as part of a larger program to study the optimum dynamic characteristics and response to turbulence of a variable stability F-100C airplane.

The aircraft used for this turbulence study and its principal dimensions are shown in Fig. 4, from Ref. 4. It is a North American F-100C which is assigned to the National Aeronautics and Space Administration and designated as NASA aircraft number 703. The F-100 is a single place, low wing aircraft, powered by a J-57 series turbojet engine with afterburner. The wing and horizontal stabilizer are swept back at an angle of 45 degrees. Low speed flight and stall characteristics are improved by the use of longitudinal leading edge slats on the standard F-100 airplane, and good longitudinal control is provided by an all-moving "slab" tail. The controls are completely power actuated. Longitudinal stick forces are provided by a simple spring bungee whose leverage on the stick is constant at all speed ranges except between a Mach number of 0.8 and 0.94 where the leverage is altered by a Mach number sensor. The F-100 airplane has a 400 cycle, 115 volt A.C. electrical system and a separate 28 volt D.C. system.

The parameters measured in flight are given by Equation (5), and the type and location of the flight instruments are shown in Table I. A continuous record of aircraft response was necessary in order to provide a complete and effective record of the turbulence encountered, therefore an oscillograph, instead of a photopanel, was required. All data were recorded on a 26 channel photographically recording oscillograph and developed on Ektachrome Aero film for analysis. As can be seen in Fig. 5, the accelerometers were positioned as close to the aircraft's center of gravity as possible. The flow vane used to measure angle of attack was located on the top of the vertical stabilizer as shown. A standard pitot static head was utilized for airspeed measurement. It is located ahead of the aircraft on the tip of the F-100's standard nose boom.

AIRPLANE DIMENSIONS

NOTE Airplane principal dimensions are taken with the landing gear struts and tires inflated to the correct pressures. Weights given are approximate and are not to be used for weight and balance computation or flight restriction.

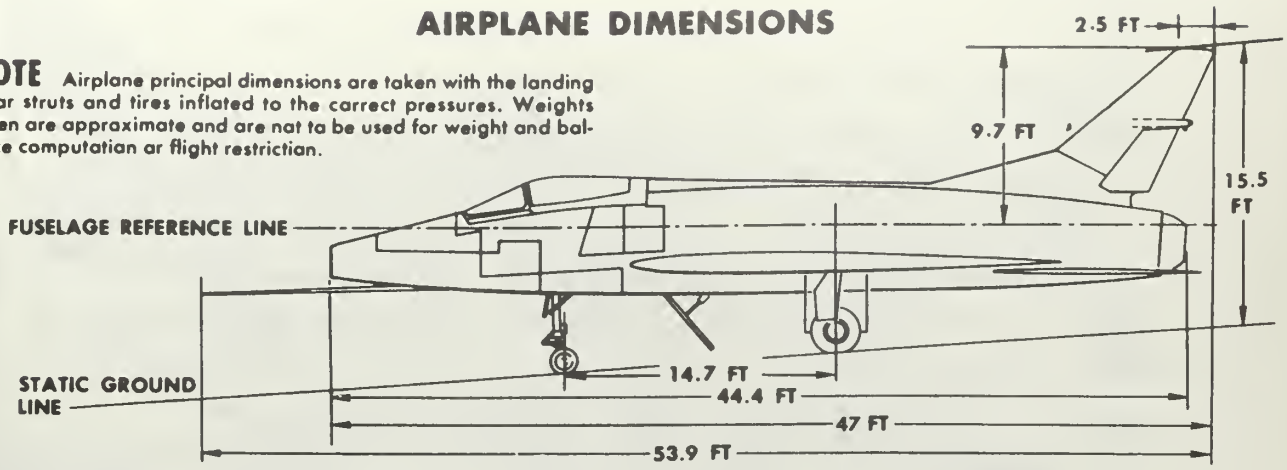

AREAS

WING (TOTAL)	385.2 SQ FT
AILERON (TOTAL AFT OF HINGE LINE)	38.6 SQ FT
WING SLATS	37.7 SQ FT
HORIZONTAL STABILIZER (TOTAL)	99.0 SQ FT
VERTICAL STABILIZER	45.2 SQ FT
RUDDER (AFT OF HINGE LINE)	6.3 SQ FT
SPEED BRAKE	12.0 SQ FT

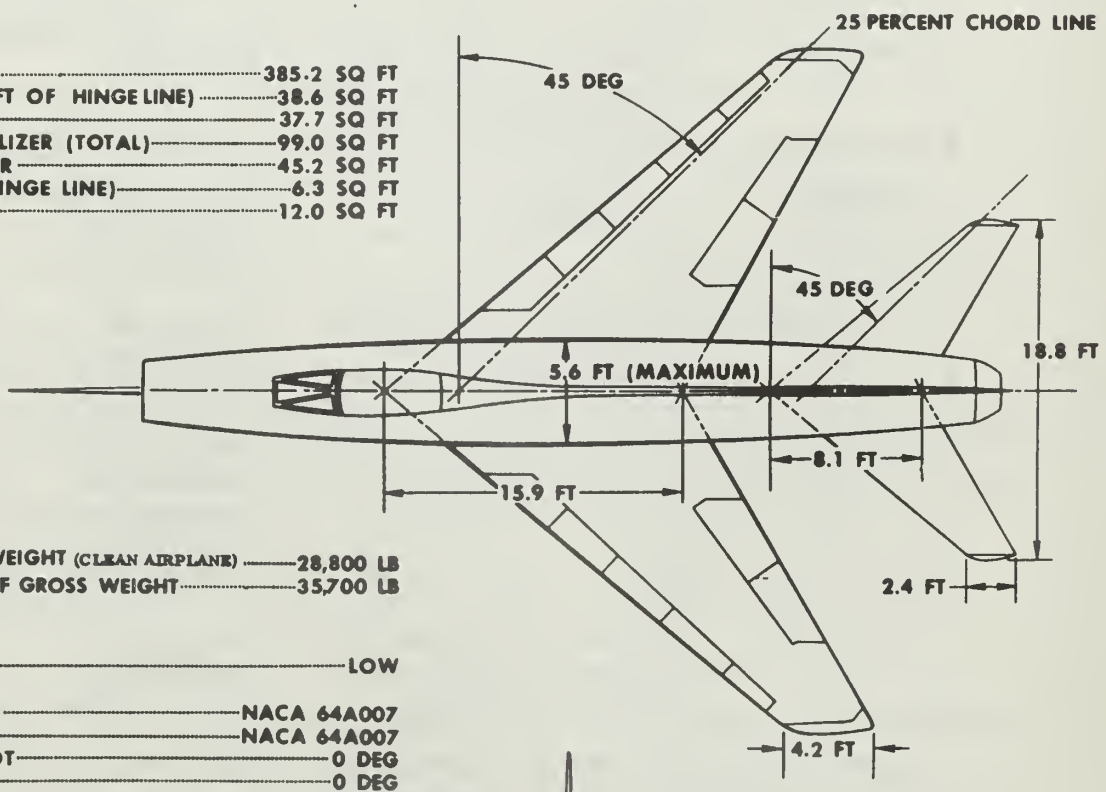

WEIGHT

TAKE-OFF GROSS WEIGHT (CLEAN AIRPLANE)	28,800 LB
MAXIMUM TAKE-OFF GROSS WEIGHT	35,700 LB

WING

TYPE	LOW
AIRFOIL SECTION	
ROOT	NACA 64A007
TIP	NACA 64A007
INCIDENCE AT ROOT	0 DEG
INCIDENCE AT TIP	0 DEG
ASPECT RATIO	3.86

DIHEDRAL

WING	0
STABILIZER	0

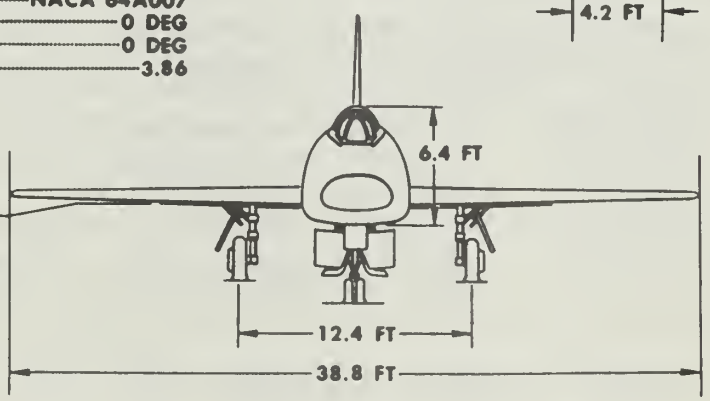

F-100C-2-00-18D

Figure 4. Airplane Dimensions

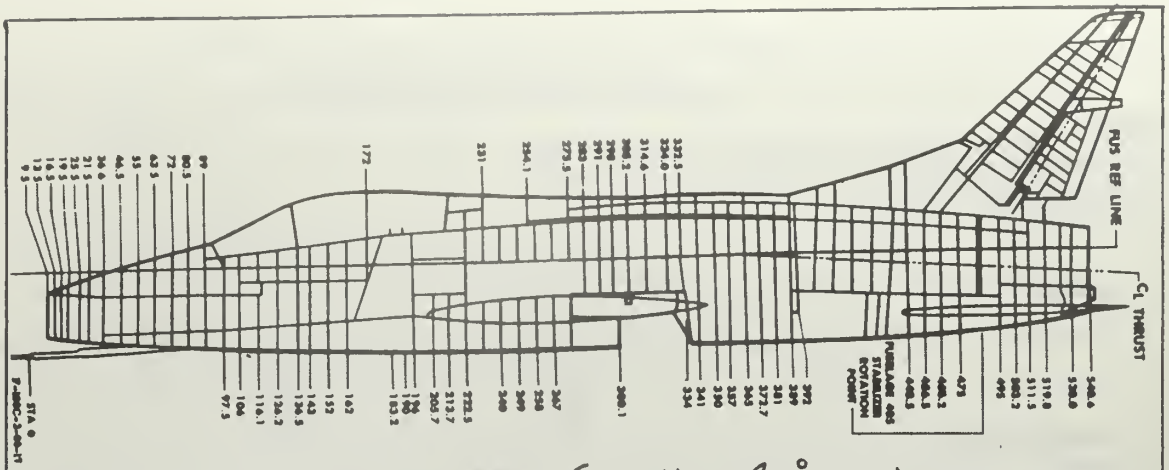

$$W_g = V\alpha_v - V\theta + \int a_z\,dt + l_x\dot{\theta} \quad (5)$$

PARAMETER MEASURED	TYPE OF INSTRUMENT	LOCATION OF INSTRUMENT	INSTRUMENT LIMITS
Airspeed V	Standard F-100 pitot-static instrument with Bourns pressure cell	Nose boom	0-500 kts
Angle of Attack α_v	400 cycle A.C. NASA instrument	Top of vertical stabilizer. Station 525	$\pm$ 10°
Pitch Angle θ	Minneapolis Honeywell attitude gyro with potentiometer pickoff	Left link compartment Station 152	$\pm$ 45°
Vertical Acceleration a_z	Statham linear strain gage accelerometer. Model CS-8-350	Wheel well on aircraft's longitudinal centerline Station 315	$\pm$ 4g's
Pitch Rate $\dot{\theta}$	Spring restrained rate gyro with a Microsyn signal generator	Left link compartment Station 143	$\pm$ 90°/sec
Longitudinal Stick Position	Potentiometer with 400 cycle A.C. output	Stick linkage on centerline	$\pm$ 19° stick deflection
Horizontal Stabilizer Position	Linear potentiometer pickoff using Markite infinite resolution pot.	Station 475	+ 25°, -5° stabilizer position
Altitude h	Statham pressure cell with strain gage pickoff	Nose compartment Station 55	0-50,000 ft

TABLE I: AIRCRAFT INSTRUMENTATION: NASA AIRCRAFT NUMBER 703

This particular F-100C had been modified by NASA for use as a variable stability airplane in order to study the effects of the interaction between the turbulence and the longitudinal stability characteristics. A planned variation in C_{m_α} and C_{m_q} was developed by NASA engineers, and these two parameters were changed to provide varying degrees of pitch response.

From basic theory, the values of C_{m_α} primarily determine the natural frequency of the short period mode and are a major factor in determining the response of the airframe to elevator motions and gusts.

The stability derivative, C_{m_q}, is usually referred to as the pitch damping derivative and is critical in longitudinal dynamics because it establishes a major portion of the damping of the short period mode. This damping effect comes mostly from the horizontal stabilizer. The appropriate C_{m_α} and C_{m_q} gain settings were obtained by means of an analog computer matching technique to produce the desired combinations of the short period frequency and damping ratio.

For this analysis, by varying C_{m_α} and C_{m_q}, a resultant value of M_α equal to -14.47 and M_q equal to .3068 was programmed into the aircraft to produce a short period frequency of .6 cycles per second and a damping ratio equal to 0.10.

The simplified schematics in Figs. 5 and 6 show how the variable stability mode of this NASA F-100C is obtained. Three modes of control may be manually selected by the pilot: a. Basic Mode, b. "Fly By Wire" Mode and c. Variable Stability Mode (includes "Fly By Wire" mode).

In the variable stability mode as shown in Fig. 5, a signal from both the angle of attack vane and the pitch rate gyro are received at the summing amplifier. The output from the summing amplifier is summed with the pilot's input and fed into a servo which controls the horizontal stabilizer's hydraulic actuating valve to provide the desired response characteristics.

A detailed schematic of the pilot's input as a closed loop system is shown in Fig. 6. A potentiometer is used to detect control stick inputs with a sensitivity such that the basic aircraft stick-to-stabilizer gearing is preserved. A torque tube between the stick and the hydraulic valve is normally mated firmly in the Basic Aircraft Mode.

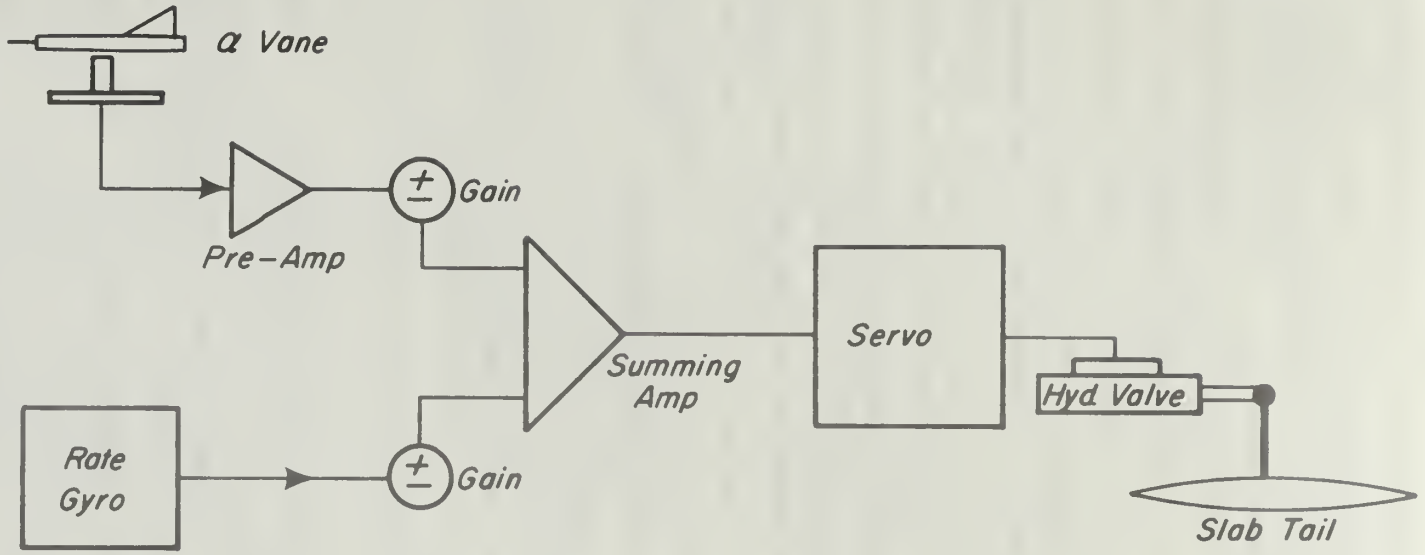

FIG. 5 SIMPLIFIED SCHEMATIC OF THE VARIABLE STABILITY MODE IN NASA F-100C AIRCRAFT NO. 703

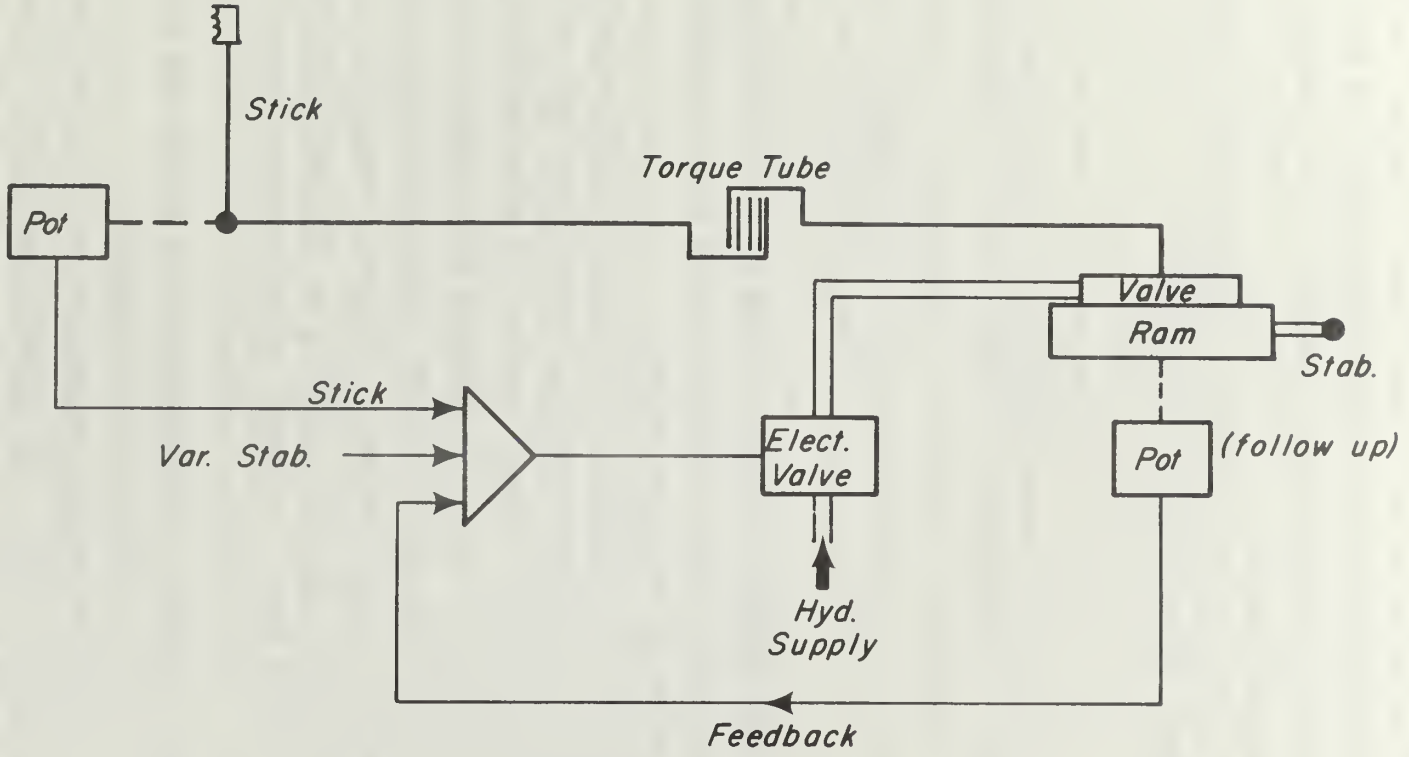

FIG. 6 SIMPLIFIED SCHEMATIC OF CLOSED LOOP CONTROL SYSTEM IN NASA F-100C AIRCRAFT NO. 703

In the "Fly By Wire" or Variable Stability Modes, the torque tube is mechanically adjusted by the system to have a greater increment of play. This adjustment prevents any feedback from the stabilizer to the stick; and allows additional commands to the stabilizer in the Variable Stability mode.

C_{m_α} and C_{m_q} are altered by the variable stability system in accordance with the following equations:

$$C_{m_\alpha\ eff} = C_{m_\alpha\ basic} + \underbrace{\boxed{\overset{SERVO}{\Delta C_{m_\alpha}}}}; \quad where\ \Delta C_{m_\alpha} = C_{m_{\delta H}}\left(\frac{\Delta H}{\Delta \alpha}\right) \tag{7}$$

$$C_{m_q\ eff} = C_{m_q\ basic} + \boxed{\overset{SERVO}{C_{m_{\delta H}}\left(\frac{2V}{\bar{c}}\right)\left(\frac{\Delta \delta H}{\Delta \dot{\theta}}\right)}} \tag{8}$$

In each example, the basic values of the F-100's stability derivatives are modified by the second term in the equation whose value is altered by the servo system.

Since the longitudinal response of the F-100 airplane to turbulence was of prime importance, all flight tests were conducted with no longitudinal control inputs, however the wings were kept level, while data were being taken, by applying minor lateral stick inputs. As a normal procedure, the turbulence was entered from a stabilized flight condition at an airspeed of 300 knots true, which is a realistic cruise airspeed for the F-100 airplane at the test altitudes selected (13,000 to 15,000 feet). Although no longitudinal control inputs were desired, both stabilizer position and control stick deflection were checked continually when analyzing the flight test data to insure the validity of the measured aircraft response.

Most of the turbulence encountered was of a mountain wave or clear air turbulence type. The leeward side of Mount Whitney and the neighboring peaks in the Sierra Nevada range were used as a flight test area.

BASIC COMPUTATION PROCEDURE

As in any statistical approach to analyzing data and predicting trends, the more information obtained, the more valid the study. This concept was tempered by the selection of that flight test data which were obtained with the F-100C programmed for the most realistic short period frequency. Accordingly, after screening the available test data, NASA Flight 26, Run 8 was selected as being a valid and optimum flight record for the power spectrum analysis. On this flight, the F-100C was programmed for a short period frequency of .6 cycles per second. It is reiterated that the intent of this thesis is to demonstrate the application of the power spectrum analysis to determine the dynamic response of an aircraft to turbulence rather than to establish any new information on the F-100C airplane.

The data for this flight were read every 0.1 seconds, and the basic parameters as outlined in Equation (5), were recorded on standard IBM eighty column digital computer cards. Due to the large quantities of data involved (six inflight parameters read at 920 intervals each) and the numerous computations required by the power spectral method, a digital computer is necessary to effectively process the data and perform the analysis efficiently. The average values of the measured flight parameters, denoted by a bar in Equation (6), were initially determined by means of a simple digital operation, and w_g itself was computed. The power spectral analysis of the measured flight data was performed by a digital program utilizing an IBM 7094/7040 direct coupled system computer for the calculations and graphing.

Both the autocorrelation function and the power spectral density of the input, w_g (referred to as series 2), and the output, $\dot{\theta}$ (referred to as series 1), were determined and graphed by the computer program. The desired transfer function, $\frac{\dot{\theta}}{w_g}$ was then computed in both phase and amplitude as a function of gust frequency. The transfer function was based upon a cross correlation and cross spectral density function which combined the average values of $\dot{\theta}$ and w_g over a common frequency interval. From the computer analysis, the phase and amplitude of $\frac{\dot{\theta}}{w_g}$ were graphed on a cross spectral density plot

versus frequency. To check the accuracy of the power spectrum method, the theoretical solution for the phase and amplitude of $\frac{\dot{\theta}}{w_g}$ was obtained by solving the longitudinal dynamic equations of motion and the pitching moment equation about the lateral axis. The phase and amplitude of the transfer function obtained theoretically were also plotted versus frequency, and the resulting curves from both methods were compared.

A detailed analysis of the steps involved in the digital computer program is presented in Appendix A; however, a proper appreciation of the digital computation can only be realized if the mathematical theory behind the power spectrum method is outlined in detail.

As discussed earlier, the vertical component of the atmospheric turbulence, w_g, was established as a stationary, ergodic form of random data. An additional stipulation is that the turbulence should represent a Gaussian process. For the turbulence to be Gaussian, the fluctuations of the turbulence must have a normal probability distribution. References 1 and 5 stipulate that if one component of the turbulence, w_g, for instance, has a normal distribution, then normality of the turbulence can be assumed. Figure 7, which is reproduced from Ref. 1, shows the cumulative frequency distribution of w_g as determined by NASA from a thunderstorm traverse. The plot is scaled in such a manner that a normal distribution of w_g will result in a straight line. The data were obtained from a 200 second record, read at 0.1 second intervals. A fitted normal distribution is shown in comparison to the data points plotted, and it may be noted that there is a good correspondence between the fitted normal distribution and the traverse data points, except at large values of w_g, therefore, from Ref. 1, the assumption that there is a Gaussian distribution of turbulence appears to be reasonable. It is reiterated that the properties of stationarity, homogeneity, and isotropy, in addition to the Gaussian assumptions, are implied. These properties specify, then, an invariance in the statistical characteristics of turbulence with respect to the position along the time history of the sampling interval and the direction through the turbulence.

From Ref. 6, Taylor's hypothesis that the variation in gust intensity existing along the flight path at any given instant will remain substantially the same until the aircraft has traversed the given body of air, is utilized. The relative length of the body of air along the flight path, therefore is large compared with the distance traversed in the reaction time of the aircraft.

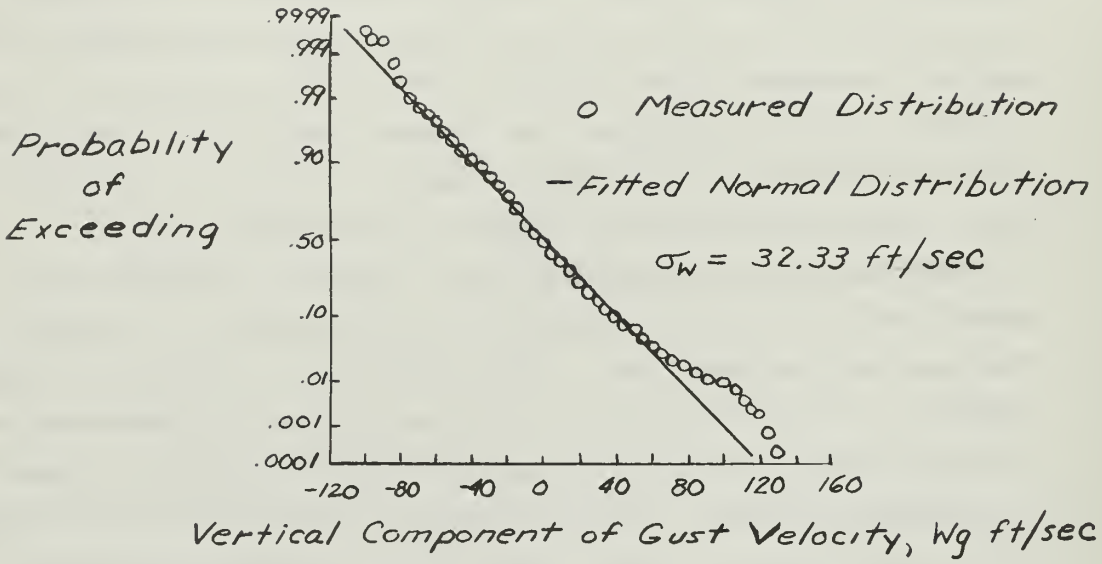

Figure 7. - Probability of equaling or exceeding given values of vertical gust velocity for thunderstorm (traverse 4). (Reproduced from Ref. 1)

With the mathematical assumptions established, a detailed analysis of the mathematical steps behind the power spectrum analysis can now be presented in conjunction with appropriate sequential reference to the computer program which is detailed in Appendix A.

A block diagram (Fig. 17) showing the steps involved in the computer analysis and the appropriate mathematical expression for each step is presented in Appendix A in order to provide a complete picture of the entire digital program involved in the power spectrum analysis.

The magnitude of $\dot{\theta}$ and w_g, as computed from Equation (6), is tabulated at 0.1 second intervals on the computer printout and referred to as series 1 and series 2 respectively. The values of the data are read from left to right in each row in chronological order. The autocorrelation function of $\dot{\theta}$ and the autocorrelation function of w_g are computed separately by taking the product of $\dot{\theta}$ or w_g at time t and at time $t + \tau$, and averaging these values over a total observation time, T. The resulting average product will approach an exact autocorrelation function (also referred to as the autocovariance function) as T approaches infinity.

In equation form the autocorrelation function is expressed as:

$$R_x(\tau) = \lim_{T \to \infty} \frac{1}{T} \int_0^T x(t) \cdot x(t+\tau)\, dt \qquad (9)$$

where $x(t)$ represents the value of either $\dot{\theta}$ or w_g at time t, and $x(t+\tau)$ is the value of $\dot{\theta}$ or w_g after a time shift whose magnitude is determined by the value of τ.

The autocorrelation functions of $\dot{\theta}$ and w_g are each computed for progressive values of τ, that vary in 0.1 second increments, from 0.1 seconds to 9.99 seconds. The autocorrelation function for $\dot{\theta}$ is tabulated on page 77 of Appendix A and plotted versus time on page 78 also. Similarly R_x for w_g is tabulated on page 82 and plotted versus time on page 83 in Appendix A.

The quantity $R_x(\tau)$, as defined above, is a real valued function with a maximum value at $\tau = 0$. Also $R_x(-\tau) = R_x(\tau)$, and $R_x(0) \geq |R_x(\tau)|$ for all τ. The mean value of x(t) can be determined from $\sqrt{R_x(\infty)}$, i.e., it is equal to the positive square root of the autocorrelation

function, as the time displacement increases toward infinity (Ref. 2). In addition, the mean square value is equal to the autocorrelation function at zero time displacement, ($\tau = 0$); i.e., $\psi_x^2 = R_x(0)$

As an example of the usefulness of the autocorrelation function, a simple autocorrelogram (plot of an autocorrelation function) is illustrated in Figure 8.

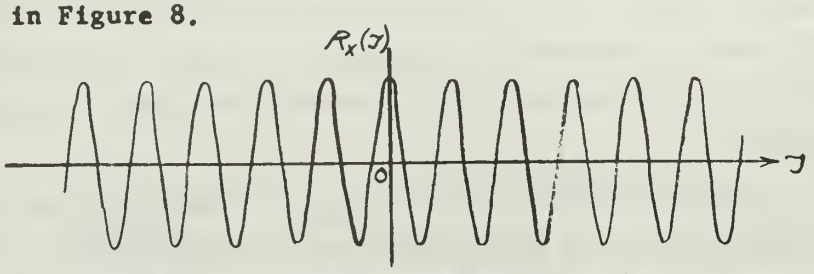

Figure 8. - Autocorrelogram for a Sine Wave.
(Reproduced from Ref. 2)

Although phase information is not available with this plot, it can be noted that the autocorrelation function for the sine wave will persist over all time displacements since it represents deterministic data. Conversely, an autocorrelogram for narrow band random noise, (non-deterministic data), will diminish to zero for large time displacements, assuming a mean value of zero. This is illustrated in Fig. 9

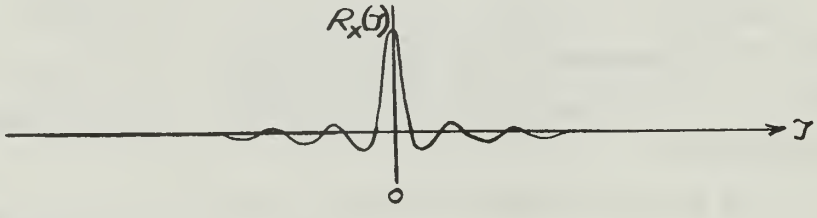

Figure 9. - Autocorrelogram for Random Noise
(Reproduced from Ref. 2)

A combined plot of the autocorrelation function of the sine wave superimposed with the autocorrelation function of the random noise will appear as in Figure 10.

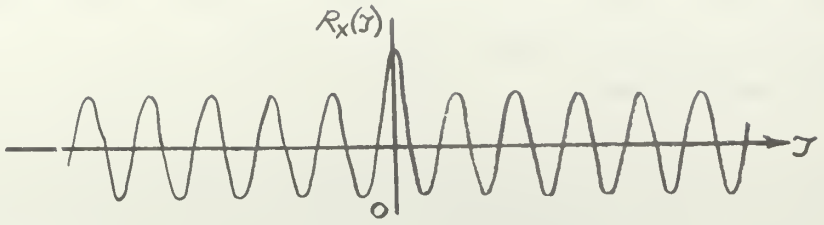

Figure 10. - Combined Autocorrelograms for a Sine Wave and Random Noise (Reproduced from Ref. 2)

The deterministic data (sine wave) can be detected from the random background of the wide band noise. This is the principle value of the autocorrelation function in that the random and non-random data may be separated into their respective categories through analysis of their combined autocorrelograms.

The autocorrelation function of $\dot{\theta}$, series 1, is noted to diminish with increasing values of time, due to the inherent longitudinal damping characteristics of the F-100 airplane. This is a typical response of a damped second order system to a random input. Refer to pages 77 and 78 of Appendix A.

It is also to be noted that the autocorrelation function of w_g, series 2, is also a maximum at $\tau = 0$ and decreases to a minimum value for increasing values of τ (pages 82 and 83, Appendix A). This is the expected characteristic of the autocorrelation function for random data.

After establishing each autocorrelation function, $R_{\dot{\theta}}$ and R_{w_g}, the power spectral estimates of both $\dot{\theta}$ and w_g are computed separately and tabulated on pages 79 and 84 of Appendix A. The power spectral estimate is simply a Fourier transform of the autocorrelation function and describes the general frequency composition of the data in terms of the spectral density of its mean square value, ψ_x^2 (Refs. 2 and 7). The time mean square value provides a measure of the disturbance energy per unit time and thus has been referred to as power in the study of turbulence and has been termed the energy or power spectrum. The power spectral density function specifies the contribution of the harmonic components to the mean square value of the random data over the specified frequency range.

The average squared value of the random data will approach an exact mean square value as the observation time, T, approaches infinity for a frequency range between f and Δ f (Ref. 2).

In equation form:

$$\Psi_x^2[f, f+\Delta f] = \lim_{T\to\infty} \frac{1}{T}\int_0^T x^2(t, f, \Delta f)\,dt \qquad (10)$$

where x(t,f, Δ f) is that portion of x(t) in the frequency range bounded by f and f + Δ f. In this analysis, of course, x(t) could represent either $\dot{\theta}$ or w_g. For small values of Δ f, the power spectral density may be computed to be:

$$G_x(f)\Delta f = \Psi_x^2(f, f+\Delta f) \qquad (11)$$

In precise form;

$$G_x(f)\Delta f = \lim_{\Delta f\to 0} \Psi_x^2 \frac{[f, f+\Delta f]}{\Delta f} = \lim_{\Delta f\to 0}\lim_{\Delta T\to\infty} \frac{1}{(\Delta f)T}\int_0^T x^2(t, f, \Delta f)\,dt \qquad (12)$$

where $G_x(f)$ represents the power spectral density function of either $\dot{\theta}$ or w_g. The power spectral density is always a real valued non-negative function.

As noted earlier, the power spectral density is a Fourier transform of the autocorrelation function and for stationary data may be expressed as:

$$G_x(f) = 2\int_{-\infty}^{\infty} R_x(\tau)e^{-j2\pi f\tau}\,d\tau = 4\int_0^{\infty} R_x(\tau)\cos 2\pi f\tau\,d\tau \qquad (13)$$

Thus, from Ref. 2, the mean value of x(t) is given by $\mu_x = \left[\int_{0^-}^{0^+} G_x(f)\,df\right]^{1/2}$, and the mean square value is given by $\Psi_x^2 = \int_0^{\infty} G_x(f)\,df$ The mean square value, therefore, is equal to the area under the plot of the power spectral density function versus frequency.

From Ref. 1, typical power spectra for the vertical component of turbulence in clear air, cumulus clouds and thunderstorms are plotted in Fig. 11. The power spectral density is in units of $(\text{ft/sec})^2$ per radian/ft, and it is plotted versus the reduced frequency in radians/ft, with an additional scale of wavelength in feet, also along the abcissa. Since the gust disturbances are essentially space

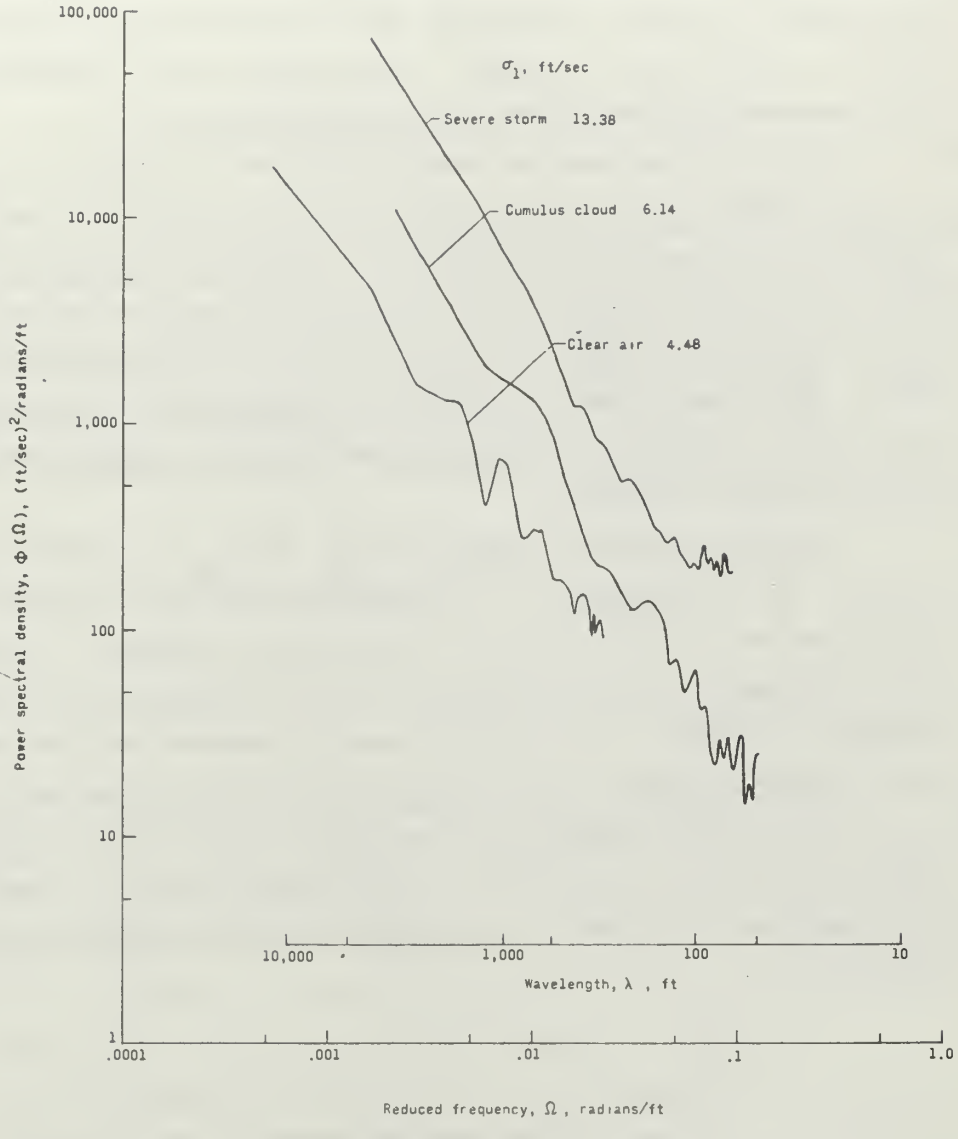

Figure 11. Typical power spectra of vertical component of turbulence measured in clear air, cumulus clouds and thunderstorm.

disturbances rather than disturbances in time, a reduced frequency, Ω, in radians/ft, is normally used in the power spectral analysis of turbulence. The relative heights of the curves in Fig. 11 indicate the variation of the intensity of the turbulence encountered under the different weather conditions. The similarity of the slopes of the power spectra is apparent, and their magnitude is equal to C/Ω^2, where C is a constant. The spectra show a characteristic rapid decrease in power with increasing frequency.

The root mean square value of the gust velocity is a measure of the intensity of the turbulence and is equal to the area under the portion of the spectrum evaluated. From Fig. 11, it may be noted that the root mean square value of the turbulence varies in magnitude from 4.48 ft/sec in clear air to a value of 13.38 ft/sec in a severe storm. The above example is presented to describe the type of information that is normally available from the power spectral density plot of a given parameter.

The power spectral density of $\dot{\theta}$ and w_g are plotted on pages 80 and 85 of Appendix A. As expected, the power spectral density of w_g (series 2) diminishes with increasing frequency. The power spectral density plot of $\dot{\theta}$ (series 1) also decreases with increasing frequency; however, a significant mode of response at the programmed short period frequency of .6 cycles per second is apparent.

The general dependence of one set of data (such as $\dot{\theta}$) upon another (w_g) may be described in more detail using the cross correlation function. From Ref. 2, two time histories of data are illustrated in Fig. 12.

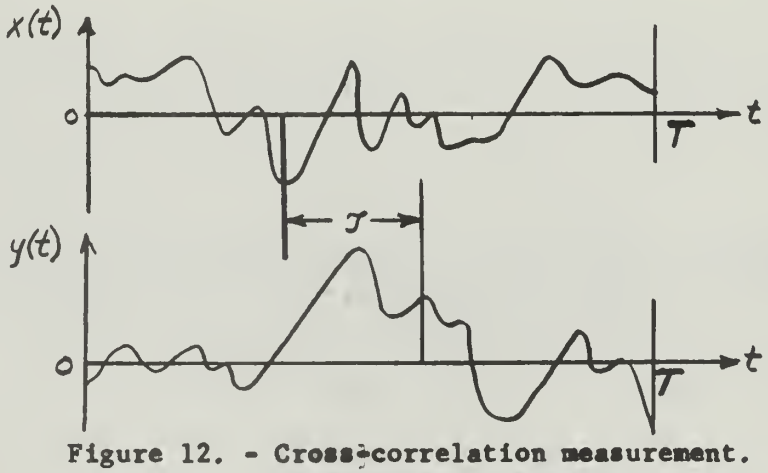

Figure 12. - Cross-correlation measurement.
(Reproduced from Ref. 2)

Like the autocorrelation function, the average product of x(t) at time t and y(t) at time $t + \tau$ is taken over the observation time t. For this analysis x(t) is comparable to $\dot{\theta}$, and y(t) is comparable to w_g or vice versa. As T becomes infinite, the resulting average product approaches an exact cross correlation function. As illustrated in Ref. 2:

$$R_{xy}(\tau) = \lim_{T \to \infty} \frac{1}{T} \int_0^T x(t) \cdot y(t+\tau) dt \qquad (14)$$

$R_{xy}(\tau)$ is always a real valued function which may be either positive or negative; however, unlike the autocorrelation for random data, $R_{xy}(\tau)$ may not necessarily have a maximum at $\tau = 0$ or be an even function only. $R_{xy}(\tau)$ displays symmetry about the ordinate when x and y are interchanged, so that $R_{xy}(\tau) = R_{xy}(-\tau)$.

The absolute value of the cross correlation function is bounded by:

$$|R_{xy}(\tau)|^2 \leq R_x(0) \cdot R_y(0)$$

$$|R_{xy}(\tau)| \leq \frac{1}{2} |R_x(0) + R_y(0)|$$

where R_x is comparable to the autocorrelation function of w_g, R_y is comparable to the autocorrelation function of $\dot{\theta}$, and R_{xy} is the cross correlation function based on $\dot{\theta}$ and w_g. The cross correlation function (labeled as cross covariance) for $\dot{\theta}$ and w_g is tabulated on page 86 of Appendix A, for both a positive τ and a negative τ, and plotted versus time on pages 87 and 88.

The Fourier transform of the cross correlation is taken to determine the cross spectral density function which is comparable to the power spectral density function for a single variable. Since the cross correlation is not an even function, the cross spectral density function is a complex number composed of the co-spectral density function (real part) and the quadrature spectral density function (imaginary part). Therefore:

$$G_{xy}(f) = C_{xy}(f) - j Q_{xy}(f) \qquad (15)$$

where C_{xy} is the co-spectral density function and Q_{xy} is the quadrature spectral density function.

The co-spectral density function is the average product of x(t) and y(t) within a narrow frequency interval between f and f + Δ f divided by the frequency interval.

The quadrature spectral density function is similar to the co-spectral density function, except that either x(t) or y(t) is shifted in time to produce a 90 degree phase shift at the frequency f.

The co-spectral density function is expressed as:

$$C_{XY}(f) = \lim_{\Delta f \to 0} \lim_{T \to \infty} \frac{1}{(\Delta f)T} \int_0^T X(t,f,\Delta f) \cdot y(t,f,\Delta f)\,dt \qquad (16)$$

and the quadrature spectral density function is:

$$Q_{XY}(f) = \lim_{\Delta f \to 0} \lim_{T \to \infty} \frac{1}{(\Delta f)T} \int_0^T X(t,f,\Delta f) \cdot y^{\circ}(t,f,\Delta f)\,dt \qquad (17)$$

where x(t,f, Δ f) and y(t,f, Δ f) are filtered portions of x(t) and y(t), and $\dot{y}^{\circ}$(t,f, Δ f) signifies a 90 degree phase shift from y(t,f,Δ f). The co-spectral density function and the quadrature spectral density function for $\dot{\theta}$ and w_g are tabulated on page 89 of Appendix A.

The cross spectral density function may also be expressed in complex polar form as:

$$G_{XY}(f) = |G_{XY}(f)|\, e^{-j\theta_{XY}(f)} \qquad (18)$$

The magnitude$|G_{xy}(f)|$ of the cross spectral density function is equal to:

$$|G_{XY}(f)| = \sqrt{C^2_{XY}(f) + Q^2_{XY}(f)} \qquad (19)$$

and the phase of the cross spectral density function $\theta_{xy}(f)$, is expressed as:

$$\theta_{XY}(f) = \tan^{-1}\left[\frac{Q_{XY}(f)}{C_{XY}(f)}\right] \qquad (20)$$

The magnitude and phase of the cross spectral density function are tabulated on page 89 of Appendix A and plotted on pages 90 and 91. Again a significant peak in the amplitude of the cross spectral density function is noted in the region of the programmed short period frequency of .6 cycles per second.

The amplitude of the transfer function, between the input, x(t), and the output, y(t), is obtained from the amplitude of the cross spectral density function, $G_{xy}(f)$, and the amplitude of the power spectral density of the input, $G_x(f)$. The amplitude of the transfer function, input x(t) to output y(t), is expressed as $H_{y/x}$ and is equal to:

$$H_{y/x} = \frac{G_{xy}(f)}{G_x} \tag{21}$$

In this analysis x(t) corresponds to w_g and y(t) is likewise $\dot{\theta}$; so that:

$$\left|\frac{\dot{\theta}}{w_g}\right| = \frac{G_{w_g \dot{\theta}}(f)}{G_{w_g}(f)} \tag{22}$$

The phase of the transfer function is the same as the phase of the cross spectral density function as outlined above.

The amplitude and phase of $\frac{\dot{\theta}}{w_g}$ versus frequency are tabulated on page 92 of Appendix A, where the phase of the transfer function is expressed as portions of a circle. The appropriate translation to angular magnitude; in degrees, is noted on the computer program beside the printed figures.

Two separate curves showing the phase and amplitude of $\frac{\dot{\theta}}{w_g}$ versus frequency were plotted from the results of the power spectral analysis and are included as Figs. 13 and 14. It is noted that the peak amplitude of $\frac{\dot{\theta}}{w_g}$, and also a phase shift of $\frac{\dot{\theta}}{w_g}$, occurs at the programmed short period frequency of .6 cycles per second. Although scatter of the data points is apparent at frequency values greater than the short period frequency, the amplitude peak of the transfer function and a distinctive phase shift may be readily determined from the plotted curves.

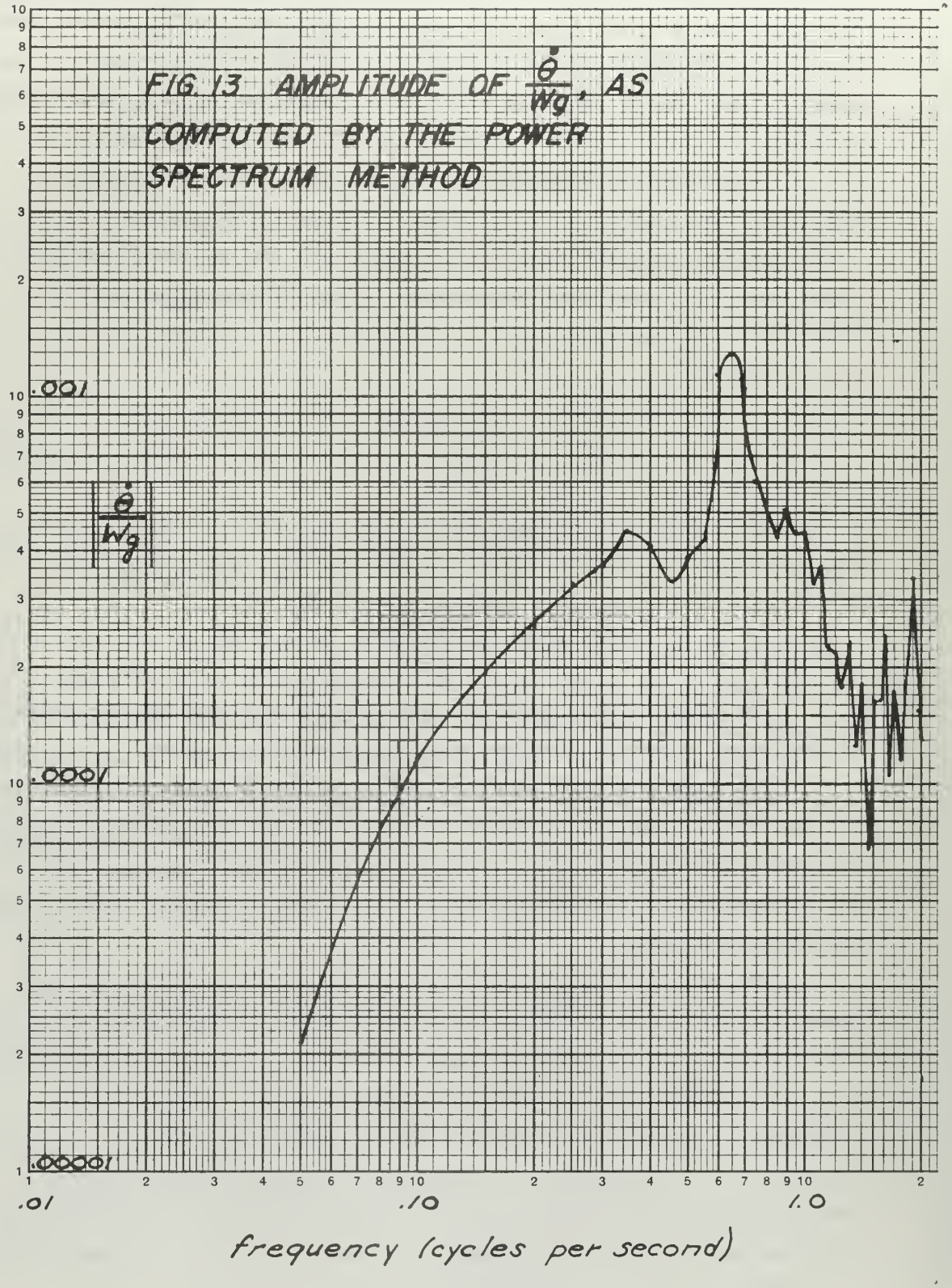
FIG. 13 AMPLITUDE OF $\frac{\dot{\theta}}{W_g}$, AS COMPUTED BY THE POWER SPECTRUM METHOD
$\left|\frac{\dot{\theta}}{W_g}\right|$
.001
.0001
.00001
.01
.10
1.0
frequency (cycles per second)

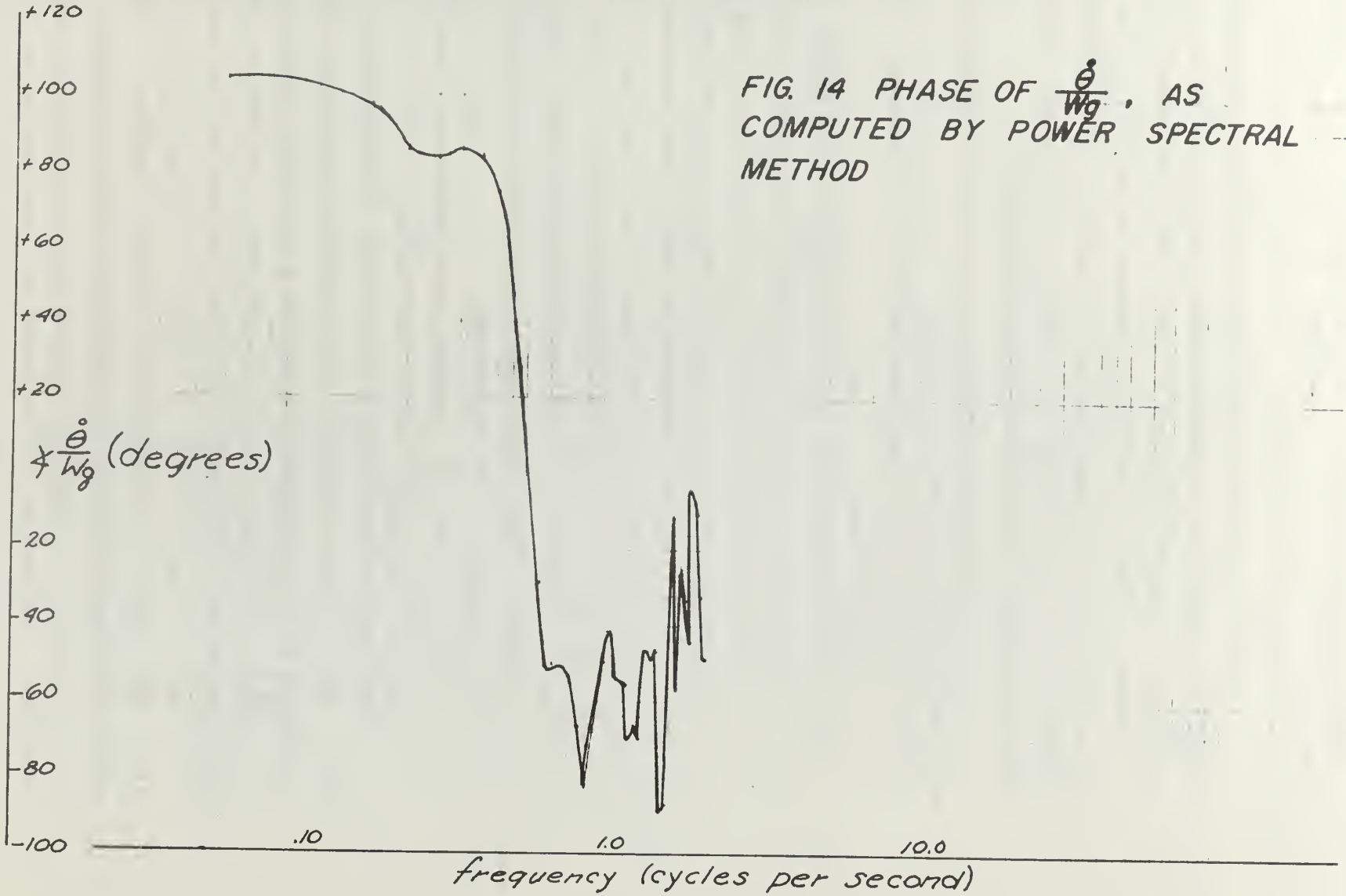

FIG. 14 PHASE OF $\frac{\dot{\theta}}{W_g}$, AS COMPUTED BY POWER SPECTRAL METHOD

THEORETICAL SOLUTION FOR THE PHASE AND AMPLITUDE OF THE TRANSFER FUNCTION

In order to determine the accuracy of the phase and amplitude of $\frac{\dot{\theta}}{w_g}$, as computed by the power spectrum method, the appropriate longitudinal equations of motion for the F-100C airplane were solved on a theoretical basis. Using the programmed values of C_{m_α} and C_{m_q}, as well as the standard stability derivatives for the F-100C; the phase and amplitude of $\frac{\dot{\theta}}{w_g}$ were computed over the same frequency range as that used for the power spectrum analysis.

The following basic assumptions were made in determining the equations of motion and solving for $\frac{\dot{\theta}}{w_g}$:

1. The equations of motion were written with respect to the stability axes.
2. The aircraft's elevator was considered to be locked, so that there were only three degrees of freedom. The equations were written therefore for linear motion along the X and Z axes and for pitching moments about the Y axis.
3. The aircraft was considered to have a linear response to the turbulence encountered.
4. No lateral/longitudinal coupling occurred.
5. The airspeed was stabilized at the beginning of the run and the engine thrust was constant throughout the run.
6. Quasi-steady flow was assumed.
7. Only the vertical component of turbulence, w_g, contributed to the aircraft's normal acceleration.

The phase and amplitude of the transfer function between w_g and $\dot{\theta}$ were initially obtained using a simplified solution in which the phugoid motion was considered to have a negligible effect upon the short period oscillations due to the turbulence. See Ref. 9. This simplified method is designated as method A in this section. To check the theoretical results, a second solution involving all of the essential terms included in the stability equations is included. This exact method is designated as method B. Both data sheets for methods A and B are included in this analysis together with the appropriate values of the stability derivatives and the important terms used in each solution. The results of both theoretical solutions were in close agreement.

The phase and amplitude of $\frac{\dot{\theta}}{Wg}$ obtained by methods A and B are plotted in Figs. 15 and 16. It can be noted that the peak amplitude and the phase shift of $\frac{\dot{\theta}}{Wg}$ occurred at the programmed short period frequency of .6 cycles per second.

From Section 13 of Ref. 9, the longitudinal equations of motion are developed with respect to the stability axes:

$$\text{X axis: } \dot{u} + ge\cos\theta_o = T_u(\cos\xi)u + T_{\delta_{RPM}}\delta_{RPM}\cos\xi + X_u u + X_q q + X_w w + X_{\dot{w}}\dot{w} + X_{\delta E}\delta E + X_{\delta F}\delta F + X_{\delta B}\delta B \quad (23)$$

$$\text{Z axis: } \dot{w} - u_o q + ge\sin\theta_o = -T_u(\sin\xi)u - T_{\delta_{RPM}}\delta_{RPM}\sin\xi + Z_u u + Z_q q + Z_w w + Z_{\dot{w}}\dot{w} + Z_{\delta E}\delta E + Z_{\delta F}\delta F + Z_{\delta B}\delta E \quad (24)$$

$$\text{Pitching Moment: } \ddot{\theta} = \frac{Z_{ym}}{I_{YY}}T_u u + \frac{Z_{ym}}{I_{YY}}T_{\delta_{RPM}}\delta_{RPM} + M_u u + M_q q + M_w w + M_{\dot{w}}\dot{w} + M_{\delta E}\delta E + M_{\delta F}\delta F + M_{\delta B}\delta E \quad (25)$$

These equations may be further simplified since the angle θ_o is assumed to be small so that $\sin\theta_o = 0$ and $\cos\theta_o = 1$. In addition, since there is no elevator deflection, flap deflection, or speed brake deflection during the run, δ_E, δ_F and δ_B all equal zero. Also under the initial conditions, the thrust is assumed to be constant; therefore, T_u is equal to zero, and the variation of the thrust with RPM, $T_{\delta RPM}$, is also zero. X_q, the variation of the force along the X axis, and Z_q, the variation of the force along the Z axis, due to the angular pitching velocity, are negligible. In addition X_w and Z_w, the variation in the forces along the X and Z axes due to the time rate of change of the vertical velocity, are negligible. For this analysis, the vertical velocity is considered to be composed of two components, w and w_g, where w is the steady state component of the vertical velocity and w_g is the fluctuation of the vertical velocity due to turbulence.

Eliminating the terms as noted above, separating the vertical velocity into the steady state and turbulent components, and introducing La-Placian notation, the equations of motion become:

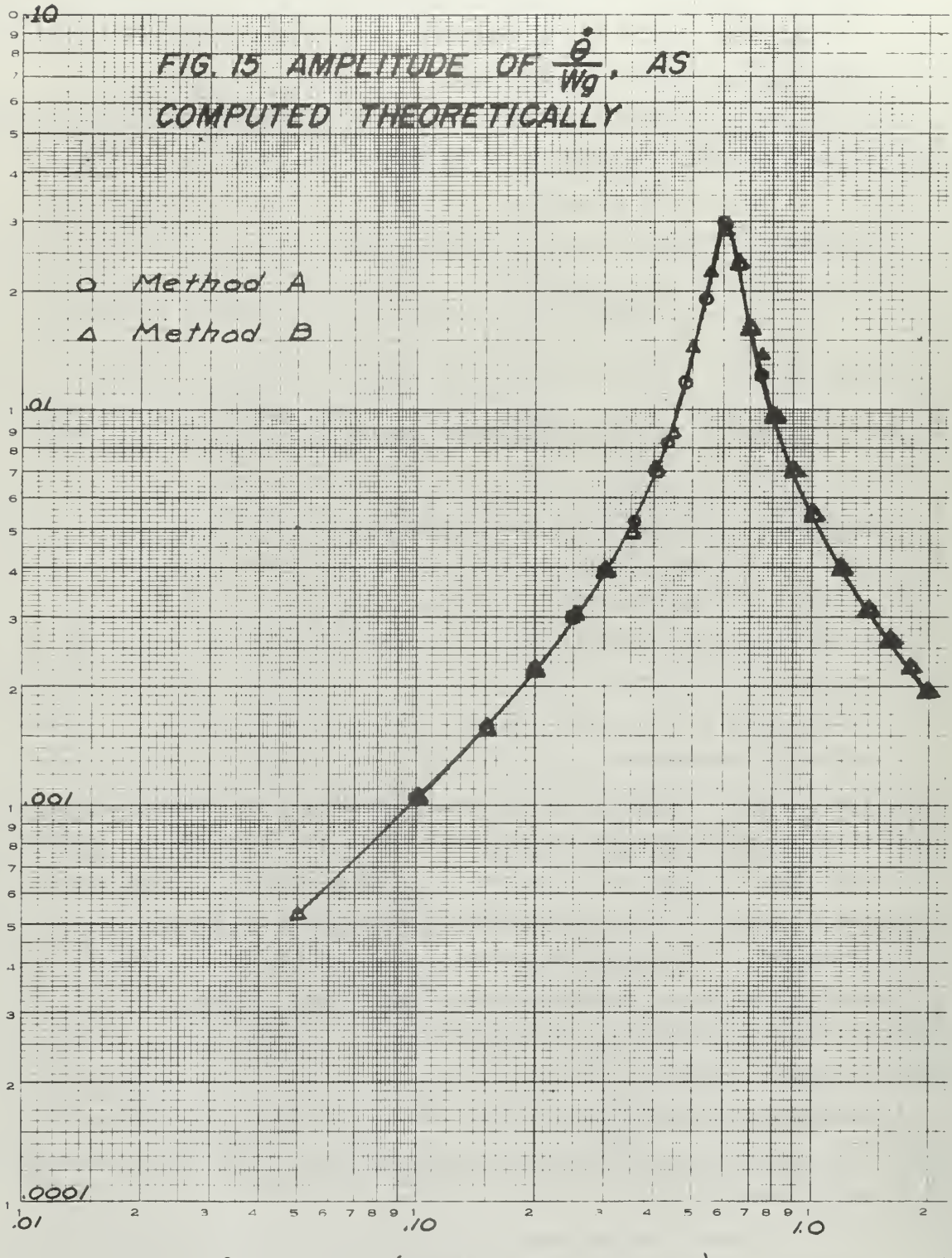
FIG. 15 AMPLITUDE OF $\frac{\dot{\theta}}{Wg}$, AS COMPUTED THEORETICALLY
○ Method A
△ Method B
.10
.01
.001
.0001
.01
.10
1.0
frequency (cycles per second)

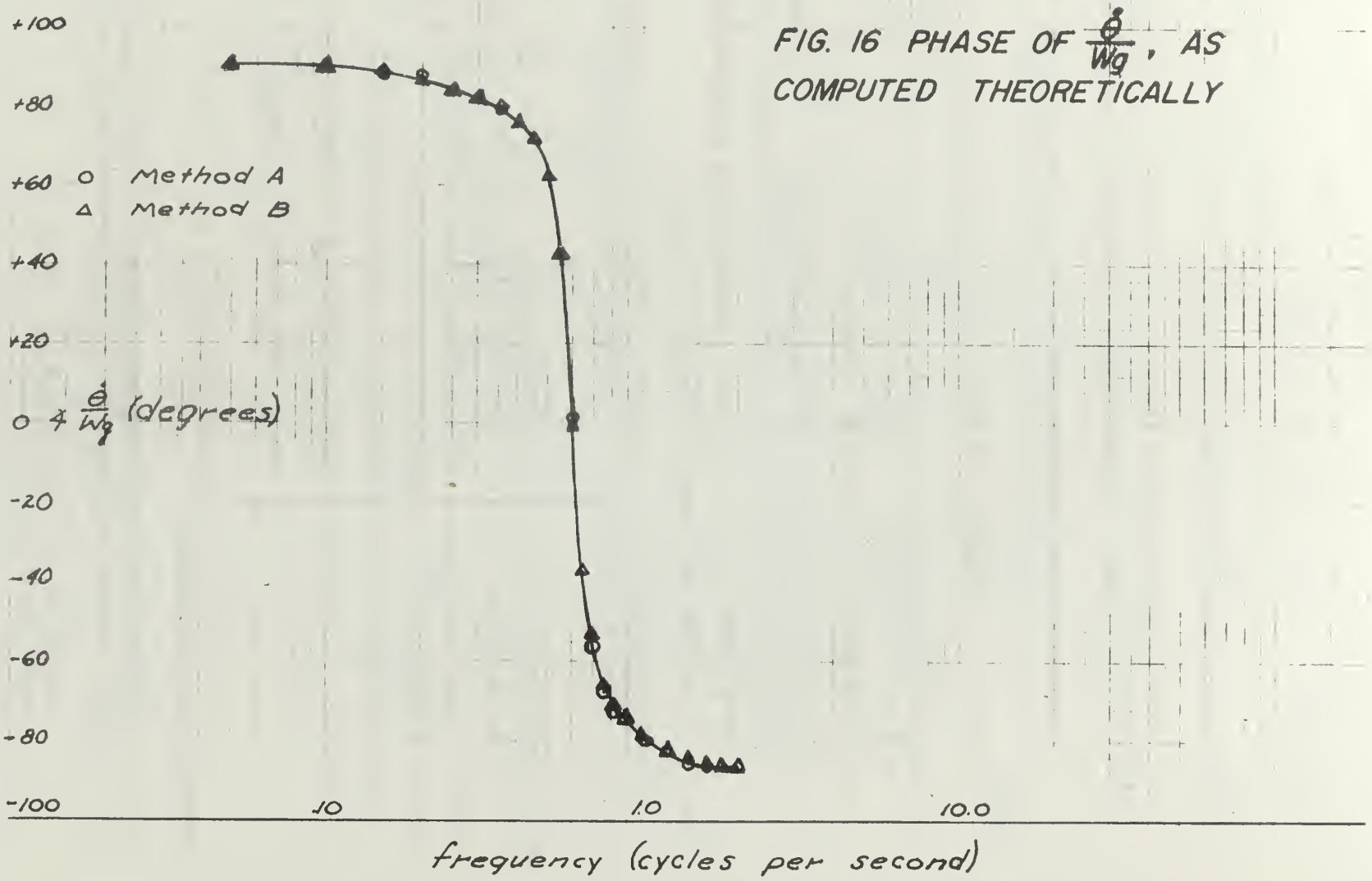

FIG. 16 PHASE OF $\frac{\phi}{wg}$, AS COMPUTED THEORETICALLY

$$su + g\theta = X_u u + X_w w + X_w w_g \tag{26}$$

$$\dot{w} - u_o s\theta = Z_u u + Z_w w + Z_w w_g \tag{27}$$

$$s^2\theta = M_u u + M_q s\theta + M_w w_g + M_w w + M_{\dot{w}} sw \tag{28}$$

Re-arranging the equations and solving for the w_g terms:

$$(s - X_u)u \quad -X_w w \quad + g\theta \quad = X_w w_g \tag{26}$$

$$-Z_u u \quad (s - Z_w)w \quad -su_o\theta \quad = Z_w w_g \tag{27}$$

$$-M_u u \quad -(M_{\dot{w}} s + M_w)w + s(s - M_q)\theta = M_w w_g \tag{28}$$

Using Cramer's rule, the above determinant is modified to solve for so that the transfer function is equal to:

$$\frac{\theta}{w_g} = \frac{\begin{vmatrix} (s-X_u) & -X_w & X_w \\ -Z_u & (s-Z_w) & Z_w \\ -M_u & -(M_{\dot{w}}s + M_w) & M_w \end{vmatrix}}{\begin{vmatrix} (s-X_u) & -X_w & g \\ -Z_u & (s-Z_w) & -su_o \\ -M_u & -(M_{\dot{w}}s + M_w) & s(s-M_q) \end{vmatrix}} \tag{29a}$$

Expanding the determinant:

$$\frac{\theta}{w_g} = \frac{X_w[Z_u(M_{\dot{w}}s + M_w) + M_u(s - Z_w)] - Z_w[-(s-X_u)(M_{\dot{w}}s + M_w)}{\Delta}$$

$$\frac{-M_u Z_w] + M_w[(s-X_u)(s-Z_w) - Z_u X_w]}{\Delta} \tag{29b}$$

where Δ denotes the original determinant in the denominator of Equation (29a). Equation (29b) can be further simplified to:

$$\frac{\theta}{w_g} = \frac{(Z_w M_{\dot{w}} + M_w)s^2 + [X_w Z_u M_{\dot{w}} + X_w M_u + Z_w(M_w - X_u M_{\dot{w}}) - M_w(X_u + Z_w)]s}{\Delta} \qquad (29c)$$

Multiplying the numerator of the ratio of the determinants by s, an expression for $\frac{\dot{\theta}}{w_g}$ is obtained, so that:

$$\frac{\dot{\theta}}{w_g} = \frac{(Z_w M_{\dot{w}} + M_w)s^3 + [X_w Z_u M_{\dot{w}} + X_w M_u + Z_w(M_w - X_u M_{\dot{w}}) - M_w(X_u + Z_w)]s^2}{\Delta} \qquad (30a)$$

Method A: The Simplified Solution of the Longitudinal Equations of Motion

For the simplified solution, the original determinant of the denominator is considered to be equivalent to the product of the quadratic expressions for the short period and phugoid motions, in Laplacian form, so that:

$$\frac{\dot{\theta}}{w_g} = \frac{(Z_w M_{\dot{w}} + M_w)s^3 + [X_w Z_u M_{\dot{w}} + X_w M_u + Z_w(M_w - X_u M_{\dot{w}}) - M_w(X_u + Z_w)]s^2}{(s^2 + 2\zeta_{ph}\omega_{ph}s + \omega^2_{ph})(s^2 + 2\zeta_{sp}\omega_{sp}s + \omega^2_{sp})} \qquad (31)$$

where ζ_{ph} and ζ_{sp} are the damping ratios of the phugoid and short period motions respectively. And ω_{ph} and ω_{sp} are equal to 2π times the phugoid and short period motion frequencies. The contribution of ω_{ph} is considered to be of negligible significance in the aircraft's dynamic response to turbulence so that the terms containing ω_{ph} can be eliminated. Therefore, the denominator can be approximated by:

$$(s^2)(s^2 + 2\zeta_{sp}\omega_{sp}s + \omega^2_{sp})$$

Canceling s^2 in both numerator and denominator and replacing the operator with jw, the simplified expression for $\frac{\dot{\theta}}{w_g}$ becomes:

$$\frac{\dot{\theta}}{w_g} = \frac{(Z_w M_{\dot{w}} + M_w)j\omega + X_w Z_u M_{\dot{w}} + X_w M_u + Z_w(M_w - X_u M_{\dot{w}}) - M_w(X_u + Z_w)}{(\omega^2_{sp} - \omega^2) + j2\zeta_{sp}\omega_{sp}\omega} \qquad (32)$$

The linear velocity along the X axis is considered to be constant so that the perturbations Z_u, M_u and X_u, may be neglected. Equation (31) therefore reduces to:

$$\frac{\dot{\theta}}{wg} = \frac{(Z_w M_w - M_w Z_w) + j\omega(Z_w M_{\dot{w}} + M_w)}{(\omega_{sp}^2 - \omega^2) + j2\zeta_{sp}\omega_{sp}\omega} \tag{33}$$

The amplitude of the transfer function (method A) is:

$$\left|\frac{\dot{\theta}}{wg}\right| = \frac{\omega(Z_w M_{\dot{w}} + M_w)}{\sqrt{(\omega_{sp}^2 - \omega^2)^2 + 4\zeta_{sp}^2\omega_{sp}^2\omega^2}} \tag{34}$$

and the phase of the transfer function is:

$$\angle\frac{\dot{\theta}}{wg} = 90^\circ - \tan^{-1}\frac{2\zeta_{sp}\omega_{sp}\omega}{(\omega_{sp}^2 - \omega^2)} \tag{35}$$

The expressions for the stability derivatives are given by Ref. 9 as:

$$Z_w = \frac{-\rho S V}{2m}(C_{L_\alpha} + C_D) \tag{36}$$

$$M_{\dot{w}} = \frac{\rho S c^2}{4I_Y}(C_{m_{\dot{\alpha}}}) \tag{37}$$

$$M_w = \frac{\rho S c V}{2I_Y}(C_{m_\alpha}) \tag{38}$$

Also from Ref. 10:

$$\omega_{sp}^2 = -L_\alpha M_q - M_\alpha \tag{39a}$$

$$2\zeta_{sp}\omega_{sp} = L_\alpha - M_q - M_{\dot{\alpha}} \tag{40a}$$

where:

$$L_{\alpha\,eff} = \frac{qS}{mV} C_{L_{\alpha\,eff}} \quad (41) \quad \text{and} \quad C_{L_{\alpha\,eff}} = C_{L_{\alpha_o}} + C_{L_{\delta H}}\left(\frac{\delta H}{\alpha}\right) \quad (42)$$

and therefore:

$$M_q = [L_{\alpha_{eff}} - M_{\dot{\alpha}}] - [2\zeta_{sp}\omega_{sp}] \tag{40b}$$

$$M_\alpha = -[L_{\alpha_{eff}}]M_q - [\omega_{sp}^2] \tag{39b}$$

The computed values of the stability derivatives noted above, as well as the quantities used to compute them, are listed in Table II. Using the values of the stability derivatives as computed in Table II, the phase and amplitude of $\frac{\dot{\theta}}{w_g}$ are computed for a range of frequencies from .05 cycles per second to 2.00 cycles per second. The values of the phase and amplitude of $\frac{\dot{\theta}}{w_g}$, as computed by the simplified solution (method A), are listed in Table III. The phase and amplitude of $\frac{\dot{\theta}}{w_g}$, as computed by the simplified solution, are plotted versus frequency in Figs. 15 and 16 .

Method B: The Exact Solution of the Longitudinal Equations of Motion.

The initial computational steps of the simplified solution, method A, as well as the same given stability equations and initial assumptions are implied for the exact solution as well; however, for the exact solution the entire determinant for w_g will be retained in the denominator of the $\frac{\dot{\theta}}{w_g}$ term throughout the analysis. Starting with Equation (30a), $\frac{\dot{\theta}}{w_g}$ is equal to:

$$\frac{\dot{\theta}}{w_g} = \frac{(Z_w M_{\dot{w}} + M_w)(-j\omega^3) + [X_w Z_u M_{\dot{w}} + X_w M_u + Z_w(M_w - X_u M_{\dot{w}}) - M_w(X_u + Z_w)]\omega^2}{\Delta} \tag{30b}$$

where Δ is equal to the expansion of the determinant formed by the longitudinal stability equations, solved for w_g.

$$\Delta = (S - X_u)[S(S - Z_w)(S - M_q) - SU_o(M_{\dot{w}}S + M_w)]$$

$$+ Z_u[-SX_w(S - M_q) + g(M_{\dot{w}}S + M_w)] - M_u[SU_oX_w - g(S - Z_w)] \tag{43a}$$

FLT. 26 RUN 8	FUEL (lbs)	WEIGHT (lbs)	V (ft/sec)	INITIAL ALTITUDE (ft)	ρ $\frac{lb\ sec^2}{ft^4}$	S (ft^2)	c (ft)	I_Y (slug-ft^2)	m (slugs)	α_o (rad)
-	3900	25,300	634	13,000	.00159	385.2	11.17	69,130	786.5	.078

$\frac{\Delta\delta_H}{\Delta\alpha_V}$	$\frac{\Delta\delta_H}{\Delta\alpha_T}$	C_L	C_{L_α}	C_D	C_{D_α}	C_{m_α}	$C_{m_{\dot\alpha}}$	$C_{L_{\delta_H}}$	$C_{L_{\alpha_o}}$	$C_{L_{\alpha_{eff}}}$
.695	.438	.2084	3.71	.0201	.192	-.738	-.908	0.483	3.50	3.71

$L_{\alpha_{eff}}$	Z_{sp}	ω_{sp} $\left(\frac{cycles}{sec}\right)$	$M_{\dot\alpha}$	M_α	M_q	Z_w	Z_u	M_w	$M_{\dot w}$	M_u
.9038	.10	.6	-.1570	-4.490	.3068	-.9087	-.1015	-.02285	-.000248	.00178

X_w	X_u
.0040	-.0098

TABLE II: FLIGHT DATA AND COMPUTED STABILITY DERIVATIVES

TABLE III: METHOD A. SIMPLIFIED SOLUTION FOR THE PHASE AND AMPLITUDE OF $\frac{\dot{\theta}}{Wg}$

f cps	ω	ω_{sp}^2	ζ_{sp}	$A\zeta_{sp}^2\omega_{sp}^2$	ω^2	$\omega_{sp}^2-\omega^2$	$(\omega_{sp}^2-\omega^2)^2$	$A\zeta_{sp}^2\omega_{sp}^2\omega^2$	$(\omega_{sp}^2-\omega^2)^2+A\zeta_{sp}^2\omega_{sp}^2\omega^2$	Z_w	$M_{\dot{w}}$	M_w
0	0	14.213	.10	.5684	0	14.213	202.009	0	202.009	-.9087	-.000248	-.02285
.05	.31415				.0987	14.114	199.205	.056	199.261			
.10	.62830				.3948	13.818	190.937	.22404	191.161			
.15	.94245				.8882	13.325	177.556	.50485	178.061			
.20	1.2556				1.5790	12.364	159.618	.897503	160.515			
.25	1.57075				2.4673	11.746	137.969	1.4024	139.371			
.30	1.88490				3.5528	10.660	113.636	2.0194	115.655			
.35	2.19905				4.8358	9.377	87.928	2.7486	90.677			
.40	2.51320				6.3162	7.897	62.363	3.5901	65.953			
.45	2.82735				7.9939	6.219	38.676	4.5437	43.219			
.50	3.14150				9.8690	4.344	18.870	5.6095	24.479			
.55	3.45565				11.9415	2.272	5.162	6.7875	11.949			
.60	3.76980				14.2114	0.002	0.000	8.07776	8.078			
.65	4.08395				16.6786	-2.466	6.081	9.48012	15.561			
.70	4.39810				19.3433	-5.130	26.317	10.99473	37.312			
.75	4.71225				22.2053	-7.992	63.872	12.6215	76.594			
.80	5.02460				25.2647	-11.052	122.147	14.3604	136.507			
.90	5.65470				31.9756	-17.763	315.524	18.1749	333.699			
1.00	6.28300				39.4761	-25.263	638.219	22.4382	660.657			
1.20	7.53960				56.8456	-42.623	1817.523	32.3110	1849.884			
1.40	8.79620				77.3731	-63.160	3989.186	43.9788	4033.165			
1.60	10.05280				101.0588	-86.846	7542.228	57.4418	7599.669			
1.80	11.30940				127.9025	-113.690	12925.416	72.6998	12998.116			
2.00	12.56600				157.9044	-143.691	20647.10	89.7529	20736.856			

TABLE III: (Continued)

f c.p.s.	$Z_w M_{\dot{w}}$	$Z_w M_{\dot{w}} + M_w$	$\omega(Z_w M_{\dot{w}} + M_w)$	$2\zeta_{sp}\omega_{sp}\omega$	$\sqrt{\text{col.11}}$	$\left\|\frac{\dot{\theta}}{\omega_g}\right\|$				$\frac{2\zeta_{sp}\omega_{sp}\omega}{(\omega_{sp}^2 - \omega^2)}$	TAN^{-1} COL.24 (degrees)	90° − COL.25
0	+.000225	−.022625	0	0	14.2129	0				0	0	90°
.05			−.007107	.23664	14.1159	.0005035				.01677	0.96	89.04
.10			−.014125	.473328	13.826	.0010282				.03425	1.96	88.04
.15			−.021322	.710527	13.3439	.0015978				.05332	3.06	86.94
.20			−.028430	.947336	12.6694	.002244				.06707	3.84	86.16
.25			−.035538	1.18423	11.8055	.00301				.10082	5.76	84.24
.30			−.042645	1.42105	10.7543	.00397				.13331	7.59	82.41
.35			−.049753	1.65789	9.5224	.00522				.17680	10.03	79.97
.40			−.056861	1.8947	8.1211	.00700				.23993	13.49	76.51
.45			−.063968	2.1315	6.5741	.00973				.34274	18.92	71.08
.50			−.07108	2.3684	4.9476	.01436				.54521	28.60	61.40
.55			−.078118	2.6053	3.4567	.02259				1.14670	48.92	41.08
.60			−.08529	2.8421	2.8422	.03000				−21.050	89.96	0.04
.65			−.092399	3.0789	3.9447	.02342				−1.24854	51.35	−38.65
.70			−.099507	3.1358	6.1084	.01629				−.64635	32.88	−57.15
.75			−.106614	3.5527	8.7518	.01281				−.44453	23.97	−66.03
.80			−.113722	3.7895	11.6836	.009733				−.34288	18.93	−71.07
.90			−.129737	4.2632	18.2675	.00700				−.2400	13.40	−76.60
1.00			−.142152	4.7368	25.7032	.00553				−.18750	10.62	−79.38
1.20			−.170583	5.6843	43.0102	.00396				−.13333	7.69	−82.31
1.40			−.199014	6.6315	63.5072	.00313				−.1049	5.99	−84.01
1.60			−.22749	7.5790	87.1761	.00261				−.08727	4.99	−85.01
1.80			−.255875	8.5264	114.0092	.00224				−.07500	4.29	−85.71
2.00	↓	↓	−.284305	9.4738	144.003	.001974				−.06593	3.76	−86.24

$$\Delta = s(s-X_u)(s-Z_w)(s-M_q) - sU_o(s-X_u)(M_{\dot{w}}s + M_w) + gZ_u(M_{\dot{w}}s+M_w)$$

$$- sX_wZ_u(s-M_q) + gM_u(s-Z_w) - sU_oX_wM_u \qquad (43b)$$

$$\Delta = s^4 - (X_u+Z_w+M_q+U_oM_{\dot{w}})s^3 + [M_q(X_u+Z_w) + X_uZ_w - X_wZ_u$$

$$- U_o(M_w - X_uM_{\dot{w}})]s^2 + [U_o(X_uM_w - X_wM_u) + M_q(X_wZ_u - X_uZ_w)$$

$$+ g(M_u + Z_uM_{\dot{w}})]s + g(Z_uM_w - M_uZ_w) \qquad (43c)$$

For simplification, the real and imaginary parts of the numerator and denominator are considered separately and designated as:

R_D The real portion of the denominator

I_D The imaginary portion of the denominator

R_N The real portion of the numerator

I_N The imaginary portion of the numerator

Therefore, the amplitude of the transfer function $\frac{\dot{\theta}}{w_g}$, is expressed as:

$$\frac{\dot{\theta}}{w_g} = \sqrt{\frac{R_N^2 + I_N^2}{R_D^2 + I_D^2}} \qquad (44)$$

and the phase of the transfer function is:

$$\not\angle \frac{\dot{\theta}}{w_g} = -\tan^{-1}\frac{I_N}{R_N} - \tan^{-1}\frac{I_D}{R_D} \qquad (45)$$

where:

$$R_N = \omega^2[M_w(X_u+Z_w) - X_wZ_uM_{\dot{w}} - X_wM_u - Z_w(M_w - X_uM_{\dot{w}})] \qquad (46)$$

$$R_N = \omega^2 A \qquad (46a)$$

$$I_N = \omega[Z_wM_{\dot{w}} + M_w] \qquad (47)$$

$$I_N = \omega^3 B \qquad (47a)$$

$$I_D = \omega\{\omega^2(X_u + Z_w + M_q + U_oM_{\dot{w}}) + U_o(X_uM_w - X_wM_u)$$

$$+ M_q(X_wZ_u - X_uZ_w) + g(M_u + Z_uM_{\dot{w}})\} \qquad (48)$$

$$I_D = \omega(\omega^2 L + K) \qquad (48a)$$

$$R_D = \omega^4 - \omega^2 \left[M_q (X_u + Z_w) + X_u Z_{\dot{w}} - X_w Z_u - U_o (M_w - X_u M_{\dot{w}}) \right] + g (Z_u M_w - M_u Z_w) \qquad (49)$$

$$R_D = \omega^4 - \omega^2 C + D \qquad (49a)$$

The stability derivatives as listed for method A, and their values as tabulated in Table II, apply to method B as well. In addition, the following derivatives, computed in accordance with Ref. 9, are used to solve for the coefficients A through F, of Equations (46a) through (49a):

$$X_u = -\frac{\rho S V}{m} C_D \quad (50), \qquad Z_u = -\frac{\rho S V}{m} C_L \qquad (52)$$

$$X_w = \frac{\rho S V}{2m} (C_L - C_{D_\alpha}) \quad (51), \qquad M_u = -\left(\frac{\rho S c V}{2 I_y}\right)(\alpha_o C_{m_\alpha}) \qquad (53)$$

The computed values of these stability derivatives, as well as the quantities used to compute them, are listed in Table II. The values of A, B, C, D, E, and F are listed in Table IV. The phase and amplitude of $\frac{\dot{\theta}}{Wg}$ are computed and listed in Table IV for a frequency range from .05 cycles per second to 2.00 cycles per second. The phase and amplitude of $\frac{\dot{\theta}}{Wg}$, as computed by the exact solution, are also plotted versus frequency, together with the values obtained from method A, on Figs. 15 and 16. The two different theoretical methods produced almost identical curves. For both methods the peak amplitude of $\frac{\dot{\theta}}{Wg}$, as well as the phase shift, occurred at the programmed short period frequency of 0.6 cycles per second.

TABLE IV: METHOD B. EXACT SOLUTION FOR THE PHASE AND AMPLITUDE OF $\frac{\ddot{\theta}}{w_g}$

f (c.p.s.)	A	B	C	D	E	F	R_N $(\omega^2 A)$	I_N $(\omega^3 B)$	$\omega^2 C$	$\omega^4 - \omega^2 C$	$\omega^4 - \omega^2 C + D$	$\omega^2 E$	$\omega^2 E + F$
0	.00022	-.02262	14.21569	.000702	.76893	.19278	0	0	0	0	.00070	0	.19278
.05	↓	↓	↓	↓	↓	↓	.00002	-.00070	1.40295	-1.39321	-1.39251	-.07589	.11699
.10							.00009	-.00561	5.61179	-5.46595	-5.45525	-.30354	-.11076
.15							.00020	-.01893	12.6765	-11.83760	-11.83690	-.68297	-.4909
.20							.00035	-.04488	22.44714	-19.95377	-19.95307	-1.21417	-1.02139
.25							.00054	-.08766	35.0738	-28.98643	-28.98573	-1.89715	-1.70437
.30							.00078	-.15148	50.5062	-37.88347	-37.88277	-2.73189	-2.53911
.35							.00106	-.24055	68.7445	-45.85936	-45.85866	-3.71841	-3.52563
.40							.00139	-.35907	89.7887	-49.89471	-49.89401	-4.85669	-4.66391
.45							.00176	-.51125	113.6389	-49.73625	-49.73565	-6.14676	-5.9593
.50							.00217	-.70130	140.2949	-42.59773	-42.89067	-7.58858	-7.3958
.55							.00263	-.93343	169.7569	-27.15705	-27.1563	-9.18219	-8.9841
.60							.00313	-1.21185	202.0247	-.06116	-.0604	-10.92756	-10.7348
.65							.00367	-1.54076	237.0985	41.67885	41.07955	-12.8247	-12.6319
.70							.00426	-1.92437	274.9781	99.18441	99.18511	-14.8736	-14.6808
.75							.00489	-2.36689	315.6630	177.41169	177.4123	-17.0743	-16.8815
.80							.00556	-2.87252	359.1551	279.14993	279.1506	-19.4267	-19.2340
.90							.00703	-4.08994	454.5555	567.88527	567.8859	-24.5870	-24.3942
1.00							.00868	-5.61040	561.1798	997.1818	997.18252	-30.3543	-30.16157
1.20							.01251	-9.69477	808.0990	2423.3198	2423.3205	-43.7102	-43.5174
1.40							.01702	-15.3949	1099.9124	4887.0464	4887.0471	-59.4945	-59.3017
1.60							.02223	-22.9802	1436.6204	8557.2586	8776.2593	-77.7071	-77.5143
1.80							.02814	-32.7198	1818.2227	14540.834	14540.835	-98.3480	-98.1553
2.00	↓	↓	↓	↓	↓	↓	.03474	-44.8832	2244.7194	22689.067	22689.0681	-121.4174	-121.2246

TABLE IV: (Continued)

f (c.p.s.)	$I_\Delta / \omega(\omega^2 E + F)$	R_N^2	I_N^2	$R_N^2 + I_N^2$	R_Δ^2	I_Δ^2	$R_\Delta^2 + I_\Delta^2$		$\frac{R_N^2 + I_N^2}{R_\Delta^2 + I_\Delta^2}$	$\left\lvert \frac{\dot{\theta}}{\omega g} \right\rvert$	$\frac{I_N}{R_N}$	$-\mathrm{Tan}^{-1}\frac{I_N}{R_N}$	$\frac{I_D}{R_D}$	$-\mathrm{Tan}^{-1}\frac{I_D}{R_D}$	$\angle \frac{\dot{\theta}}{\omega g}$ (degrees)
0	0	0×10^{-6}	0×10^{-6}	$\times 10^{-6}$	0	0	0		0×10^{-6}	0					
.05	.03675	0	.49	.49	1.9391	.0014	1.9404		.25252	100.503	-35.0	+88.37	-.0264	+1.52	+89.89
.10	-.06959	.6018	31.47721	31.4739	29.7598	.0048	29.7646		1.05742	.001028	-62.3	+89.08	+.01276	-.73	+88.35
.15	-.46198	.0400	358.4449	358.385	140.1122	.2134	140.3256		2.55395	.001598	-94.5	+89.40	+.03902	-2.23	+87.17
.20	-1.28348	.1225	2014.2144	2014.337	398.1250	1.6463	399.7723		5.03891	.002245	-128.22	+89.55	+.06432	-3.68	+85.87
.25	-2.67714	.2716	7684.275	7684.547	840.1725	4.4899	844.6625		9.09780	.003016	-162.22	+89.65	+.09236	-5.28	+84.37
.30	-4.78597	.6084	22946.190	22946.80	1435.104	22.9055	1458.010		15.73843	.003967	-194.2	+89.70	+.12634	-7.20	+82.50
.35	-7.75304	1.1236	33809.302	33810.43	2067.408	60.1096	2117.518		15.96700	.003996	-226.93	+89.75	+.17092	-9.70	+80.05
.40	-11.72134	1.9321	128931.26	128933.2	2489.412	137.390	2626.802		49.08371	.00706	-56.182	+88.90	+.23492	-13.22	+76.68
.45	-16.8339	3.0976	261376.56	261379.7	2473.465	283.383	3757.018		94.80522	.009737	-290.48	+89.80	+.33846	-18.70	+71.10
.50	-23.2339	4.7089	491821.69	491826.4	1840.124	539.815	2379.939		206.6550	.014375	-323.18	+89.83	+.54162	-28.44	+61.39
.55	-31.0642	6.9469	871291.56	871298.5	737.467	964.988	1702.455		511.7894	.022623	-354.91	+89.84	+1.1439	-48.83	+41.01
.60	-40.4679	9.7969	1,461,580	1,468,546	.003819	1637.657	1637.660		896.7612	.028404	-387.50	+89.85	+670.0	-89.92	-.07
.65	-51.5881	13.4687	2,373,941	2,373,954	687.529	2661.339	3348.869		545.8785	.023364	-419.82	-89.86	-1.2558	+51.46	-38.41
.70	-64.5678	18.1476	3,703,200	3,703,218	9837.636	4169.007	14006.693		264.3892	.016260	-451.73	-89.82	-.72397	+35.80	-54.02
.75	-79.5500	23.9101	5602,218	5602192	18884.16	6328.209	25210.373		222.2177	.014007	-484.03	-89.88	-.14839	+24.15	-65.86
.80	-96.6798	30.9136	8251,371	8251412	17925.07	9346.603	87,271,677		94.5484	.009724	-516.64	-89.90	-.34633	+19.10	-70.70
.90	-137.9421	49.4207	16,727,936	16727985	3224915	19028.126	3451225		48.9806	.006999	-581.78	-89.91	-.242904	+13.65	-76.24
1.00	-189.5051	75.3424	31,476,588	31.47666 3	994373.0	35912.20	1030285.2		30.5514	.005527	-646.36	-89.92	-.19004	+10.76	-79.15
1.20	-308.1043	156.500	93,988,565	93988721	5872.482	107652.15	5480135		15.7168	.003964	-774.96	-89.93	-.13539	+7.71	-82.21
1.40	-521.6299	289.680	237,004,466	237004966	23883203	2702921	24155296		9.81169	.003132	-904.52	-89.95	-.10671	+6.10	-83.83
1.60	-779.2363	494.172	528,900,592	528900086	770227.6	7607209.3	7776.9937		6.80266	.002608	-1033.75	-89.95	-.08879	+5.08	-84.66
1.80	-1110.0776	791.8596	1,070,858,084	1070858932	21143588	123327.24	2126816.0		5.03408	.002244	-1162.75	-89.95	-.076342	+4.37	-85.58
2.00	-1523.3085	1206.867	2,014,502,847	2014502847	5747.7938	23204.69	5171.49283		3.89566	.001974	-1290.82	-89.95	-.06715	+3.84	-86.11

Comparing the power spectral solution and the theoretical solution (Figs. 13, 14, 15, and 16) by matching the phase and amplitude curves for $\frac{\dot{\theta}}{wg}$, it is noted that in both cases the phase shift of the transfer function is in close agreement and the greatest amplitude of $\frac{\dot{\theta}}{wg}$, as established by both solutions, occurs at the same frequency, 0.6 cycles per second, however a discrepancy in the value of the peak amplitude of $\frac{\dot{\theta}}{wg}$ is apparent. The amplitude of the transfer function, as determined by the power spectral method, is consistently less, by an almost constant difference, than the amplitude as established by the theoretical solution for the same range of frequencies. The validity of the transfer function amplitude as established theoretically is considered to be accurate inasmuch as two different solutions produced identical results and the peak amplitude of 0.3 is a realistic value for an aircraft such as the F-100. Refer to Myslett and Smith (10). The power spectral solution, as derived, would imply that in flight the aircraft was not as disturbed by the turbulence as the theoretical solution predicted. This is more obvious when examining the autocorrelation function for $\dot{\theta}$ as computed and graphed by the digital program. Although the distribution of the fluctuations of the autocorrelation function for $\dot{\theta}$ was in agreement with theory; the magnitude of the fluctuations was extremely small with an average absolute value of .000001.

The computational results and the observation mentioned above led to a close scrutiny of the instrument sensitivity on the test aircraft used to gather the data. In particular, the sensitivities of the instruments measuring pitch angle, pitch rate, normal acceleration at the C.G., and angle of attack were checked because these parameters provide the most vital information regarding the actual dynamic response of the aircraft to turbulence. The entire flight record for Run number 8 was re-examined for the typical inflight measurements of the parameters mentioned above. The results are summarized in Table V.

Table V: Instrument Sensitivity and In-Flight Measurements for Flt. 26, Run 8.

Parameter Measured	Inst. Sensitivity (in terms of trace deflection)	Average Deflection Flight Record	Typical Resultant Value
θ	12°/inch	.22 inch	$\pm$ 1.6°
$\dot{\theta}$	$\frac{9.1^{\circ}}{\text{sec/inch}}$	.07 inch	$\pm$ $.7^{\circ}$/sec
a_z	4g's/inch	.09 inch	$\pm$ .36g
α_v	4.5°/inch	.15 inch .05 inch	$.9^{\circ}(+\alpha_v)$ $.2^{\circ}(-\alpha_v)$

The tabulations above indicate a generally small response of the aircraft to the clear air turbulence encountered. The data from Table V, the diminished magnitude of the autocorrelation function for $\dot{\theta}$, and the consistent trend of the power spectral solution for the amplitude of $\frac{\dot{\theta}}{Wg}$ to be less than the theoretical amplitude of $\frac{\dot{\theta}}{Wg}$ indicate that the sensitivity of the instrumentation aboard the test aircraft was insufficient. This conclusion was further verified during the investigation of the instrument sensitivity at NASA when discussion with the NASA engineers revealed that the aircraft used in collecting this data had been originally instrumented for the purpose of collecting maneuvering type data. The instrument sensitivity requirements for this type of maneuvering flight are not as stringent as those necessary for the power spectral type analysis of turbulence. The accuracy of the response is even more critical in a power spectral analysis since the associated digital computation is of such length that any initial discrepancies will be magnified by "rounding off" errors which are carried throughout the computer program. The amplitude discrepancy of the transfer function noted above, however, was of indirect value in an academic sense in that it generated a thorough secondary analysis of the

flight test data and a better appreciation of the entire flight test program from considerations of the instrument location and sensitivity, to the digital program itself.

Despite the single discrepancy in the solution for the transfer function, $\frac{\dot{\theta}}{w_g}$, it is felt that this analysis did represent a significant and unique application of power spectral methods because the transfer function between a random input and the resultant aircraft dynamic response was established on a continuous basis over a finite frequency range. The amplitude discrepancy between the theoretical and power spectral solutions for the transfer function is considered to be entirely due to improper instrument sensitivity and not to the mathematical computations or the power spectral analysis itself. A closer correlation between the amplitudes of the transfer functions would be realized using the same analytical procedures if the in-flight response measurements were more accurate.

Future effort in turbulence response analysis, particularly with power spectral applications, will require that more sensitive instrumentation be incorporated on the test aircraft. In addition, the angle of attack vane should be re-located from its present position on the vertical stabilizer to a position at least two and a half fuselage diameters ahead of the aircraft as proposed in Refs. 1 and 11.

Although this analysis considered a singular application of the power spectral method, additional areas of investigation related to gust loading would be worthwhile for future research. A preliminary study, by Press and Houbolt (12), has been conducted to determine the variation in normal acceleration with center of gravity position for a fighter type aircraft. Through power spectral analysis, the ratio of the root mean square values of the normal acceleration, determined by the area under the gust spectrum, was readily established between center of gravity positions. It was determined that as the center of gravity position is shifted aft, the peak frequency response moves to a lower frequency and diminishes slightly. Other significant areas of future study and investigation include the effect of low short period damping on the gust loads of aircraft in continuous turbulence and the magnification in gust load stresses that results from wing flexibility. Refer to Press and Tukey (13).

In general, the power spectral methods of analysis may be regarded as an effective and accurate tool for analysis of a random type disturbance. In particular, it is a powerful method for further exploration of the science of gust loading.

BIBLIOGRAPHY

1. Houbolt, J. C., Steiner, R., and Pratt, K. G. "Dynamic Response of Airplanes to Atmospheric Turbulence Including Flight Data on Input and Response," NASA Technical Report R-199, June 1964.

2. Bendat, J. S. and Piersol, R. G. Measurement and Analysis of Random Data, John Wiley and Sons, New York, N. Y., 1966.

3. Chilton, R. G. "Some Measurements of Atmospheric Turbulence Obtained from Flow-Direction Vanes Mounted on an Airplane," NACA Technical Note 3313, November 1964.

4. U. S. A. F. Technical Order 1F-100C-2-5, "Maintenance Handbook Flight Control Systems, F-100C Aircraft," November 1956.

5. Press, H., Meadows, M. F., and Hadlock, I. "Estimates of Probability Distribution of Root-Mean-Square Gust Velocity of Atmospheric Turbulence from Occasional Gust Load Data by Random Process Theory," NACA Technical Note 3362, March 1955.

6. Diederich, F. W. "The Response of an Airplane to Random Atmospheric Disturbances," NACA Report 1345, 1958.

7. Etkin, B. Dynamics of Flight, John Wiley and Sons, New York, N. Y., 1959.

8. Pratt, K. G. and Bennett, F. V. "Charts for Estimating the Effects of Short Period Stability Characteristics on Airplane Vertical Acceleration and Pitch Angle Response in Continuous Atmospheric Turbulence," NACA Technical Note 3992, June 1957.

9. "Dynamics of The Airplane," BuAer Report AE-61-4II, prepared by the Servomechanisms Section and Aerodynamic Section, Northrop Aircraft, Inc., 1952.

10. Myslett, W. C. and Smith, A. G. "Longitudinal Frequency Response Characteristics of a 35° Swept Wing Airplane as Determined from Flight Measurements Including a Method for the Evaluation of Transfer Functions," NACA Research Memorandum RM A 51627, June 1954.

11. Press, H. and Mazelsky, B. "A Study of the Application of Power Spectral Methods of Generalized Harmonic Analysis to Gust Loads on Airplanes," NACA Report 1172, May 1954.

12. Press, H. and Houbolt, J. C. "Some Applications of Generalized Harmonic Analysis to Gust Loads on Airplanes," Journal of the Aeronautical Sciences, January 1955.

13. Press, H. and Tukey, J. W. "Power Spectral Methods of Analysis and Their Application to Problems in Airplane Dynamics," Flight Test Manual, NATO Advisory Group for Aeronautical Research and Development, IV-C, June 1956.

14. UCLA BioMedical Computer Handbook, BMD02T, June 1964.

Appendix A

The Sequence of Digital Computer Steps in the Power Spectrum Analysis

The mathematical steps outlined in Table VI explain the computational procedure behind each of the digital computer steps in the power spectrum analysis (Ref. 14). All information in Table VI refers to Fig. 17, and each step in the table is related to the appropriate computer operation by the computer sequence number.

The symbols used in Table VI are defined as follows:

X_i — i^{th} value of discrete, equi-spaced time series X(t)

X_i — i^{th} value of time series X(t) after subtracting mean

Y_i — i^{th} value of time series Y(t) after subtracting mean

P — Lag

n — Number of discrete data points

m — Maximum lag

t — Constant time interval

$R_x^{(p)}$ — Autocovariance of series X at lag p, $R_x^{(p)} = R_x^{(p\Delta t)}$

$P_x^{(h)}$ — Power spectral estimate of series X at frequency $\frac{h\pi}{m\Delta t}$

$P_x^{(h)} = P_{x\frac{h\pi}{m\Delta t}}$

$SP_x^{(h)}$ — Smoothed power spectral estimate of series X at frequency $\frac{h\pi}{m\Delta t}$

$R_{xy}^{(p)}$ — Cross-covariance between series X and Y at lag p

$P_{xy}^{(h)}$ — Cross-power spectral estimate at frequency $\frac{h\pi}{m\Delta t}$

$C_{xy}^{(h)}$ — Cospectrum, the real part of $P_{xy}^{(h)}$ at frequency $\frac{h\pi}{m\Delta t}$

$Q_{xy}^{(h)}$ — Quadrature spectrum, the imaginary part of $P_{xy}^{(h)}$ at frequency $\frac{h\pi}{m\Delta t}$

$SC_{xy}^{(h)}$ — Smoothed cospectrum at frequency $\frac{h\pi}{m\Delta t}$

$SQ_{xy}^{(h)}$ Smoothed quadrature spectrum at frequency $\frac{h\pi}{m\Delta t}$

$AM_{xy}^{(h)}$ Amplitude of cross spectrum at frequency $\frac{h\pi}{m\Delta t}$

$PHAS_{xy}^{(h)}$ Phase of cross-spectrum at frequency $\frac{h\pi}{m\Delta t}$

$T_{xy}^{(h)}$ Transfer function at frequency $\frac{h\pi}{m\Delta t}$

$TAM_{xy}^{(h)}$ Amplitude of transfer function at frequency $\frac{h\pi}{m\Delta t}$

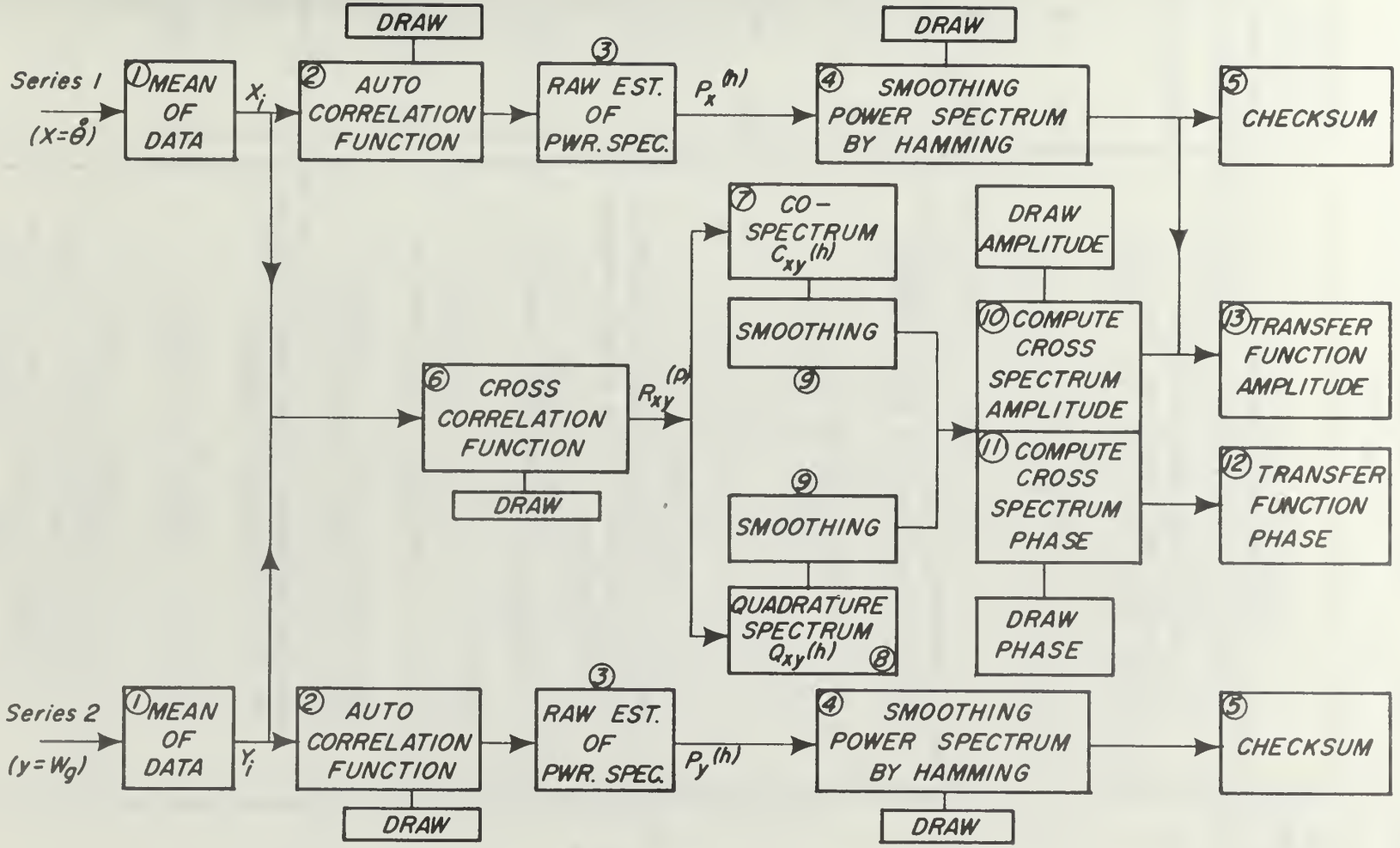

FIG. 17 SEQUENCE OF DIGITAL COMPUTER STEPS IN POWER SPECTRUM ANALYSIS

1. X and y correspond to $\dot{\theta}$ and Wg respectively.
2. Wg is computed from eqn. (5): $Wg = V\alpha_v - V\theta + \int a_z\, dt + l_x\dot{\theta}$.
3. Computer sequence numbers are circled.

TABLE VI: Sequence of Digital Computer Steps In The Power Spectrum Analysis

COMPUTER SEQUENCE NUMBER	MATHEMATICAL OPERATION	REFER TO PAGE:
(1)	The mean of the data is first calculated and subtracted from each value of X'.	(Original Data)
	$m_x = \frac{1}{n} \sum_{i=1}^{n} X_i'$	$\dot{\theta}$ 76
	$X_i = X_i' - m_x \qquad i = 1, 2, \ldots, n$	Wg 81
(2)	The autocovariance is then computed.	
	$R_x^{(p)} = \frac{1}{n-p} \sum_{q=1}^{n-p} X_q \cdot X_{q+p}$	$\dot{\theta}$ 77,78
	$p = 0, 1, 2, \ldots, m$	Wg 82,83
	$R_x^{(p)} = R_x(p\Delta t)$	
(3)	The raw estimate of the power spectrum is obtained by	
	$P_x^{(h)} = \frac{2\Delta t}{\pi} \sum_{p=0}^{m} \epsilon_p R_x^{(p)} \cos \frac{hp\pi}{m}, \quad h = 0, 1, \ldots, m$	$\dot{\theta}$ 79
	where $\epsilon_p = \begin{cases} 1 & 0 < p < m \\ 1/2 & p = 0, m \end{cases}$	Wg 84
	NOTE: $P_x^{(h)} = P_x(\omega_h) = P_x\left(\frac{h\pi}{m\Delta t}\right)$	
(4)	The raw estimates of the power spectrum are then smoothed by "hamming"	
	$SP_x^{(0)} = .54P_x^{(0)} + .46P_x^{(1)}$	$\dot{\theta}$ 80
	$SP_x^{(h)} = .23P_x^{(h-1)} + .54P_x^{(h)} + .23P_x^{(h+1)}, \quad 0 < h < m$	
	$SP_x^{(m)} = .54P_x^{(m)} + .46P_x^{(m-1)}$	Wg 85

TABLE VI (Continued)

COMPUTER SEQUENCE NUMBER	MATHEMATICAL OPERATION	REFER TO PAGE:
(5)	A check sum is computed to check the computations of the estimates. $\text{CHKSUM} = \frac{\pi}{m\Delta t}\left[\frac{1}{2}\left(SP_x^{(0)} + SP_x^{(m)}\right) + \sum_{h=1}^{m-1} SP_x^{(h)}\right]$ This should equal $R_x^{(0)}$, the autocovariance at zero lag.	$\mathring{\theta}$ 79 W_g 84
(6)	The cross-covariance is computed by the formula $R_{xy}^{(p)} = \frac{1}{n-p}\sum_{q=1}^{n-p} X_q Y_{q+p}, \quad p = 0,1,2,\ldots,m$ $R_{xy}^{(-p)} = \frac{1}{n-p}\sum_{q=1}^{n-p} X_{q+p} Y_q, \quad p = 0,1,2\ldots,m$	86,87, 88
(7)	The cross-spectrum, $P_{xy}^{(h)}$, is given by $P_{xy}^{(h)} = C_{xy}^{(h)} + i\,Q_{xy}^{(h)}$ The cospectrum is obtained from $C_{xy}^{(h)} = \frac{\Delta t}{\pi}\sum_{p=0}^{m} \epsilon_p \left(R_{xy}^{(p)} + R_{xy}^{(-p)}\right)\cos\frac{hp\pi}{m}$	89
(8)	The quadrature spectrum is obtained from $Q_{xy}^{(h)} = \frac{\Delta t}{\pi}\sum_{p=0}^{m} \epsilon_p \left(R_{xy}^{(p)} + R_{xy}^{(-p)}\right)\sin\frac{hp\pi}{m}$ $h = 0, 1, 2, \ldots, m$ $\epsilon_p = \begin{cases} 1/2 & p = 0, m \\ 1 & 0 < p < m \end{cases}$	89
(9)	Both the cospectrum and quadrature spectrum are smoothed by "hamming" as shown in step 4.	

TABLE VI (Continued)

COMPUTER SEQUENCE NUMBER	MATHEMATICAL OPERATION	REFER TO PAGE:
(10)	The amplitude and phase of the cross-spectrum are computed. $$AM_{xy}^{(h)} = \sqrt{[SC_{xy}^{(h)}]^2 + [SQ_{xy}^{(h)}]^2}$$	89,90
(11)	$$PHAS_{xy}^{(h)} = ARCTAN\left(\frac{SQ_{xy}^{(h)}}{SC_{xy}^{(h)}}\right)$$ The phase angle computed is the phase shift of series Y with respect to series X.	89,91
(12)	The transfer function from series X to Y is given by $$T_{xy}^{(h)} = \frac{P_{xy}^{(h)}}{P_x(h)} = TAM_{xy}^{(h)} e^{i PHAS_{xy}^{(h)}}$$	92
(13)	The amplitude is given by $$TAM_{xy}^{(h)} = AM_{xy}^{(h)} / SP_x^{(h)}$$ The phase shift from X to Y is the same as that of the cross-spectrum. Both the transfer function amplitudes from X to Y and Y to X are printed.	92

BMD02T-AUTOCOVARIANCE AND POWER SPECTRAL ANALYSIS - VERSION OF MAR. 22, 1964
HEALTH SCIENCES COMPUTING FACILITY, UCLA

PROBLEM NUMBER RUN 8

INPUT DATA TO BE PRINTED OUT---YES

INPUT SERIES TO BE PLOTTED OUT---

DETRENDING---

PREWHITENING---

FLIGHT 26, RUN 8
SERIES 1 = θ
SERIES 2 = w_g

VALUE OF CONSTANT C USED IN THE PREWHITENING TRANSFORMATION Z(T)=X(T+1)-CX(T) --- -0.

NUMBER OF SERIES = 2

NUMBER OF DATA POINTS = 920

NUMBER OF LAGS CHOSEN = 100

NUMBER OF SELECTION CARDS = 1

USE PREVIOUS DATA---

CONSTANT TIME INTERVAL = 0.10000 SECOND

NUMBER OF VARIABLE FORMAT CARDS = 1

(7) ORIGINAL DATA OF SERIES 1

-0.00061	-0.00048	0.00027	0.00027	0.00027	0.00027	0.00027	0.00027	0.00027	0.00027
0.00027	0.00027	0.00002	0.00002	0.00002	0.00002	0.00002	0.00002	0.00002	0.00002
0.00052	0.00102	0.00202	0.00290	0.00315	0.00240	0.00152	0.00064	0.00002	-0.00023
-0.00023	-0.00023	-0.00023	-0.00023	0.00064	0.00190	0.00315	0.00403	0.00378	0.00278
0.00140	0.00077	0.00014	-0.00023	-0.00111	-0.00211	-0.00211	-0.00211	-0.00149	-0.00048
-0.00023	0.00115	0.00115	0.00115	0.00190	0.00177	0.00090	0.00002	-0.00012	-0.00011
-0.00023	-0.00023	-0.00023	-0.00099	-0.00136	-0.00249	-0.00249	-0.00249	-0.00048	0.00064
0.00127	0.00265	0.00202	0.00152	0.00077	0.00039	-0.00023	-0.00023	-0.00024	-0.00023
-0.00023	-0.00023	-0.00023	-0.00023	-0.00023	0.00052	0.00002	-0.00099	-0.00086	-0.00023
-0.00073	-0.00086	-0.00161	-0.00211	-0.00199	-0.00199	-0.00161	-0.00136	-0.00011	0.00240
0.00428	0.00278	0.00278	0.00215	0.00140	0.00039	0.00039	0.00039	0.00064	0.00115
0.00152	0.00152	0.00152	0.00340	0.00416	0.00416	0.00654	0.00654	0.00428	0.00165
-0.00011	-0.00161	-0.00349	-0.00387	-0.00387	-0.00362	-0.00036	0.00039	0.00177	0.00403
0.00516	0.00667	0.00667	0.00604	0.00253	-0.00048	-0.00211	-0.00437	-0.00437	-0.00437
-0.00249	-0.00124	0.00014	0.00014	0.00014	0.00014	0.00014	-0.00061	-0.00061	-0.00036
-0.00036	-0.00036	-0.00036	-0.00036	-0.00036	-0.00036	-0.00036	-0.00036	0.00077	0.00416
0.00729	0.00842	0.00830	0.00840	0.00729	0.00403	0.00152	0.00014	-0.00086	0.00002
0.00090	0.00090	0.00090	0.00090	0.00064	0.00014	0.00014	0.00014	0.00014	0.00014
0.00064	0.00115	0.00115	0.00102	0.00052	0.00027	0.00027	0.00027	0.00027	0.00027
0.00027	0.00027	0.00027	0.00027	-0.00073	-0.00111	-0.00161	-0.00186	-0.00161	-0.00099
-0.00023	0.00014	0.00064	0.00039	-0.00036	-0.00111	-0.00186	-0.00249	-0.00312	-0.00312
-0.00237	-0.00111	-0.00061	-0.00011	-0.00011	-0.00011	-0.00011	-0.00011	-0.00048	-0.00086
-0.00086	-0.00086	-0.00086	-0.00086	-0.00086	-0.00136	-0.00199	-0.00224	-0.00224	-0.00199
-0.00099	-0.00099	-0.00099	-0.00099	-0.00099	-0.00161	-0.00211	-0.00349	-0.00362	-0.00312
-0.00324	-0.00487	-0.00312	-0.00312	-0.00124	0.00190	0.00441	0.00491	0.00693	0.00629
0.00315	0.00039	-0.00061	-0.00124	-0.00111	-0.00111	-0.00149	-0.00211	-0.00212	-0.00199
-0.00161	-0.00099	-0.00036	-0.00011	0.00052	0.00090	0.00090	-0.00011	-0.00111	-0.00161
-0.00262	-0.00249	-0.00186	-0.00099	-0.00048	0.00014	0.00027	0.00014	-0.00012	-0.00048
-0.00086	-0.00136	-0.00211	-0.00124	-0.00086	-0.00099	-0.00099	-0.00099	-0.00099	-0.00099
-0.00099	-0.00099	-0.00099	-0.00099	-0.00099	-0.00099	-0.00099	-0.00099	-0.00098	-0.00086
0.00014	0.00039	0.00039	0.00039	0.00027	0.00002	-0.00086	-0.00199	-0.00287	-0.00287
-0.00287	-0.00287	-0.00249	-0.00186	-0.00136	-0.00111	-0.00111	-0.00136	-0.00161	-0.00199
-0.00199	-0.00199	-0.00199	-0.00186	-0.00161	0.00014	0.00090	0.00240	0.00391	0.00403
0.00366	0.00177	-0.00036	-0.00149	-0.00161	-0.00287	-0.00287	-0.00287	-0.00287	-0.00237
-0.00161	-0.00086	-0.00061	-0.00086	-0.00023	0.00014	0.00102	0.00090	0.00052	-0.00011
-0.00023	-0.00023	-0.00023	-0.00023	-0.00099	-0.00161	-0.00161	-0.00149	-0.00149	-0.00149
-0.00149	-0.00149	-0.00149	-0.00149	-0.00149	-0.00149	-0.00149	-0.00224	-0.00425	-0.00563
-0.00563	-0.00487	-0.00337	-0.00186	-0.00136	-0.00086	-0.00086	-0.00061	-0.00061	-0.00011
0.00039	0.00115	0.00190	0.00177	0.00177	0.00027	0.00002	0.00002	0.00002	0.00090
0.00253	0.00278	0.00353	0.00340	0.00340	0.00366	0.00228	0.00064	0.00002	-0.00048
-0.00061	-0.00061	-0.00048	-0.00048	-0.00048	-0.00048	-0.00048	-0.00048	-0.00048	-0.00011
0.00115	0.00240	0.00416	0.00416	0.00190	-0.00011	-0.00073	-0.00224	-0.00199	-0.00199
-0.00124	-0.00099	-0.00023	0.00077	0.00077	0.00027	-0.00086	-0.00073	-0.00099	-0.00073
-0.00174	-0.00174	-0.00174	-0.00174	-0.00124	-0.00073	-0.00036	-0.00023	-0.00024	-0.00023
-0.00099	-0.00099	-0.00111	-0.00149	-0.00111	-0.00048	0.00002	0.00090	0.00127	0.00127
0.00090	0.00052	0.00052	0.00052	0.00014	-0.00048	-0.00086	-0.00124	-0.00124	-0.00111
-0.00061	0.00052	0.00052	0.00052	0.00052	0.00014	-0.00023	-0.00136	-0.00186	-0.00124
-0.00061	0.00115	0.00290	0.00290	0.00278	0.00202	0.00052	-0.00073	-0.00324	-0.00475
-0.00588	-0.00525	-0.00274	-0.00086	0.00052	0.00077	0.00265	0.00428	0.00478	0.00441
0.00340	0.00177	0.00039	-0.00011	-0.00124	-0.00224	-0.00211	-0.00211	-0.00211	-0.00111
-0.00136	-0.00061	0.00039	0.00140	0.00315	0.00453	0.00453	0.00453	0.00453	0.00453
0.00391	0.00165	0.00014	0.00014	-0.00036	-0.00023	0.00090	0.00315	0.00478	0.00541
0.00566	0.00491	0.00315	0.00090	-0.00011	-0.00136	-0.00349	-0.00688	-0.00839	-0.00625
-0.00475	-0.00186	0.00014	0.00090	0.00240	0.00240	0.00240	0.00240	0.00202	0.00077
0.00062	0.00014	0.00014	0.00014	0.00014	0.00014	0.00014	-0.00036	-0.00011	0.00165
0.00328	0.00453	0.00428	0.00391	0.00328	0.00253	0.00064	-0.00199	-0.00387	-0.00613
-0.00663	-0.00575	-0.00237	-0.00124	-0.00048	0.00039	0.00165	0.00240	0.00265	0.00265
0.00202	0.00052	-0.00011	-0.00086	-0.00287	-0.00287	-0.00287	-0.00287	-0.00136	-0.00048
-0.00036	0.00027	0.00303	0.00278	0.00253	0.00228	0.00177	0.00077	0.00039	-0.00048
-0.00124	-0.00149	-0.00149	-0.00149	-0.00149	-0.00073	-0.00048	-0.00023	0.00077	0.00177
0.00190	0.00115	0.00027	-0.00073	-0.00073	-0.00073	-0.00048	-0.00023	0.00014	0.00077
0.00115	0.00115	0.00115	0.00115	0.00077	-0.00011	-0.00023	-0.00048	-0.00061	-0.00048
-0.00048	-0.00048	-0.00048	-0.00048	-0.00048	-0.00048	-0.00036	-0.00036	-0.00024	0.00027
0.00102	0.00127	0.00140	0.00102	0.00027	-0.00036	-0.00073	-0.00174	-0.00124	-0.00061
0.00052	0.00177	0.00290	0.00378	0.00378	0.00278	0.00102	-0.00011	-0.00073	-0.00161
-0.00161	-0.00099	-0.00023	0.00077	0.00228	0.00378	0.00579	0.00729	0.00654	0.00504
0.00240	-0.00011	-0.00149	-0.00375	-0.00337	-0.00299	-0.00237	-0.00174	-0.00073	-0.00048
-0.00061	-0.00061	-0.00061	-0.00111	-0.00262	-0.00262	-0.00262	-0.00262	-0.00262	-0.00262
-0.00262	-0.00136	-0.00073	-0.00036	0.00177	0.00391	0.00491	0.00491	0.00491	0.00441
0.00240	0.00064	-0.00011	-0.00061	-0.00099	-0.00174	-0.00174	-0.00186	-0.00186	-0.00186
-0.00186	-0.00186	-0.00186	-0.00124	-0.00086	-0.00073	-0.00061	-0.00036	0.00014	0.00014
0.00014	0.00002	-0.00036	-0.00086	-0.00086	-0.00086	-0.00099	-0.00099	-0.00099	-0.00086
-0.00086	-0.00023	-0.00011	0.00090	0.00140	0.00115	0.00039	-0.00011	-0.00073	-0.00086
-0.00149	-0.00161	-0.00174	-0.00186	-0.00161	-0.00073	0.00152	0.00328	0.00391	0.00391
0.00378	-0.00011	-0.00023	-0.00036	-0.00036	-0.00061	-0.00061	-0.00036	-0.00036	0.00027
0.00077	0.00077	0.00127	0.00190	0.00152	0.00090	0.00064	0.00014	-0.00011	-0.00011
-0.00011	-0.00023	-0.00036	-0.00036	-0.00023	0.00014	0.00077	0.00077	0.00077	0.00052
0.00014	-0.00011	-0.00023	-0.00036	-0.00036	-0.00036	-0.00048	-0.00061	-0.00061	-0.00061
-0.00073	-0.00086	-0.00136	-0.00111	-0.00061	-0.00023	-0.00023	-0.00036	-0.00086	-0.00111
-0.00161	-0.00174	-0.00174	-0.00174	-0.00161	-0.00061	0.00090	0.00240	0.00403	0.00403
0.00391	0.00265	0.00140	-0.00036	-0.00086	-0.00174	-0.00237	-0.00249	-0.00262	-0.00262
-0.00211	-0.00136	-0.00061	-0.00036	0.00014	0.00064	0.00140	0.00290	0.00315	0.00290
0.00215	0.00366	0.00240	0.00014	0.00002	-0.00011	-0.00011	-0.00011	-0.00011	-0.00011
-0.00048	-0.00099	-0.00086	-0.00099	-0.00099	-0.00036	0.00077	0.00240	0.00340	0.00340
0.00340	0.00353	0.00253	0.00215	0.00115	-0.00011	-0.00023	-0.00086	-0.00161	-0.00174
-0.00161	-0.00161	-0.00149	-0.00161	-0.00161	-0.00161	-0.00149	-0.00086	-0.00099	-0.00099
-0.00099	-0.00099	-0.00011	0.00014	-0.00011	-0.00011	-0.00011	-0.00011	-0.00011	-0.00011
-0.00011	-0.00011	-0.00011	0.00014	0.00002	0.00002	0.00002	0.00002	-0.00011	-0.00036
-0.00174	-0.00324	-0.00324	-0.00237	-0.00099	0.00039	0.00102	0.00115	0.00240	0.00240
0.00240	0.00140	0.00014	-0.00036	-0.00099	-0.00086	-0.00036	0.00002	0.00014	0.00002
-0.00023	-0.00048	-0.00073	-0.00061	-0.00061	-0.00061	-0.00061	-0.00061	-0.00061	-0.00061
-0.00061	-0.00061	-0.00061	-0.00048	-0.00036	-0.00011	-0.00011	-0.00011	-0.00023	-0.00073

LAG (SECOND)	(2) AUTOCOVARIANCE OF SERIES 1
-0.	0.000004
0.1000000	0.000004
0.2000000	0.000003
0.3000000	0.000002
0.4000000	0.000001
0.5000000	-0.000000
0.6000000	-0.000001
0.7000000	-0.000001
0.8000000	-0.000002
0.9000000	-0.000001
1.0000000	-0.000001
1.0999999	-0.000000
1.1999999	0.000000
1.2999999	0.000001
1.3999999	0.000001
1.4999999	0.000001
1.5999999	0.000001
1.6999999	0.000001
1.7999999	0.000001
1.8999999	0.000000
1.9999999	-0.000000
2.0999999	-0.000001
2.1999999	-0.000001
2.2999999	-0.000001
2.3999999	-0.000001
2.4999999	-0.000001
2.5999998	-0.000000
2.6999998	0.000000
2.7999998	0.000001
2.8999998	0.000001
2.9999998	0.000001
3.0999998	0.000001
3.1999998	0.000001
3.2999998	0.000001
3.3999998	0.000000
3.4999998	0.000000
3.5999998	-0.000000
3.6999998	-0.000001
3.7999998	-0.000001
3.8999998	-0.000001
3.9999998	-0.000001
4.0999997	-0.000001
4.1999997	-0.000000
4.2999997	-0.000000
4.3999996	0.000000
4.4999996	0.000001
4.5999995	0.000001
4.6999995	0.000001
4.7999995	0.000001
4.8999994	0.000001
4.9999994	0.000000
5.0999994	0.000000
5.1999993	-0.000000
5.2999993	-0.000000
5.3999993	-0.000000
5.4999992	-0.000000
5.5999992	-0.000000
5.6999992	-0.000000
5.7999991	0.000000
5.8999991	0.000000
5.9999990	0.000001
6.0999990	0.000001
6.1999990	0.000001
6.2999989	0.000001
6.3999989	0.000000
6.4999989	0.000000
6.5999988	-0.000000
6.6999988	-0.000000
6.7999988	-0.000000
6.8999987	-0.000000
6.9999987	-0.000001
7.0999987	-0.000000
7.1999986	-0.000000
7.2999986	-0.000000
7.3999985	-0.000000
7.4999985	0.000000
7.5999985	0.000000
7.6999984	0.000000
7.7999984	0.000000
7.8999984	0.000001
7.9999983	0.000001
8.0999982	0.000000
8.1999981	0.000000
8.2999980	0.000000
8.3999979	-0.000000
8.4999979	-0.000000
8.5999978	-0.000000
8.6999977	-0.000000
8.7999976	-0.000000
8.8999975	0.000000
8.9999974	0.000000
9.0999973	0.000000
9.1999972	0.000000
9.2999971	0.000000
9.3999970	0.000000
9.4999969	0.000000
9.5999968	0.000000
9.6999967	-0.000000
9.7999966	-0.000000
9.8999965	-0.000000
9.9999964	-0.000000

(2) GRAPH OF AUTOCOVARIANCE FUNCTION OF SERIES 1 PLOTTED AGAINST TIME UP TO A LAG OF 10.0000 SECOND

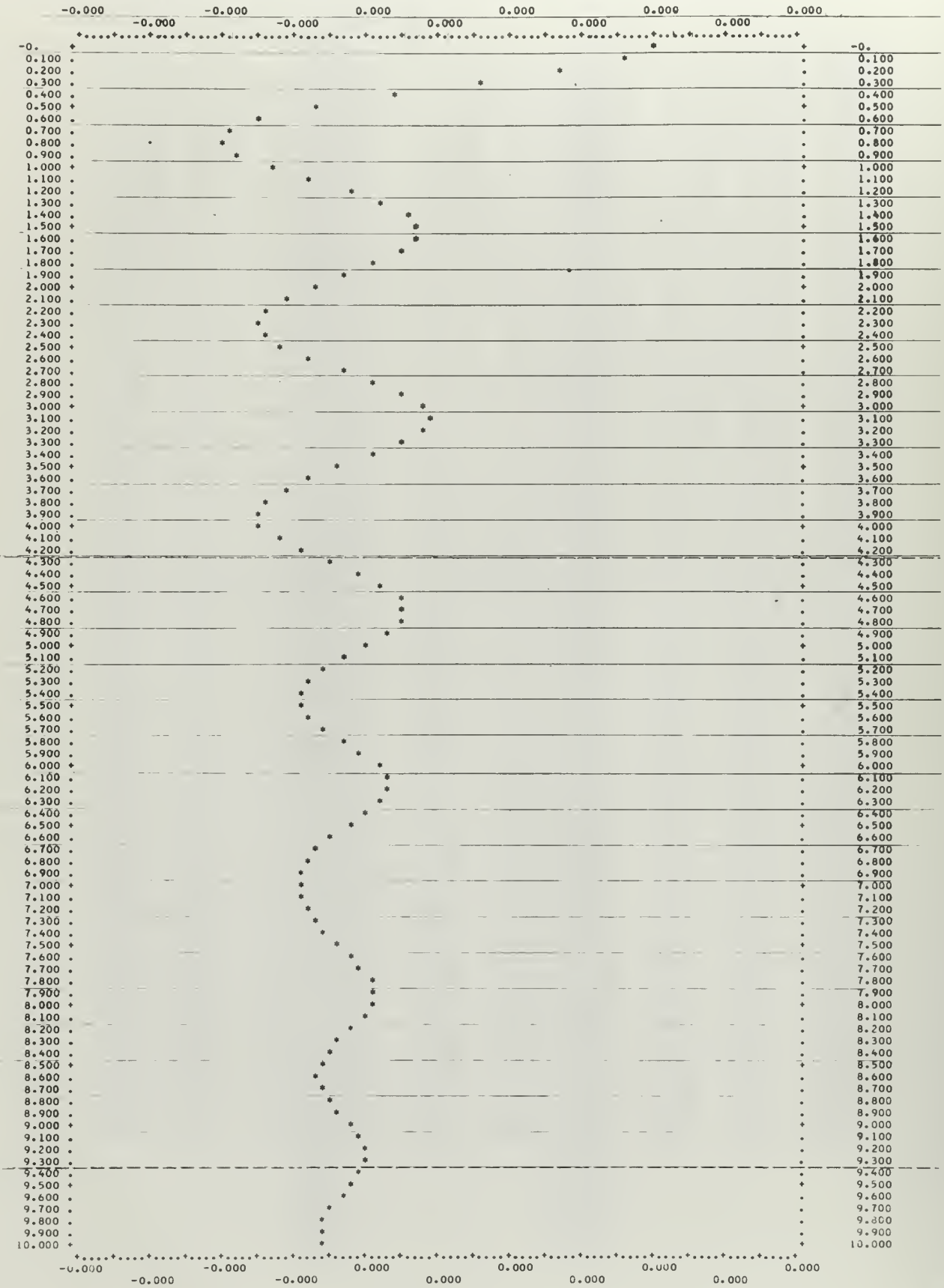

FREQUENCY (CYCLES/SECOND)	(4) POWER SPECTRAL ESTIMATES OF SERIES 1
-0.	0.0000006
0.050000	0.0000005
0.100000	0.0000004
0.150000	0.0000005
0.200000	0.0000005
0.250000	0.0000005
0.300000	0.0000005
0.350000	0.0000007
0.400000	0.0000006
0.450000	0.0000004
0.500000	0.0000004
0.550000	0.0000007
0.600000	0.0000016
0.650000	0.0000021
0.700000	0.0000012
0.750000	0.0000005
0.800000	0.0000003
0.850000	0.0000003
0.900000	0.0000003
0.950000	0.0000002
1.000000	0.0000002
1.050000	0.0000001
1.100000	0.0000001
1.150000	0.0000001
1.200000	0.0000000
1.250000	0.0000000
1.300000	0.0000000
1.350000	0.0000000
1.400000	0.0000000
1.450000	0.0000000
1.500000	0.0000000
1.550000	0.0000000
1.600000	0.0000000
1.650000	0.0000000
1.700000	0.0000000
1.750000	0.0000000
1.800000	0.0000000
1.850000	0.0000000
1.900000	0.0000000
1.950000	0.0000000
2.000000	0.0000000
2.050000	0.0000000
2.100000	0.0000000
2.150000	0.0000000
2.200000	0.0000000
2.250000	0.0000000
2.300000	0.0000000
2.350000	0.0000000
2.400000	0.0000000
2.450000	0.0000000
2.500000	0.0000000
2.550000	0.0000000
2.600000	0.0000000
2.650000	0.0000000
2.700000	0.0000000
2.750000	0.0000000
2.800000	0.0000000
2.850000	0.0000000
2.900000	0.0000000
2.950000	0.0000000
3.000000	0.0000000
3.050000	0.0000000
3.100000	0.0000000
3.149999	0.0000000
3.199999	0.0000000
3.249999	0.0000000
3.299999	0.0000000
3.349999	0.0000000
3.399999	0.0000000
3.449999	0.0000000
3.499999	0.0000000
3.549999	0.0000000
3.599999	0.0000000
3.649999	0.0000000
3.699999	0.0000000
3.749999	0.0000000
3.799999	0.0000000
3.849999	0.0000000
3.899999	0.0000000
3.949999	0.0000000
3.999999	0.0000000
4.049999	0.0000000
4.099999	0.0000000
4.149999	0.0000000
4.199999	0.0000000
4.249999	0.0000000
4.299999	0.0000000
4.349999	0.0000000
4.399999	0.0000000
4.449999	0.0000000
4.499999	0.0000000
4.549999	0.0000000
4.599999	0.0000000
4.649999	0.0000000
4.699999	0.0000000
4.749999	0.0000000
4.799998	0.0000000
4.849998	0.0000000
4.899998	0.0000000
4.949998	0.0000000
4.999998	0.0000000

(5) THE CHECK SUM OF POWER SPECTRAL ESTIMATES IS 0.0000043 AND SHOULD BE 0.0000043
THE DIFFERENCE IS -0.0000000

(4) POWER SPECTRAL ESTIMATES OF SERIES 1 PLOTTED IN A LOG SCALE AGAINST FREQUENCY (CYCLES/SECOND)

(7) ORIGINAL DATA OF SERIES 2

-15.43277	-15.29394	-15.10733	-11.80424	-11.70203	-11.78810	-13.47460	-15.34940	-14.05897	-13.57583
-14.04283	-12.90932	-12.12568	-11.92757	-11.31092	-11.05609	-11.61874	-15.32039	-14.17087	-14.18820
-13.61904	-14.38157	-13.91715	-10.33656	-10.65099	-11.93192	-12.39502	-12.47955	-16.54546	-17.26991
-16.60439	-15.30753	-15.32660	-15.32085	-16.47856	-16.38701	-15.66165	-15.90909	-15.05836	-14.55498
-14.05848	-14.87849	-16.59164	-15.25259	-15.38477	-15.30114	-17.44583	-17.55157	-16.23585	-15.08140
-14.29750	-12.26106	-15.88715	-11.22409	-9.57749	-10.42566	-10.06645	-9.11165	-9.04369	-19.50860
-22.83710	-15.22941	-16.31275	-15.19923	-13.76868	-13.92849	-15.55961	-14.96937	-12.06889	-9.03887
-7.10161	-9.00367	-8.86902	-10.68258	-10.05777	-9.06746	-9.23427	-9.24713	-9.35188	-6.32852
-13.29531	-12.12243	-9.33356	-13.25176	-19.60020	-11.51876	-9.81310	-15.88639	-15.22819	-11.44710
-10.12201	-7.63157	-5.12908	-3.46897	-2.15593	-0.67296	-4.35722	-11.31423	-10.54917	-6.70130
0.76946	-1.35449	-2.19794	-2.87070	-3.45984	-9.02522	-9.09664	-9.49191	-10.47744	-11.41185
-10.74977	-11.95252	-15.80720	-20.37070	-19.15086	-16.57658	-15.59370	-14.44475	-13.83926	-18.13411
-19.12252	-18.40204	-18.49179	-22.29091	-22.93767	-22.02923	-22.22168	-21.33889	-19.50782	-19.62828
-21.01191	-21.26067	-19.99551	-15.44501	-17.20754	-15.15773	-21.00320	-23.09451	-23.78207	-23.37892
-21.74918	-20.22999	-18.87147	-16.82727	-14.12521	-10.98244	-11.28710	-11.92698	-12.49872	-9.97014
-13.47497	-11.37651	-9.89464	-8.90579	-7.58826	-6.27074	-7.86946	-11.54388	-11.53768	-11.10305
-11.55557	-11.84985	-12.18782	-11.62840	-10.89800	-13.15686	-14.85344	-26.02188	-23.92791	-28.32216
-26.61552	-25.14459	-26.41387	-23.45079	-26.89276	-27.26791	-27.61689	-28.20733	-27.34940	-26.54587
-26.23083	-25.76622	-25.60109	-24.95452	-24.93943	-24.92915	-24.92370	-24.91824	-24.91278	-24.90733
-24.90187	-24.88989	-25.11925	-24.11328	-24.27152	-24.00075	-23.98697	-26.12838	-24.98822	-24.08652
-24.22899	-24.11975	-21.58329	-20.36052	-20.75534	-21.18972	-20.35847	-22.39156	-22.88960	-23.92908
-24.21073	-24.17246	-22.62595	-21.54044	-22.54461	-23.08240	-23.36730	-22.88107	-22.85399	-22.92019
-24.80041	-24.02889	-22.59973	-22.59612	-21.01001	-20.01981	-17.35620	-19.94379	-21.80551	-23.20279
-20.70920	-18.85594	-18.76769	-17.60037	-14.19982	-9.89346	-10.96181	-16.15361	-13.87977	-10.73554
-9.35524	-8.53354	-8.84044	-10.07023	-9.41517	-7.73080	-6.67854	-8.78346	-8.11031	-3.96354
-4.58238	-8.50506	-12.02255	-12.16427	-11.86035	-10.91563	-8.61857	-9.38055	-11.22497	-11.68276
-12.27613	-17.81541	-18.12724	-12.18717	-12.49961	-14.20678	-7.85556	-6.63608	-5.56750	-4.35214
-8.93367	-8.98343	-7.66393	-7.67292	-7.65276	-4.65167	-3.43329	-2.65960	-2.64436	-2.63299
-4.56024	-4.36182	-6.17442	-5.90503	-6.03990	-5.54560	-4.77676	-4.83876	-4.80845	-4.77813
-6.31717	-3.80087	-3.03229	-3.00066	-2.86667	-2.81240	-1.26019	-1.45551	-4.87907	-1.06793
-1.55663	-2.81897	-3.76982	-4.24187	-0.77055	0.46422	1.02727	1.46690	0.57775	-0.83160
-2.45227	-1.36178	1.12094	1.77654	2.87295	2.97021	5.64611	6.84752	7.97080	9.25862
8.99957	4.70342	5.27462	5.08356	5.27034	5.29146	5.29913	4.35946	5.37813	8.17693
9.99344	8.75954	7.49446	6.57922	5.01274	3.67349	3.57089	3.60779	3.14079	4.06259
5.85840	6.95164	8.06906	8.78438	8.36725	7.56357	9.58640	8.08225	7.56639	7.12033
6.40829	6.31440	5.20111	6.30060	6.30821	6.21162	2.26396	3.37622	10.35930	7.81597
7.75790	7.75088	7.81562	7.81320	10.51547	12.61159	12.47804	14.44117	15.72693	14.83219
12.95480	12.33502	13.28797	13.37325	16.18349	16.18873	17.50811	15.55749	15.10434	15.94763
15.94086	16.34670	17.88741	22.04780	21.00901	9.51846	3.84834	0.04300	-1.18325	0.40083
1.08627	1.70292	-0.03187	-0.36278	3.02381	3.98414	3.49026	0.92911	-0.60736	-3.21541
-3.22063	-5.89794	3.81913	-1.74070	4.07467	3.18537	1.56628	-0.79152	-4.54876	-5.24879
-4.36221	-1.85926	5.56699	4.74202	3.44222	2.28739	1.39569	0.14121	2.23816	0.53966
0.34584	-3.71852	-2.78949	-1.73032	4.82515	5.50472	6.26699	8.52146	8.57228	7.91901
1.88128	7.40257	8.10762	7.78603	7.68642	7.79244	10.21796	9.59086	9.99200	10.47578
11.65311	14.13510	14.67151	13.61131	11.44726	10.02621	9.84496	10.21518	11.38130	10.53300
12.24798	13.69941	12.52977	12.52214	12.52174	12.52616	8.37081	9.13525	9.57219	10.14492
9.91822	10.05246	9.95686	12.31722	14.77786	17.42979	17.45981	12.11613	10.86524	8.10563
6.94626	6.68126	13.91504	5.47372	5.50772	5.67533	5.68816	4.55030	7.12113	9.28310
1.65958	5.87784	8.70570	9.81654	9.83214	9.71180	11.43511	14.07626	15.89603	16.61397
15.21282	13.71671	13.92760	13.90212	9.42284	7.43111	0.44024	6.94663	11.28884	13.54554
12.10280	7.97936	8.61612	10.23179	13.18778	15.77438	16.41386	16.06433	15.64834	15.29233
17.34109	16.00382	11.93497	10.00638	7.50251	3.95238	2.65741	5.77466	5.73322	5.40328
8.27966	5.79799	3.73207	3.49401	3.32661	7.82436	7.89817	4.24387	4.60350	2.72065
3.92710	8.13536	9.54884	12.51593	13.64236	12.11652	8.91645	11.32518	10.55893	11.59392
10.65686	10.65336	10.61965	10.64307	10.68902	10.65654	6.27616	5.89965	6.06567	6.12810
7.24027	5.50807	4.65863	5.13942	6.61672	9.53526	11.50198	8.27239	9.39098	9.43077
2.06712	5.43301	7.63076	8.47442	8.54069	9.43676	12.69759	12.10513	12.26175	12.17246
10.79523	12.31425	13.63002	13.42154	13.03320	14.28858	10.83886	10.36048	10.45024	10.23958
9.40230	8.13304	12.50450	14.94671	13.36600	12.53981	11.44370	10.19099	10.16318	10.33135
10.84246	10.39247	10.04213	11.16625	10.88072	8.79745	6.04909	5.08421	7.36475	9.45424
11.79835	13.03440	11.63125	11.36029	11.21494	6.27198	8.02868	9.13076	10.16107	11.01480
11.03534	11.16100	10.94672	11.22201	11.22161	10.02038	10.20139	11.39026	10.34293	4.69062
2.10471	7.25508	9.50407	7.43672	7.66781	8.70688	7.49752	7.68425	7.61549	7.55884
9.12649	10.86250	11.75197	13.46063	13.10821	10.70411	10.34472	4.92193	6.56989	4.52726
12.61522	13.74301	13.73772	16.19705	21.60622	19.47628	18.15808	16.53778	15.14948	15.38765
14.63116	13.47012	11.84286	9.89484	7.30000	3.50035	2.71851	4.47925	6.97640	4.93545
6.96720	8.00693	7.45808	5.45430	1.86626	-3.43706	1.45160	0.66441	5.96300	10.94904
11.53239	12.35054	11.83731	11.57269	9.21297	12.84823	13.77739	15.02490	16.27242	18.16575
13.19590	12.36017	11.42819	8.65964	10.79142	11.92395	10.42804	9.80625	9.55196	9.16695
9.76589	8.66221	7.50813	7.64513	7.94088	9.21084	9.11178	10.15373	10.93676	11.57769
10.75781	11.59329	11.76998	12.44009	12.74404	12.73400	12.72397	12.23332	11.89726	11.88963
12.53407	13.40637	14.52535	14.42635	14.13142	14.45963	14.52525	14.17078	13.46358	13.07705
12.80174	10.94728	11.10842	10.29630	11.74354	11.58339	11.54261	11.46760	12.50092	12.68706
12.20654	14.25188	15.28302	8.62409	7.10040	7.09245	8.05601	7.12306	7.88431	10.16580
9.02841	12.42090	12.97416	4.58978	5.80362	7.50307	7.42992	2.21389	2.06170	5.77683
4.09788	4.10334	5.82768	5.51232	6.13178	5.98401	5.81178	5.64280	5.62821	2.16622
2.23986	2.94099	2.45623	3.00813	2.64823	3.10012	4.01081	3.23404	1.95280	2.04302
2.97298	2.29115	0.89951	0.88146	2.76986	2.74784	3.36504	4.30064	4.27862	4.25660
7.66486	6.42442	2.52312	2.82069	5.01006	6.46455	8.24171	10.31553	10.12194	9.35582
9.88404	10.19054	7.09435	6.61671	4.97482	5.26411	6.76164	6.18004	8.43909	8.27486
9.15361	7.64339	6.52691	6.51899	5.65466	3.09716	4.73765	6.21600	5.49785	7.00641
5.31958	5.31974	5.31991	5.32971	4.62370	5.09163	5.85837	5.46741	4.59657	4.29997
5.29049	5.02686	2.81128	2.40527	2.20989	2.12974	2.03780	2.15109	1.88741	1.87976
0.74866	0.39408	-0.21870	-1.55230	-3.09669	-3.45793	-3.45975	-0.70336	2.57968	1.79982
1.05706	0.42898	-2.03297	-0.02930	0.29118	-1.89379	-1.90032	-1.89721	-4.63511	-6.52237
-6.11569	-5.07483	0.42722	-0.03672	-0.71626	0.54184	1.79754	2.72782	3.19889	3.82543
-1.48380	-1.09507	6.21192	5.51204	4.26385	3.17571	4.83964	4.68648	4.85317	5.96537
5.92871	5.91433	4.25136	4.25331	4.26248	4.11123	4.11799	6.71686	9.42935	12.05823
10.28951	8.15274	6.05476	3.15848	4.87175	8.44544	8.11253	5.71297	6.07033	7.31816
10.46128	9.21817	9.22940	6.73487	4.79002	5.09665	5.51501	5.68552	6.11110	7.16098
5.99795	5.32348	6.07614	7.56941	6.53230	5.62648	5.03656	4.89385	4.91108	4.45446
4.62964	4.96278	5.29591	5.62664	5.64146	5.49593	7.72848	9.31490	9.33454	9.36141

LAG (SECOND)	(2) AUTOCOVARIANCE OF SERIES 2
-0.	136.719803
0.1000000	134.240084
0.2000000	131.581932
0.3000000	129.585528
0.4000000	127.921975
0.5000000	126.609322
0.6000000	125.920371
0.7000000	125.486989
0.8000000	124.593373
0.9000000	123.793691
1.0000000	123.072532
1.0999999	121.941852
1.1999999	120.731608
1.2999999	119.777925
1.3999999	118.849810
1.4999999	117.890696
1.5999999	117.133982
1.6999999	116.442049
1.7999999	115.699091
1.8999999	114.813326
1.9999999	114.211069
2.0999999	113.906106
2.1999999	113.501927
2.2999999	113.036245
2.3999999	112.740736
2.4999999	112.334232
2.5999998	111.902419
2.6999998	111.688000
2.7999998	111.562537
2.8999998	111.016543
2.9999998	110.366092
3.0999998	109.921986
3.1999998	109.528613
3.2999998	109.178701
3.3999998	108.681991
3.4999998	108.327072
3.5999998	107.943579
3.6999998	107.695281
3.7999998	107.496702
3.8999998	107.057416
3.9999998	106.584144
4.0999997	106.180769
4.1999997	105.817260
4.2999997	105.476593
4.3999996	105.365089
4.4999996	105.434935
4.5999995	105.246566
4.6999995	104.829396
4.7999995	104.419641
4.8999994	104.152740
4.9999994	104.080753
5.0999994	103.839989
5.1999993	103.589747
5.2999993	103.218030
5.3999993	102.741178
5.4999992	102.118905
5.5999992	101.668960
5.6999992	101.382447
5.7999991	101.394451
5.8999991	101.581653
5.9999990	101.319965
6.0999990	100.600062
6.1999990	99.943790
6.2999989	99.288632
6.3999989	98.585267
6.4999989	98.001596
6.5999988	97.774487
6.6999988	97.353745
6.7999988	96.929824
6.8999987	96.771644
6.9999987	96.674341
7.0999987	96.245048
7.1999986	95.781318
7.2999986	95.475562
7.3999985	95.122528
7.4999985	94.918305
7.5999985	94.807581
7.6999984	94.825804
7.7999984	94.575465
7.8999984	94.218449
7.9999983	93.865534
8.0999982	93.277043
8.1999981	92.947791
8.2999980	92.765900
8.3999979	92.383802
8.4999979	91.735512
8.5999978	91.172016
8.6999977	90.622938
8.7999976	89.914673
8.8999975	89.238074
8.9999974	88.793876
9.0999973	88.343747
9.1999972	87.748139
9.2999971	87.221180
9.3999970	86.829659
9.4999969	86.542577
9.5999968	85.949423
9.6999967	85.175899
9.7999966	84.460137
9.8999965	83.717133
9.9999964	83.336562

(2) GRAPH OF AUTOCOVARIANCE FUNCTION OF SERIES 2 PLOTTED AGAINST TIME UP TO A LAG OF 10.0000 SECOND

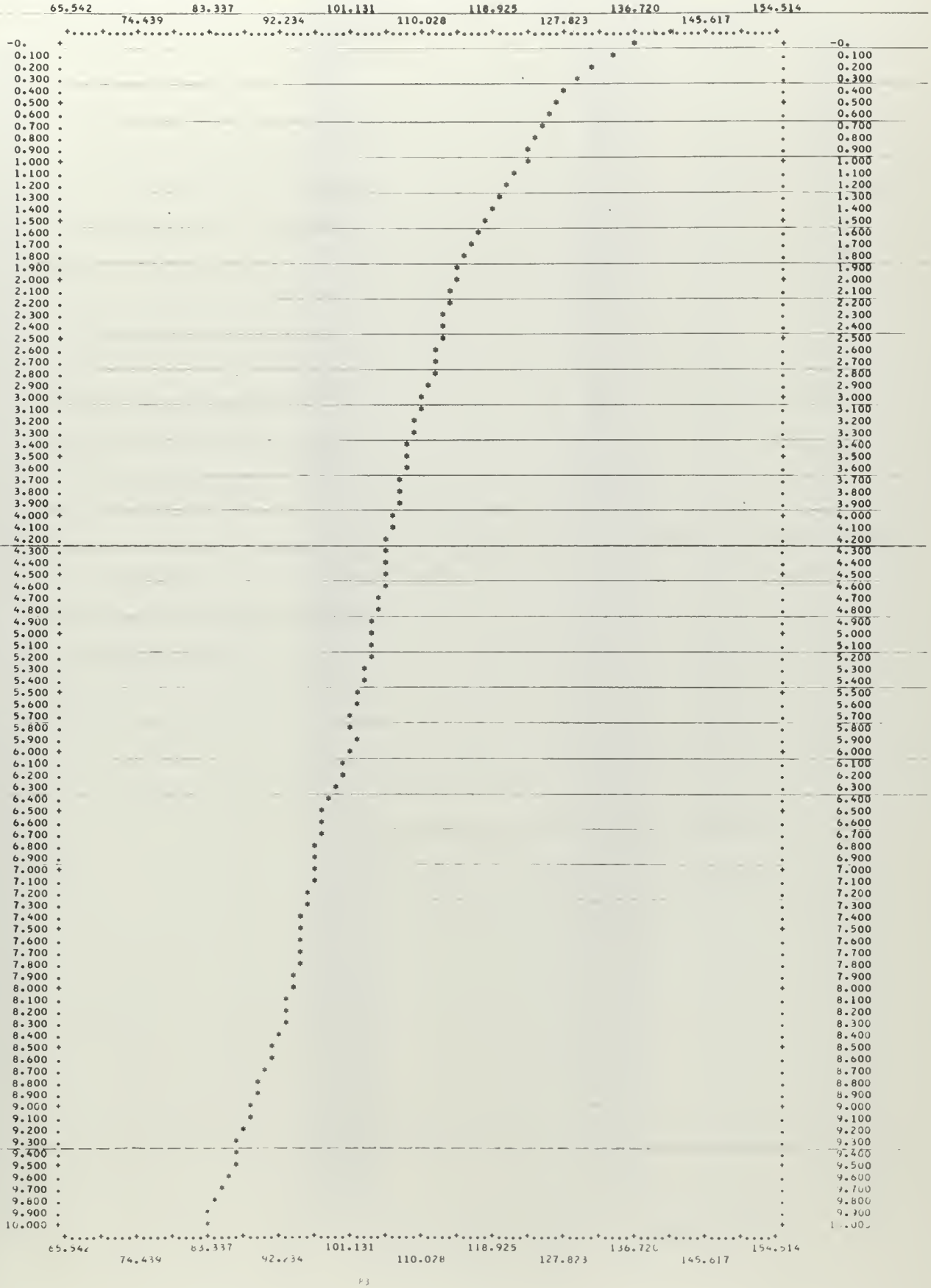

FREQUENCY (CYCLES/SECOND)	③ POWER SPECTRAL ESTIMATES OF SERIES 2
-0.	383.7285881
0.050000	182.6911449
0.100000	17.5962090
0.150000	8.4628992
0.200000	5.9579135
0.250000	4.0517607
0.300000	2.6287237
0.350000	2.3770285
0.400000	1.5715009
0.450000	0.9300798
0.500000	0.7405255
0.550000	0.6149712
0.600000	0.6493334
0.650000	0.8312680
0.700000	0.7522334
0.750000	0.7580444
0.800000	0.8241192
0.850000	0.7903058
0.900000	0.5287128
0.950000	0.5986931
1.000000	0.7000603
1.050000	0.6201725
1.100000	0.5461514
1.150000	0.6196621
1.200000	0.4137453
1.250000	0.3527345
1.300000	0.4807013
1.350000	0.4302773
1.400000	0.2442606
1.450000	0.2064999
1.500000	0.2690425
1.550000	0.2498153
1.600000	0.1055194
1.650000	0.1510822
1.700000	0.2169964
1.750000	0.2253814
1.800000	0.2266283
1.850000	0.1850663
1.900000	0.1082196
1.950000	0.0878182
2.000000	0.1065000
2.050000	0.1020795
2.100000	0.1037366
2.150000	0.1398452
2.200000	0.1294576
2.250000	0.0743691
2.300000	0.0553440
2.350000	0.0858689
2.400000	0.1243207
2.450000	0.0852670
2.500000	0.0582651
2.550000	0.0651205
2.600000	0.0524829
2.650000	0.0591246
2.700000	0.0817738
2.750000	0.1007028
2.800000	0.1209391
2.850000	0.1759721
2.900000	0.1336417
2.950000	0.0824582
3.000000	0.0847758
3.050000	0.0630463
3.100000	0.0583861
3.149999	0.0793020
3.199999	0.0699261
3.249999	0.0520203
3.299999	0.0446261
3.349999	0.0475723
3.399999	0.0300561
3.449999	0.0187037
3.499999	0.0194987
3.549999	0.0272510
3.599999	0.0330077
3.649999	0.0339645
3.699999	0.0363169
3.749999	0.0403523
3.799999	0.0334528
3.849999	0.0377382
3.899999	0.0427226
3.949999	0.0421150
3.999999	0.0418114
4.049999	0.0300238
4.099999	0.0245524
4.149999	0.0303787
4.199999	0.0441823
4.249999	0.0509428
4.299999	0.0358283
4.349999	0.0291407
4.399999	0.0361181
4.449999	0.0316606
4.499999	0.0365714
4.549999	0.0405647
4.599999	0.0361531
4.649999	0.0318768
4.699999	0.0233634
4.749999	0.0236066
4.799998	0.0334033
4.849998	0.0361747
4.899998	0.0302330
4.949998	0.0338973
4.999998	0.0402399

⑤ THE CHECK SUM OF POWER SPECTRAL ESTIMATES IS 136.7196331 AND SHOULD BE 136.7198029
THE DIFFERENCE IS -0.0001698

④ POWER SPECTRAL ESTIMATES OF SERIES 2 PLOTTED IN A LOG SCALE AGAINST FREQUENCY (CYCLES/SECOND)

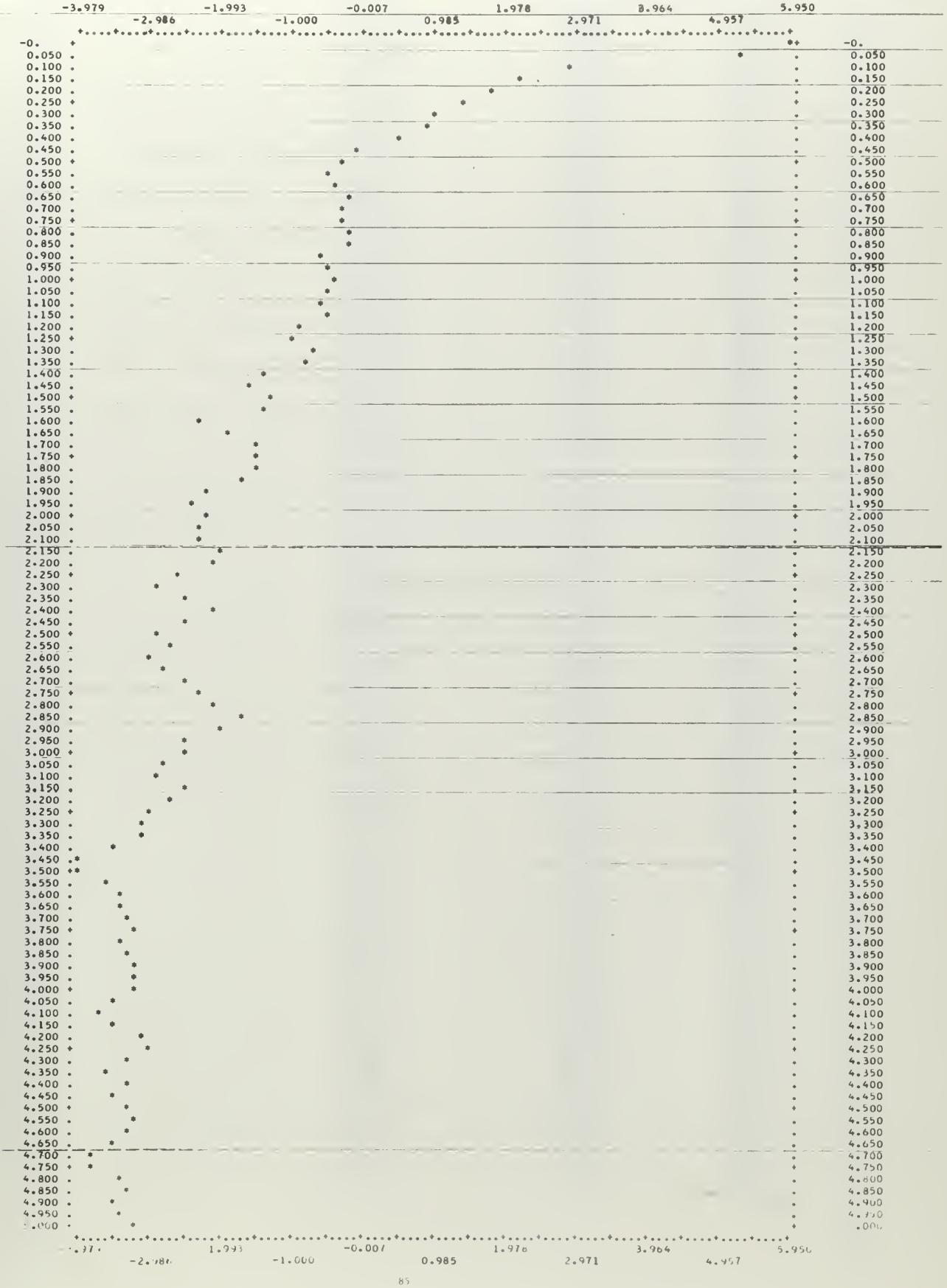

LAG (SECONO)	⑥ CROSSCOVARIANCE OF SERIES 1 ANO 2 (POSITIVE TAU)	⑥ CROSSCOVARIANCE OF SERIES 1 ANO 2 (NEGATIVE TAU)
-0.	0.000349	0.000349
0.1000	0.000444	-0.000202
0.2000	0.000076	-0.000782
0.3000	-0.000740	-0.000942
0.4000	-0.001713	-0.000726
0.5000	-0.002795	-0.000261
0.6000	-0.003751	0.000370
0.7000	-0.004492	0.001021
0.8000	-0.004957	0.001583
0.9000	-0.005073	0.001980
1.0000	-0.004926	0.002243
1.1000	-0.004590	0.002306
1.2000	-0.004196	0.002163
1.3000	-0.003774	0.001917
1.4000	-0.003308	0.001660
1.5000	-0.002807	0.001329
1.6000	-0.002360	0.001004
1.7000	-0.002002	0.000735
1.8000	-0.001768	0.000464
1.9000	-0.001724	0.000197
2.0000	-0.001740	0.000116
2.1000	-0.001862	0.000132
2.2000	-0.002088	0.000140
2.3000	-0.002320	0.000236
2.4000	-0.002501	0.000390
2.5000	-0.002610	0.000549
2.6000	-0.002579	0.000745
2.7000	-0.002411	0.000938
2.8000	-0.002174	0.001039
2.9000	-0.001927	0.001080
3.0000	-0.001673	0.001123
3.1000	-0.001521	0.001152
3.2000	-0.001494	0.001056
3.3000	-0.001567	0.000874
3.4000	-0.001759	0.000754
3.5000	-0.001926	0.000637
3.6000	-0.002033	0.000584
3.7000	-0.002031	0.000659
3.8000	-0.001997	0.000765
3.9000	-0.001960	0.000875
4.0000	-0.001925	0.001066
4.1000	-0.001892	0.001312
4.2000	-0.001829	0.001472
4.3000	-0.001749	0.001587
4.4000	-0.001627	0.001692
4.5000	-0.001462	0.001714
4.6000	-0.001372	0.001592
4.7000	-0.001333	0.001405
4.8000	-0.001343	0.001164
4.9000	-0.001378	0.000931
5.0000	-0.001471	0.000837
5.1000	-0.001531	0.000829
5.2000	-0.001572	0.000918
5.3000	-0.001691	0.001045
5.4000	-0.001874	0.001199
5.5000	-0.002099	0.001437
5.6000	-0.002260	0.001686
5.7000	-0.002391	0.001966
5.8000	-0.002417	0.002263
5.9000	-0.002363	0.002483
6.0000	-0.002294	0.002483
6.1000	-0.002250	0.002318
6.2000	-0.002174	0.002118
6.3000	-0.002155	0.001937
6.4000	-0.002178	0.001751
6.5000	-0.002248	0.001636
6.6000	-0.002329	0.001511
6.7000	-0.002440	0.001484
6.8000	-0.002477	0.001488
6.9000	-0.002433	0.001503
7.0000	-0.002356	0.001517
7.1000	-0.002293	0.001459
7.2000	-0.002262	0.001428
7.3000	-0.002237	0.001453
7.4000	-0.002188	0.001591
7.5000	-0.002129	0.001765
7.6000	-0.002067	0.001930
7.7000	-0.002001	0.002069
7.8000	-0.001960	0.002126
7.9000	-0.001935	0.002101
8.0000	-0.001961	0.002050
8.1000	-0.002096	0.001962
8.2000	-0.002279	0.001886
8.3000	-0.002495	0.001836
8.4000	-0.002651	0.001828
8.5000	-0.002856	0.001838
8.6000	-0.003043	0.001872
8.7000	-0.003218	0.001963
8.8000	-0.003311	0.002079
8.9000	-0.003251	0.002236
9.0000	-0.003091	0.002405
9.1000	-0.002906	0.002453
9.2000	-0.002699	0.002401
9.3000	-0.002504	0.002307
9.4000	-0.002405	0.002063
9.5000	-0.002351	0.001764
9.6000	-0.002369	0.001463
9.7000	-0.002438	0.001258
9.8000	-0.002593	0.001168
9.9000	-0.002772	0.001182
10.0000	-0.002956	0.001313

(6) GRAPH OF CROSS-COVARIANCE FUNCTION OF SERIES 1 AND 2 PLOTTED AGAINST TIME UP TO A LAG OF 10.0000 SECOND

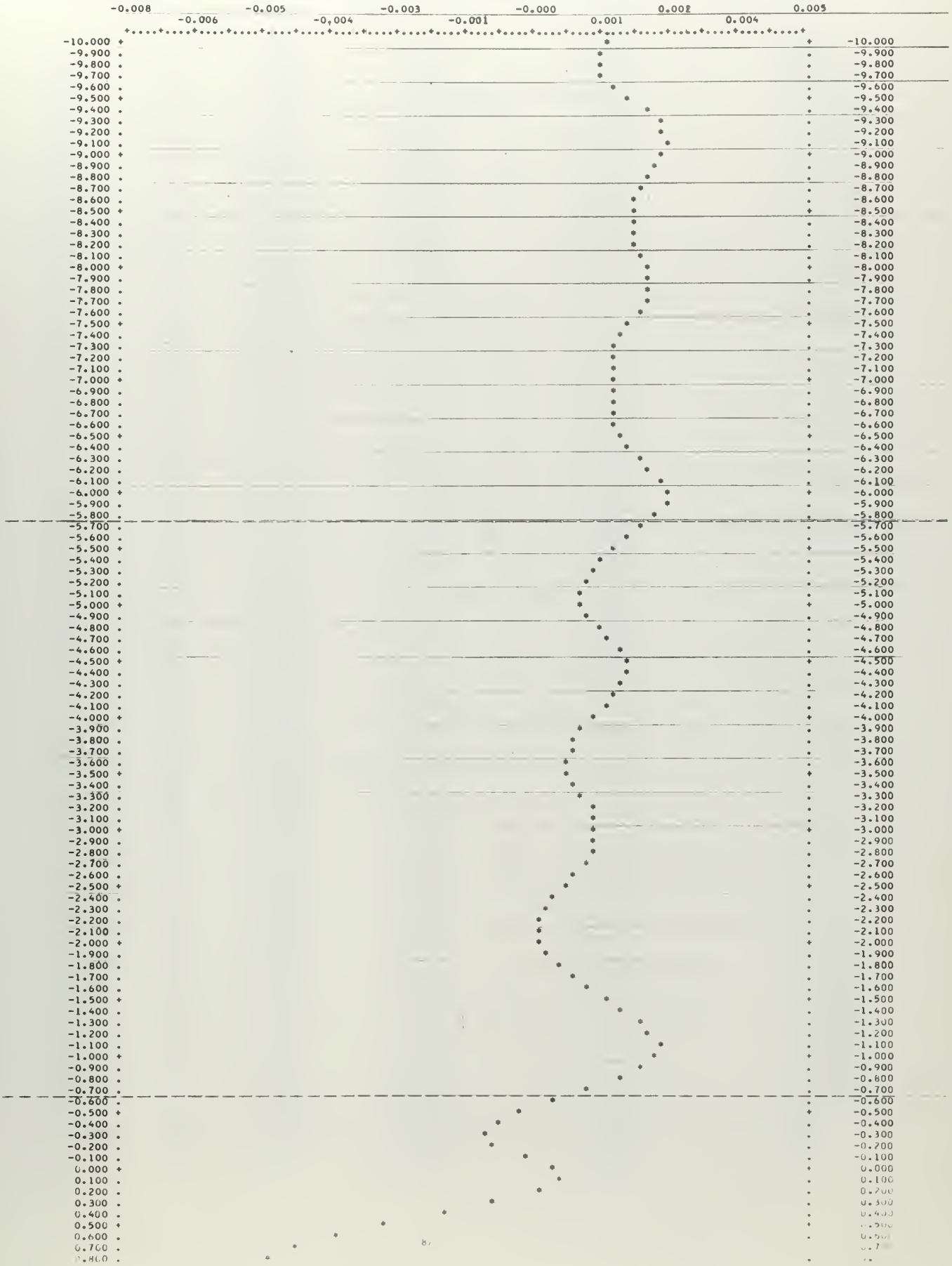

GRAPH OF CROSS-COVARIANCE FUNCTION
OF SERIES 1 AND 2 (CONTINUED)

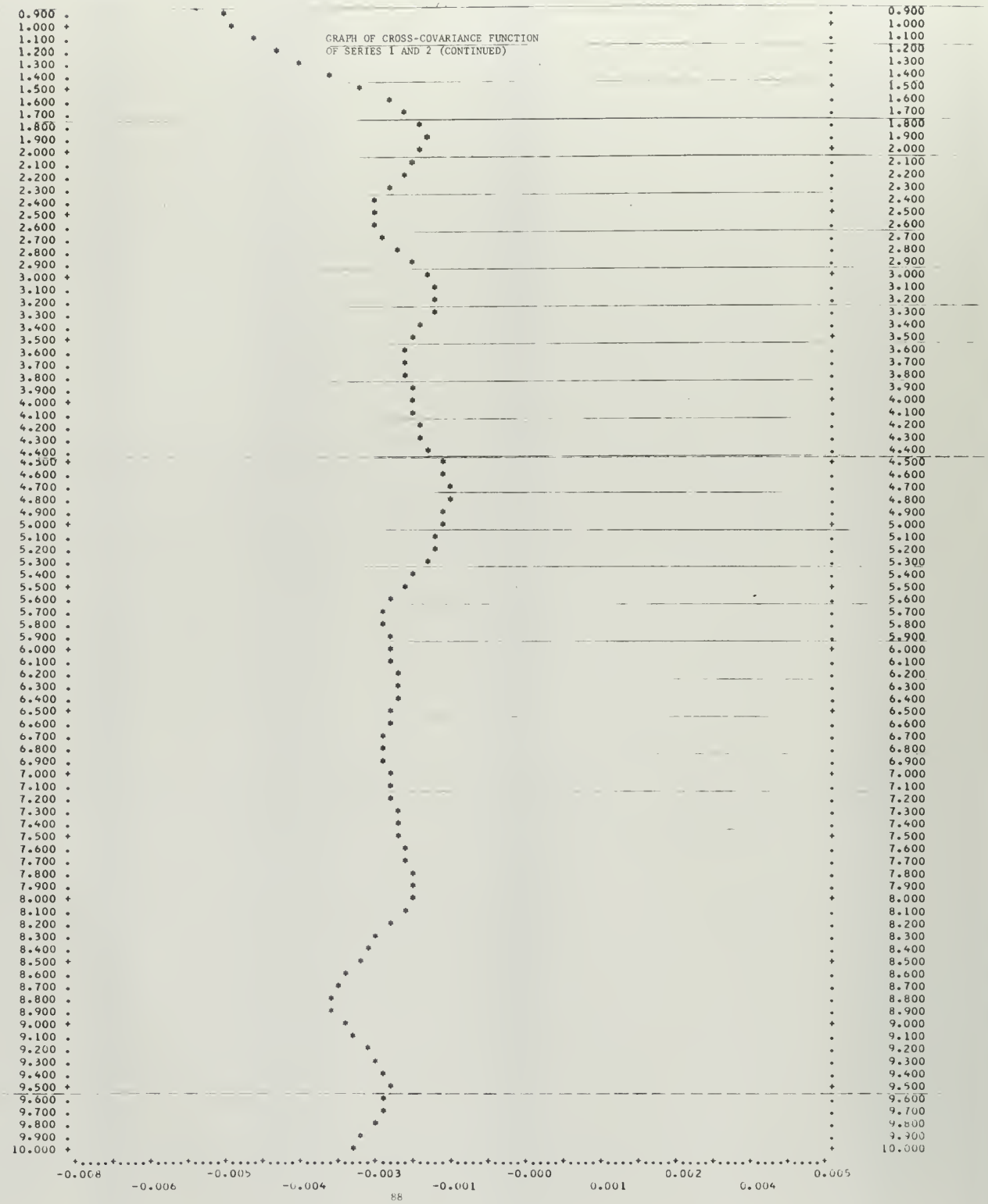

FREQUENCY (CYCLES/SECOND)	(7) CO-SPECTRUM OF SERIES 1 AND 2	(8) QUADRATURE SPECTRUM OF SERIES 1 AND 2	(10) AMPLITUDE OF CROSS-SPECTRUM OF SERIES 1 AND 2	(11) PHASE OF CROSS-SPECTRUM OF SERIES 1 AND 2 *
-0.	-0.0021232	-0.D032847	0.0039111	0.6586698
0.050	-0.0014642	-0.0036339	0.0039178	0.689D397
0.100	-0.0007291	-0.D018874	0.0020233	0.6913315
0.150	-0.0002058	-0.0016613	0.DD16740	0.7303843
0.200	0.0000841	-0.0015001	0.0D15024	0.7589148
0.250	0.0001300	-0.0D13435	0.0013498	0.7653466
0.300	0.0CD0567	-0.0009808	0.0009824	0.7591837
0.350	0.0001186	-0.0010761	0.DD10826	0.7674672
0.400	0.0D01705	-0.00D6342	0.DD06567	0.7917943
0.450	0.0002059	-0.0002335	0.D003113	0.865D182
0.500	0.0002811	-0.0000399	0.0DD2839	0.9775740
0.550	0.0002331	0.0001258	0.0002649	0.0787852
0.600	0.0D03949	0.0D063D9	0.0007443	0.1609982
0.650	0.0006710	0.D008557	0.0D10874	0.1441602
0.700	0.0004431	0.DD06563	0.DDD7918	0.1554885
0.750	0.00D1871	0.0004414	0.0004794	0.1861861
0.800	0.D000596	0.0004297	0.0004338	0.2280736
0.850	0.D001251	0.0003221	0.0003455	0.1910421
0.900	0.D0D1735	0.D002081	0.0D02709	0.1393655
0.950	0.DD02DD2	0.D001729	0.0D02645	0.1133860
1.000	0.0001898	0.0002451	0.0003100	0.1451075
1.050	0.0DD1140	0.00D1750	0.0002088	0.1580855
1.100	0.0D0D712	0.0001851	0.0001983	0.1915373
1.150	0.0000592	0.0001287	0.0001417	0.1813452
1.200	0.0000335	0.0000819	0.0D00885	0.1882467
1.250	0.0000442	0.0000451	0.0000632	0.1265222
1.300	0.DD00758	0.0000837	0.0001129	0.1329414
1.350	0.0000383	0.D000385	0.00D0543	0.1254156
1.400	0.0000010	0.0000441	0.0000441	0.2465480
1.45D	0.0000008	0.0000140	0.D000141	0.2411736
1.500	0.0000329	0.DD003D6	0.0D00449	0.1190123
1.550	0.0000403	0.DD00080	0.0000411	0.0311476
1.600	0.0000137	0.0000218	0.D000258	0.1605806
1.650	0.0000146	0.0000063	0.0000159	0.0647518
1.700	0.0DD0304	0.0000218	0.0000375	0.0991182
1.750	0.0000267	0.0000012	0.D000267	0.DD73651
1.800	0.00DD251	0.0000235	0.0DD0344	0.1197049
1.850	0.0000391	0.0000081	0.0000399	0.0323389
1.900	0.0D00310	0.0DDD2D1	0.0000370	0.0915918
1.950	0.000D138	-0.0000D20	0.00D0139	0.9776278
2.000	0.0000087	0.0DD0108	0.D00D139	0.1418096
2.050	-0.0DDD002	-0.00D0041	0.000D041	0.7435969
2.100	0.0DDD019	0.D000169	0.0000170	0.2321248
2.150	0.0000097	0.0000053	0.000D111	0.0799590
2.200	0.0000107	0.0000098	0.0000145	0.1186766
2.250	0.0000076	-0.00DD064	0.0000099	0.8884183
2.300	0.0000043	0.D000083	0.0D00093	0.1733896
2.350	0.0000069	-0.D000064	0.D00D094	0.8814613
2.400	0.0D00071	0.DD00D38	0.D000D81	0.0779053
2.450	0.0000066	-0.0000047	0.0000081	0.9016696
2.500	0.000DD48	0.0000092	0.D0001D4	0.1728165
2.550	0.0000D41	-0.0000039	0.0000056	0.8782449
2.600	0.000D033	0.0000053	0.0000063	0.1610474
2.650	0.0000072	-0.0000031	0.0000078	0.9357431
2.700	0.0000D77	0.0000062	0.00D0099	0.1082187
2.750	0.000D014	-0.0000033	0.0000036	0.8121454
2.8DD	0.0000032	0.0000070	0.DDD0077	0.1811776
2.850	0.000D147	-0.0000011	0.0000147	0.9884785
2.900	0.0000170	0.0000034	0.00D0173	0.0315632
2.950	0.00D0080	-0.0000118	0.00D0142	0.8448193
3.000	0.00D0DD7	-0.000D063	0.0000063	0.7666611
3.D50	-0.0D00049	-0.D000078	0.0000093	0.6603585
3.100	-0.D00D064	0.D0D0040	0.0000076	0.4118942
3.150	-0.0D0D052	-0.DD0D037	0.00D0064	0.5991808
3.200	0.0000003	0.0000006	0.0000007	0.1898396
3.250	0.0000013	-0.D000070	0.0000071	0.7788337
3.300	0.0000014	0.0000029	0.0000032	0.1772105
3.350	0.00DD050	0.0000003	0.0000050	0.0097569
3.40D	0.0000048	0.00DDD53	0.0D00072	0.1331675
3.450	0.0000024	-0.0000042	0.0000048	0.8324596
3.500	0.0000003	0.D000009	0.0000010	0.2018086
3.550	-0.0000DD4	-0.D000044	0.DDD0045	0.7342104
3.600	-0.000D028	-0.0000002	0.0000028	0.5132156
3.650	-0.0000032	-0.D000050	0.0000059	0.6595750
3.700	-0.0000022	0.0DDD014	0.0DDDD26	0.4075344
3.750	-0.0000005	-0.0000028	0.0000028	0.7229510
3.800	0.0000007	-0.0000001	0.0C00007	0.9710475
3.850	0.0DDDDD5	-0.00DD067	0.0000067	0.7624584
3.900	-0.0000003	-0.0000031	0.0000031	0.7358648
3.950	-0.0000006	-0.0000036	0.D000037	0.7248844
4.DDD	0.DDDDD15	-0.DDDDD06	0.0000016	0.9387038
4.05D	-0.0000004	-0.0000038	0.00D0038	0.7319391
4.100	-0.0CD0024	0.0000010	0.0000026	0.4360235
4.15D	-0.D000D14	-0.00D0042	0.0000044	0.6974187
4.200	-0.0000006	-0.0000040	0.0000041	0.7273278
4.250	0.C0D0004	-0.0000050	0.0000050	0.7632795
4.30D	0.0D0CD14	0.D00D002	0.00D0D14	0.D195076
4.350	0.0CCC006	-0.0000025	0.0000026	0.7865818
4.400	0.0000018	-0.0000016	0.0000024	0.8842748
4.45C	0.CCCCC21	-0.0D00D49	0.CC0DD53	0.8155177
4.500	0.CCCCC15	-0.0000020	0.0C00025	0.8491784
4.550	0.0CCC00e	-0.0000007	0.0C00010	0.8894575
4.600	0.C00C016	-0.DDDDD01	0.00DDD16	0.9939513
4.650	0.CCCC016	-0.0000008	0.0C00018	0.9235846
4.700	0.CCCCCCC	0.0000025	0.CCCC025	0.2474827
4.750	0.CCCCCC2	0.CCCCCCC	0.CCCCCC2	0.0356658
4.800	0.CCCCCC6	-0.0000008	0.0C00010	0.8483709
4.850	0.CCCCC24	0.0000001	0.0CCCC24	0.0044560
4.900	0.0000025	0.0000014	0.0000028	0.0815476
4.950	0.0000023	-0.0000006	0.0000023	0.9586746
[illegible]	0.CCCCC2[illegible]	-0.0000015	0.CCCCC3C	0.9144167

[illegible] IRC[illegible]

(10) GRAPH OF AMPLITUDE OF CROSS-SPECTRUM OF SERIES 1 AND 2 (IN LOG SCALE) AGAINST FREQUENCY (CYCLES/SECOND)

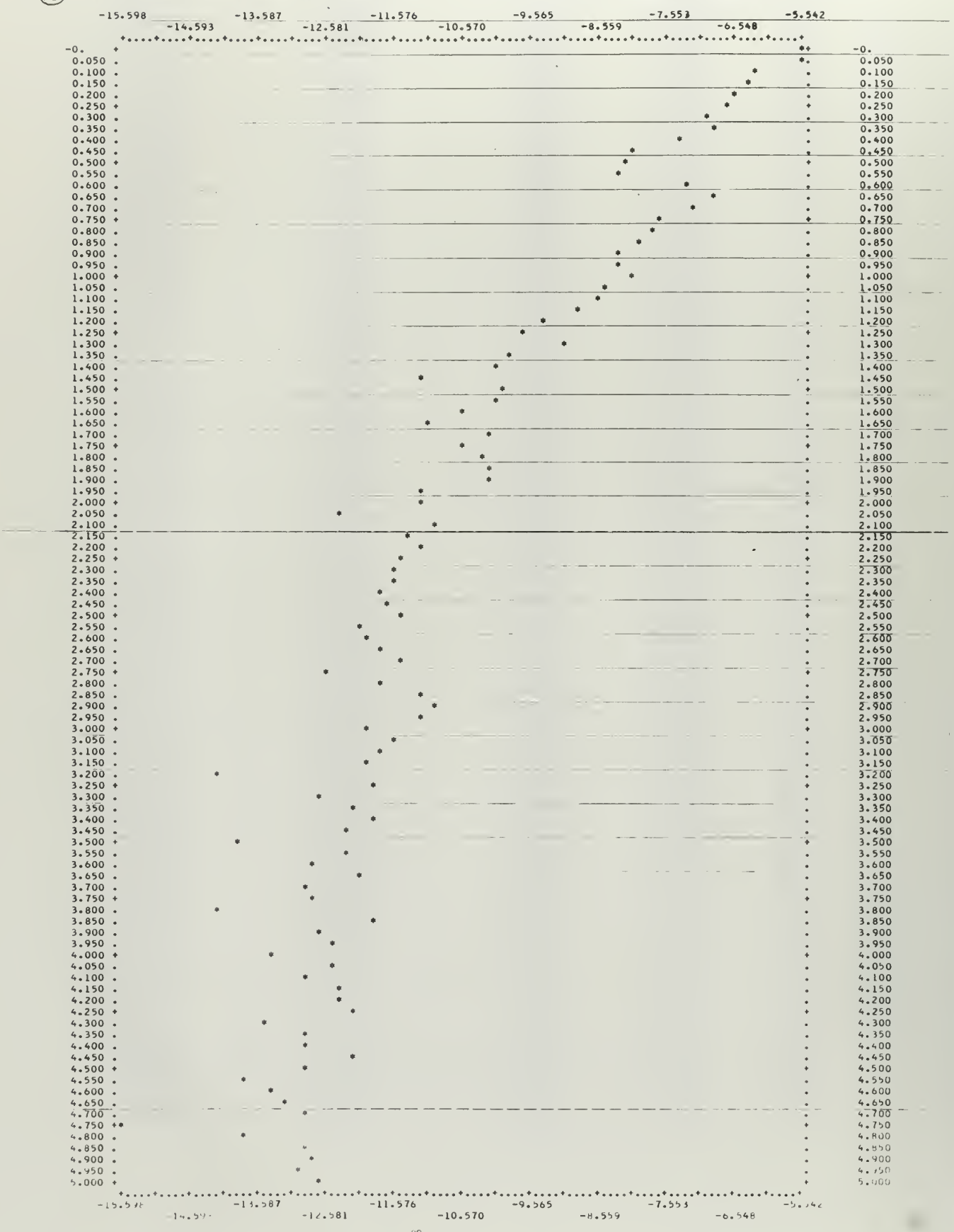

(11) PHASE OF CROSS-SPECTRUM OF SERIES 1 AND 2 -- PLOTTED IN FRACTIONS OF A CIRCLE AGAINST FREQUENCY (CYCLES/SECOND)

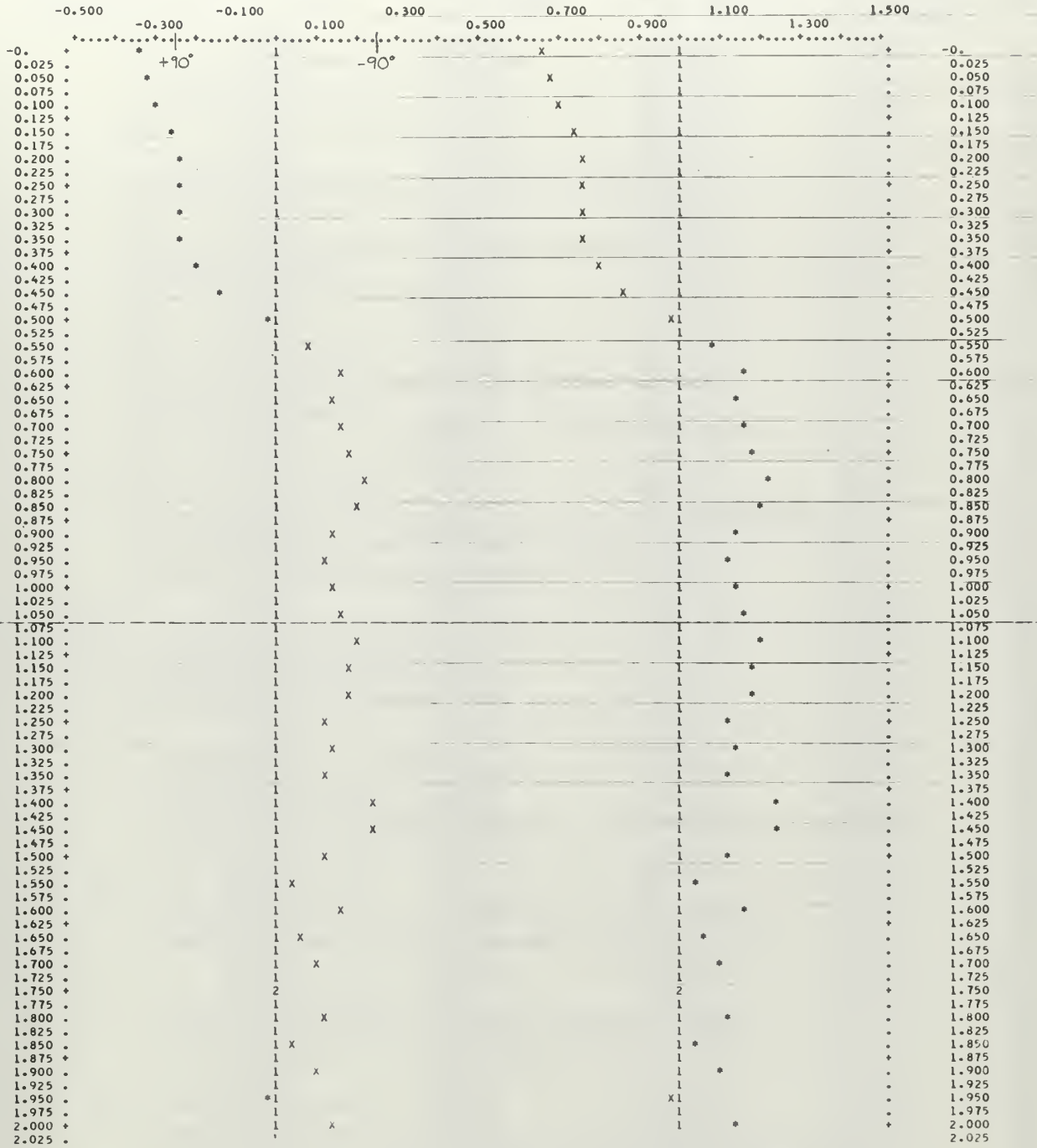

FREQUENCY (CYCLES/SECOND)	COHERENCE SQUARE OF SERIES 1 AND 2	(13) AMPLITUDE OF TRANSFER FUNCTION FROM 1 TO 2	(13) AMPLITUDE OF TRANSFER FUNCTION FROM 2 TO 1	(12) PHASE OF TRANSFER FUNCTION FROM 1 TO 2 *	(12) PHASE OF TRANSFER FUNCTION FROM 1 TO 2 (degrees)
-0.	0.0619165	6074.7177734	0.0000102	0.6586698	123.0
0.0500	0.1614117	7526.7287598	0.0000214	0.6890397	112.1
0.1000	0.5300088	4609.3800659	0.0001150	0.6913315	111.1
0.1500	0.6889446	3483.0234375	0.0001978	0.7303843	97.1
0.2000	0.7242599	2872.0730286	0.0002522	0.7589148	86.9
0.2500	0.9594974	2880.1491394	0.0003331	0.7653466	84.7
0.3000	0.6903551	1847.2368774	0.0003737	0.7591837	86.6
0.3500	0.6757946	1483.8199463	0.0004554	0.7674672	83.8
0.4000	0.4400037	1052.9419556	0.0004179	0.7917943	75.0
0.4500	0.2456576	733.9263306	0.0003347	0.8650182	49.6
0.5000	0.2757262	719.2819901	0.0003833	0.9775740	8.1
0.5500	0.1686972	391.6125259	0.0004308	0.0787852	28.3
0.6000	0.5212792	454.7567940	0.0011463	0.1609982	52.5
0.6500	0.6685881	511.1045265	0.0013081	0.1441602	51.9
0.7000	0.8822397	648.1295166	0.0010526	0.1554885	55.9
0.7500	0.6187247	978.2851639	0.0006325	0.1861861	67.0
0.8000	0.6741928	1280.8452759	0.0005264	0.2280736	82.2
0.8500	0.4412994	1009.3552246	0.0004372	0.1910421	68.7
0.9000	0.5377295	1049.2672119	0.0005125	0.1393655	50.1
0.9500	0.5397015	1221.4488831	0.0004418	0.1133860	40.8
1.0000	0.6581574	1486.2371521	0.0004428	0.1451075	52.3
1.0500	0.5283800	1569.1015778	0.0003367	0.1580855	56.9
1.1000	0.6613693	1821.7242432	0.0003630	0.1915373	68.9
1.1500	0.4437273	1940.5514069	0.0002287	0.1813452	65.3
1.2000	0.6364876	2976.3462524	0.0002138	0.1882467	67.7
1.2500	0.3351934	1872.0773163	0.0001790	0.1265222	45.5
1.3000	0.5603038	2384.6016235	0.0002350	0.1329414	47.8
1.3500	0.1766725	1400.0268097	0.0001262	0.1254156	45.1
1.4000	0.3567112	1976.2814636	0.0001805	0.2465480	88.7
1.4500	0.0603871	886.6184082	0.0000681	0.2411736	86.8
1.5000	0.3647295	2183.8581543	0.0001670	0.1190123	42.5
1.5500	0.3726450	2263.4462585	0.0001646	0.0311476	11.2
1.6000	0.3357297	1372.8514557	0.0002445	0.1605806	57.8
1.6500	0.0976866	930.6552048	0.0001050	0.0647518	23.3
1.7000	0.5087685	2947.2337952	0.0001726	0.0991182	35.7
1.7500	0.3973063	3354.8771667	0.0001184	0.0073651	2.7
1.8000	0.5725720	3776.2563477	0.0001516	0.1197049	43.1
1.8500	0.5433132	2517.9406433	0.0002158	0.0323389	11.6
1.9000	0.6925161	2026.1054230	0.0003418	0.0915918	33.0
1.9500	0.2104636	1324.4456482	0.0001589	0.9776278	351.9
2.0000	0.4060428	3108.2918091	0.0001306	0.1418096	51.0
2.0500	0.0568191	1423.4937134	0.0000399	0.7435969	
2.1000	0.4143999	2534.3022461	0.0001635	0.2321248	
2.1500	0.1160870	1467.5696869	0.0000791	0.0799590	
2.2000	0.3373034	3010.0081787	0.0001121	0.1186766	
2.2500	0.3391165	2542.1031189	0.0001334	0.8884183	
2.3000	0.3951004	2339.2106323	0.0001689	0.1733896	
2.3500	0.2073879	1897.1470947	0.0001093	0.8814613	
2.4000	0.0762371	1174.1041107	0.0000649	0.0779053	
2.4500	0.0967490	1012.1558762	0.0000956	0.9016696	
2.5000	0.3335481	1869.1534729	0.0001784	0.1728165	
2.5500	0.1620380	1876.8699493	0.0000863	0.8782449	
2.6000	0.3285159	2753.6622009	0.0001193	0.1610474	
2.6500	0.4141135	3138.3084717	0.0001319	0.9357431	
2.7000	0.5032876	4148.7296143	0.0001213	0.1082187	
2.7500	0.0605351	1708.0550995	0.0000354	0.8121454	
2.8000	0.1319702	2058.9215393	0.0000641	0.1811776	
2.8500	0.3315270	3962.8581238	0.0000837	0.9884785	
2.9000	0.4106817	3165.8064880	0.0001297	0.0315632	
2.9500	0.3866681	2239.2727661	0.0001727	0.8448193	
3.0000	0.0876520	1178.8600616	0.0000743	0.7666611	
3.0500	0.2599313	1767.2790833	0.0001471	0.6603585	
3.1000	0.2062179	1589.3707428	0.0001297	0.4118942	
3.1500	0.1158226	1444.4833832	0.0000802	0.5991808	
3.2000	0.0019717	197.2228985	0.0000100	0.1898396	
3.2500	0.4477476	3288.1257629	0.0001362	0.7788337	
3.3000	0.1373497	1917.8540192	0.0000716	0.1772105	
3.3500	0.2815928	2685.6484680	0.0001048	0.0097569	
3.4000	0.6578453	2743.4693298	0.0002398	0.1331675	
3.4500	0.5462859	2131.6284485	0.0002563	0.8324596	
3.5000	0.0266906	534.1774063	0.0000500	0.2018086	
3.5500	0.3734227	2274.2352905	0.0001642	0.7342104	
3.6000	0.0917691	1079.4534607	0.0000850	0.5132156	
3.6500	0.4369779	2512.2828369	0.0001739	0.6595750	
3.7000	0.0951813	1324.5124817	0.0000719	0.4075344	
3.7500	0.1409936	2000.5970917	0.0000705	0.7229510	
3.8000	0.0124684	623.6468735	0.0000200	0.9710475	
3.8500	1.0855527	6093.4472656	0.0001782	0.7624584	
3.9000	0.1534083	2117.1085510	0.0000725	0.7358648	
3.9500	0.2499397	2859.4440918	0.0000874	0.7248844	
4.0000	0.0353635	935.8715439	0.0000378	0.9387038	
4.0500	0.3604958	2818.8566284	0.0001279	0.7319391	
4.1000	0.1919961	1806.6541748	0.0001063	0.4360235	
4.1500	0.2832790	1950.9380035	0.0001452	0.6974187	
4.2000	0.1815312	1961.1654358	0.0000926	0.7273278	
4.2500	0.5055732	5117.8895264	0.0000988	0.7632795	
4.3000	0.0627275	1609.4082031	0.0000390	0.0195076	
4.3500	0.2640604	2948.5805054	0.0000895	0.7865818	
4.4000	0.1507886	2235.9115295	0.0000674	0.8842748	
4.4500	0.5587885	3309.3141479	0.0001689	0.8155177	
4.5000	0.0994396	1450.1022034	0.0000686	0.8491784	
4.5500	0.0204393	803.9247055	0.0000254	0.8894575	
4.6000	0.0490170	1102.0391388	0.0000445	0.9939513	
4.6500	0.0819387	1413.5077515	0.0000580	0.9235846	
4.7000	0.2198924	2064.6186829	0.0001065	0.2474822	
4.7500	0.0010840	152.1559296	0.0000071	0.0356658	
4.8000	0.0292708	968.6815491	0.0000302	0.8483709	
4.8500	0.1724146	2569.9429626	0.0000671	0.0044560	
4.9000	0.2382646	2537.3323975	0.0000939	0.0815476	
4.9500	0.1540685	2235.0189209	0.0000689	0.9586748	
5.0000	0.1996510	2663.2410278	0.0000750	0.9144567	

+ ↑
− ↓

* PHASE GIVEN IN FRACTION OF A CIRCLE

INITIAL DISTRIBUTION LIST

		No. Copies
1.	Defense Documentation Center Cameron Station Alexandria, Virginia	20
2.	Library Naval Postgraduate School, Monterey, California	2
3.	Commander, Naval Air Systems Command Navy Department Washington, D. C. 20360	1
4.	Dr. E. S. Lamar Chief Scientist, Naval Air Systems Command Navy Department Washington, D. C. 20360	1
5.	Mr. G. L. Desmond Aerodynamics and Structures Technical Administrator Naval Air Systems Command Navy Department, Washington, D. C. 20360	1
6.	Commander D. M. Layton Department of Aeronautics Naval Postgraduate School Monterey, California 93940	1
7.	Professor E. J. Andrews Department of Aeronautics Naval Postgraduate School Monterey, California 93940	1
8.	Mr. Walter McNeil Flight Test Division, NASA Ames Research Center Moffett Field, California 94035	1
9.	Mr. William Crawford Computer Facility, NASA Ames Research Center Moffett Field, California 94035	1
10.	Lieutenant John K. Ready Carrier Suitability Branch, Flight Test Division Naval Air Test Center, Patuxent River, Maryland 20670	1
11.	Lieutenant Paul S. Norton Naval Test Pilot School Naval Air Test Center, Patuxent River, Maryland 20670	1

INITIAL DISTRIBUTION LIST (Continued)

		No. of Copies
12.	Professor A. E. Fuhs Department of Aeronautics Naval Postgraduate School, Monterey, California 93940	1
13.	Chairman, Department of Aeronautics Naval Postgraduate School, Monterey, California 93940	1
14.	Lieutenant William M. McDonald SMC #2855 Naval Postgraduate School, Monterey, California 93940	1

DOCUMENT CONTROL DATA - R&D

(Security classification of title, body of abstract and indexing annotation must be entered when the overall report is classified)

1. ORIGINATING ACTIVITY *(Corporate author)*
Naval Postgraduate School
Monterey, California 93940

2a. REPORT SECURITY CLASSIFICATION
UNCLASSIFIED

2b. GROUP

3. REPORT TITLE
THE DETERMINATION OF THE DYNAMIC RESPONSE OF A SMALL SWEPT WING JET FIGHTER TO ATMOSPHERIC TURBULENCE USING THE POWER SPECTRUM METHOD OF ANALYSIS

4. DESCRIPTIVE NOTES *(Type of report and inclusive dates)*
Thesis

5. AUTHOR(S) *(Last name, first name, initial)*
NORTON, Paul S.
LT, U.S. Navy

6. REPORT DATE	7a. TOTAL NO. OF PAGES	7b. NO. OF REFS
December 1967	92	14

8a. CONTRACT OR GRANT NO.	9a. ORIGINATOR'S REPORT NUMBER(S)
b. PROJECT NO.	
c.	9b. OTHER REPORT NO(S) *(Any other numbers that may be assigned this report)*
d.	

10. AVAILABILITY/LIMITATION NOTICES
[redacted] to special export controls and each transmittal to foreign government or foreign nationals may be made only with prior approval of the U. S. Naval Postgraduate School.

11. SUPPLEMENTARY NOTES	12. SPONSORING MILITARY ACTIVITY
None	Naval Postgraduate School Monterey, California 93940

13. ABSTRACT

The power spectral techniques of generalized harmonic analysis were applied to determine the phase and amplitude of the transfer function between the vertical component of turbulence and the resultant pitch rate of a small swept wing jet fighter. The power spectrum analysis was based on actual flight test data. In addition, the amplitude and phase of the aircraft's transfer function are determined theoretically by two different methods and compared with the results of the power spectrum analysis. It was established that the power spectrum method, as applied to random turbulence, can be used to determine an aircraft's response to this random input on a continuous basis and that power spectrum techniques have considerable potential value in the study of aircraft gust loading.

14 KEY WORDS	LINK A		LINK B		LINK C	
	ROLE	WT	ROLE	WT	ROLE	WT
Response to Turbulence						
Power Spectrum Methods						
Harmonic Analysis of Turbulence						